National Library of Canada
Acquisitions and Bibliographic Services Branch
395 Wellington Street
Ottawa, Ontario
K1A 0N4

Bibliothèque nationale du Canada
Direction des acquisitions et des services bibliographiques
395, rue Wellington
Ottawa (Ontario)
K1A 0N4

Your file Votre référence

Our file Notre référence

NOTICE

The quality of this microform is heavily dependent upon the quality of the original thesis submitted for microfilming. Every effort has been made to ensure the highest quality of reproduction possible.

If pages are missing, contact the university which granted the degree.

Some pages may have indistinct print especially if the original pages were typed with a poor typewriter ribbon or if the university sent us an inferior photocopy.

AVIS

La qualité de cette microforme dépend grandement de la qualité de la thèse soumise au microfilmage. Nous avons tout fait pour assurer une qualité supérieure de reproduction.

S'il manque des pages, veuillez communiquer avec l'université qui a conféré le grade.

La qualité d'impression de certaines pages peut laisser à désirer, surtout si les pages originales ont été dactylographiées à l'aide d'un ruban usé ou si l'université nous a fait parvenir une photocopie de qualité inférieure.

Canada

Particle Fractionation

by

Elutriation-Spouting

by

MAHER AL-JABARI

A Thesis Submitted to the Faculty of Graduate Studies and Research
in Partial Fulfillment of the Requirements for the Degree of
Doctor of Philosophy

Department of Chemical Engineering
McGill University
Montreal, Quebec, Canada

August, 1994

ISBN 0-612-00072-9

Abstract

Pulp fibers can be spouted in a conical vessel if the inlet Reynolds number is above a critical value which varies linearly with mass of pulp in the vessel. Continuous pulp spouting is also feasible in a wedge-like vessel within certain limits of flow rate and inlet pulp consistency. Spouting hydrodynamics and particle separation behavior in both vessels were investigated for pulp fibers and recycled pulp suspensions.

The minimum spouting velocity (MSV), spouting stability and the pressure drop-flow rate relationship were determined for liquid spouting of pulp fibers and of rigid particles. Liquid spouting of rigid particles is similar to gaseous spouting; pulp spouting is different. The liquid flow field in a conical spouted bed of pulp fibers is of a jet expansion type. A model for predicting the MSV for spouting pulp fibers was developed based on visual observation of the transition of the jet flow patterns in the conical vessel.

Small particles including both ink and pulp fines can be elutriated from a spouted bed of a recycled pulp suspension, with little fiber loss, in both semi-batch and continuous modes using conical and wedge-like vessels, respectively. Both processes were studied using on-line measurement of the exit particle concentration.

For the semi-batch process, the first order elutriation coefficient increased with the flow rate, but was about the same for all pulps. Based on the analysis of the flow field around a porous spherical particle in a shear flow, an elutriation model was developed for fine particle removal from a suspension of porous coarse particles. For the continuous operation, the particle separation mechanism and the fractional particle removal were investigated. Separation occurs by excluding fibers from the top stream, while fines are split according to the ratio of top to bottom flow rates.

Résumé

Dans un réacteur conique, une suspension de fibres de bois peut être fluidisée si le nombre de Reynolds est porté au dessus d'une certaine valeur critique. Cette valeur critique varie avec la masse totale de pâte contenue dans le réacteur. La fluidisation est aussi possible dans un réacteur à paroies divergeantes. L'hydrodynamique de la fluidisation et le phénomène de la séparation des particules ont été étudiés pour les deux types de réacteurs, avec des fibres vierges et recyclées.

La vitesse minimale de fluidisation (MSV), la stabilité de la fluidisation et la corrélation entre la perte de charge et le débit ont été déterminés pour des fibres et des particules rigides. La fluidisation de particules rigides à l'aide d'un liquide ou d'un gaz est similaire. Mais le comportement est différent pour une suspension de fibres. Le champ de vitesses du liquide dans le réacteur conique est un jet divergeant. Un model qui prédit la MSV pour la fluidisation des fibres a été développé a partir d'une observation visuelle.

Les plus petites particules comme l'encre et les fines peuvent être separées en semi-cuvé et en continu à l' aide des réacteurs conique et à parois divergeantes respectivement. Le procédé comportait un système de lecture de la concentration des particules à la sortie.

Pour le réateur conique, le coefficient du model d'évacuation augmente avec le débit, mais il demeure le même pour toute les suspensions de fibres. Basé sur l'analyse du champ de vitesse autour d'une particule poreuse sphérique soumise à un cisaillement, un model d'évacuation a été developpé pour les petites particules poreuses et allongées. Pour le procédé en continu, le mécanisme de séparation des particules et le fractionnement ont été etudiés. La ségrégation apparaît en excluant les fibres de la partie suspérieure, tandis que les fines sont dispersées selon le ratio des vitesse du haut et du bas du réacteur.

Acknowledgement

My sincere thanks and appreciation go to my thesis directors for their teaching, guidance, and encouragement: To

Prof. T.G.M. van de Ven and *Prof. M.E. Weber*

I express my appreciation to the Pulp and Paper Research Institute of Canada and the Department of Chemical Engineering for their financial support during my graduate studies.

I would like also to thank all the members of the "suspension group" for the interesting points and discussions during group meetings. In particularly I like to mention Dr. J.Petlicki and my colleges with whom I discussed politics and religion in parallel with science and colloidal chemistry: Dr. M. Kamiti, Marco Polverari, Xin Wu and Alain Carignan. Also, I express my thanks to Mr. Fred Kluck and Mr. William Bastian from the workshop, whose help in building and maintaining my experimental devices is appreciated. Great thanks to Mrs. P.A. McCaffery, Mrs. A. McGuinness, Mrs. S. Shaieb and Mrs. S. Mosher who have kindly made my stay in the Pulp and Paper Building very easy.

My greatest thanks are expressed deeply to my father, who supported and encouraged me through all the period of my university education, to my mother who is always waiting for me to return home and to my brother and sisters for their permanent love and wishes.

My real acknowledgement is for the lord of the universe who created me and provided the power of thinking which links an observation with information to reach a conclusion.

To

Whom I owe the largest favour in my life;
Understanding the life itself,
the meaning of existence,
the law of nature,
and the importance of discovering natural laws.

To those who are
giving their lives to enlighten the lives of others,
giving their freedom to free others
and working hard to establish
justice,
and fair international society.

To those who are calling for
the satisfaction of the "ROUTES"
of HUMAN existence:
the "Mind",
the "Needs",
and the "Instincts".

M.A.J.

Table of Content

Chapter Two

Spouting of Pulp Fibers in a Conical Vessel

Chapter Three

A Model for the Minimum Spouting Velocity

of Pulp Fibers in a Conical Vessel

Chapter Four

Particle Elutriation From a Spouted Bed of Recycled Pulp Fibers

Chapter Five

Modeling Particle Elutriation from

a Spouted Bed of Pulp Fibers

Chapter Six

Continuous Elutriation Process

Chapter Seven

Summary, Contributions to Knowledge

and Recommendations for Further Research

List of Figures

Chapter One

Chapter Two

Chapter Three

Chapter Four

Chapter Five

Chapter Six

List of Tables

Chapter One

Introduction

1.1. General Introduction

The process of paper recycling is primarily concerned with the removal of contaminating materials prior to reuse of the cellulose fibers in paper production [1]. Secondary recycled fibers are used in several applications: in North America over 50% of the deinked pulps are used for superior quality wood-free products; in Europe and Japan, 55% of the deinked stocks are used for newsprint. World wide statistics show that 47% of deinked stock is used for newsprint and 32% for superior quality products such as tissue papers, printing and writing grades [2].

The need for paper recycling has increased over the last three decades due to the rising cost and restrictions of waste disposal. Although paper recycling should reduce pollution, the disposal of waste water from the deinking plant often causes a serious enviromental problem whose solution may be difficult and expensive [3].

The cost of secondary fibers is less than that of virgin fibers since virgin pulp is manufactured according to precise mill specifications, it is easier to use than secondary fibers [4]. The cost of secondary fiber depends not only on the price of waste papers but also on the type and the cost of the deinking treatment as well as its yield, quality, and the type of furnish produced. Although certain waste papers are easier to deink, the kind of paper stock available for recycling is determined by the market demand for papers regardless of their ability for easy deinking. Waste papers come from different sources and include different types of papers such as newspapers, magazines, books, office papers, etc. A plant might use a mixture of different types of papers (e.g. newsprint and magazine). In a paper production plant using secondary fiber, the price of secondary fiber is the largest part of the final paper cost [3]. This fact provides an economic incentive to improve deinking technology.

In a paper recycling plant the deinking process comes after the repulping and cooking stage, i.e. after the disintegration of the waste papers and the detachment

of contaminants (e.g. ink particles) from the surface of the fibers by mechanical, thermal and/or chemical action. The suspended ink particles are separated from the pulp fibers using one of several mechanisms [2]. The removal of ink particles is achieved most often either mechanically by washing or chemimechanically by flotation. Washing processes are based on the difference in sizes between ink particles and fibers, whereas flotation processes depend on surface properties. Of the deinking plants installed worldwide about 65% utilize flotation and 35% utilize washing. Washing is the dominant technique in North America (90%) while flotation is more popular in Europe and Japan (87%) [2]. Some modern deinking plants use both washing and flotation.

This thesis investigates a hydrodynamic separation technique, which utilizes the principles of elutriation and spouting (see sec. 1.3.). It is based on the difference in terminal settling velocity between ink particles and pulp fibers. When a deinking suspension is subjected to an upward liquid flow in a vessel designed to drop the velocity at some height to a value that is less than the settling velocity of fibers, the fibers will descend while ink particles will ascend provided that the upward liquid velocity is higher than the terminal settling velocity of the ink. This thesis demonstrates the two aspects of such separation process, i.e. spouting and elutriation, for both semi-batch and continuous modes of operation.

In the following two sections of this chapter, the principles of deinking, spouting and elutriation are reviewed. The final two sections summarize the objectives and the outline of the thesis.

1.2. Deinking

Deinking is the removal of ink particles from a slurry of recycled paper after the particles are dislodged from the paper and dispersed. This process is achieved through two main steps: the detachment of ink particles from the surface of the fibers into the suspension producing the so-called deinking slurry, and then the

separation of the particles from the pulp fibers using one or more techniques. A complete deinking plant includes additional steps [6-12], depending upon the nature of the recycled fibers and the requirements of the finished pulp. Crow and Secor [10] distinguished ten general steps in deinking: repulping, prewashing, screening, cleaning (reverse and forward), washing, flotation, dispersion, bleaching and water recirculation and makeup. An example of a simple flowsheet for a deinking plant is shown in Fig.1.1. The suitability of a certain step for ink removal depends on particle size and ink surface properties [12]. The nature of the recycled papers determines the characteristics of the deinking slurry, while the requirements of the finished pulp determine whether a selective removal of ink particles is needed or the removal of all small particles including the fillers.

1.2.1. Repulping and Cooking

In a deinking plant, the waste papers are first disintegrated in water to form the pulp slurry, in which the contaminant particles are dislodged from the fiber surface by mechanical, thermal and chemical means during the repulping stage. Repulping [13] involves two operations: defibering, which is accomplished mainly mechanically by agitation, and deanchoring of contaminants from the fibers and dispersion of the contaminants in the aqueous phase.

For some grades of paper, the contaminants may be detached from the paper flakes or from the fibers by mechanical action only; e.g. Turai and Teng [14,15] showed that ultrasonically-induced cavitation dispersed inks from waste papers with high-gloss printed or overprint varnished ink films without the use of chemicals. Nevertheless, ink detachment is generally accomplished with the aid of several chemicals at moderately elevated temperature; this process is usually referred to as cooking. Although, repulping and cooking are commonly carried out simultaneously, consecutive operation is also possible. The cooking temperature depends on the source of the waste paper, the nature of chemicals used, the type of bleaching operation and the end product. Increasing the temperature reduces the cooking time

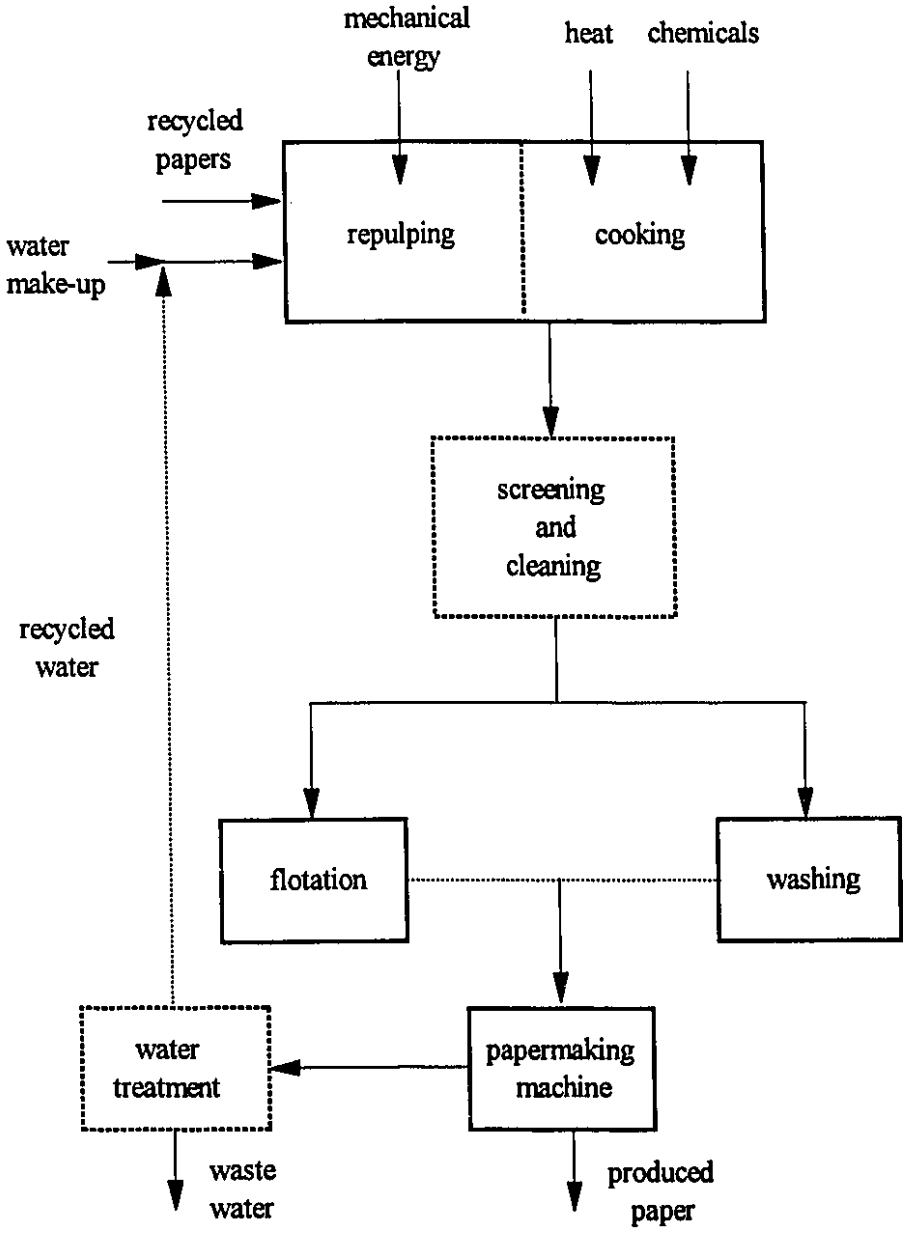

Figure 1.1: A simple flowsheet for a deinking plant

because heat softens ink; also high temperature allows rapid defibering [3]. In general, cooking temperature is in the range of 38-99 °C. Repulpers are operated either at low consistency (4-8%) or high consistency (>12%), depending on the equipment and waste paper used.

1.2.1.1. Deinking Chemicals

The basic chemical recipe for deinking consists of alkali, detergent and dispersing agents [16]. The alkali breaks down the oil-based vehicle by a saponification reaction to release ink pigment. In addition, alkali increases fiber swelling, which assists in ink dispersion. Once the pigment is released, the detergent makes it hydrophillic so that it becomes wetted by water and remains dispersed. Although wetting may be accomplished through the action of the soaps resulting from the saponification reaction, detergents are essential when deinking papers with non-oil-based inks (which do not undergo the saponification reaction). Once the pigment is wetted, dispersing agents are needed to prevent ink from re-agglomerating or redepositing on the fibers. In addition to these deinking chemicals hydrogen peroxide is often used as bleaching agent. The exact type and concentration of each chemical depends on the source of the waste paper, the desired product and the type of deinking technique [16].

1.2.1.2. Characteristics of the Deinking Slurry

The deinking slurry contains certain cellulosic and non-cellulosic components depending on the source of the recycled papers, such as newsprint, magazines, photocopy waste paper, etc. The deinkability of a furnish depends on the paper grade, the nature and amount of ink, and the ink setting and printing process. In this thesis, the interest is in newsprint source, which covers most of recycled papers, specially in North America (in US over 90%) [17]. The printing process for newsprint grades is mainly by letterpress and flexography, methods for which the ink is relatively easy to disperse.

The two main pulp components are fibers and fines. The fibers resemble hollow cylinders with a wide range of sizes; depending on the original source of the pulp, an average fiber has a diameter of about 30 μm and a length of about 1 mm. Fibers are often present as flocs composed of a number of fibers in a three dimensional network with a size of the order of fiber length. Floc size depends on pulp consistency, the chemicals present in the suspension and the shear rate [18]; high shear rate leads to the break-up of flocs. Fines, the smallest component of the pulp, are normally less that 0.2 mm in size. The percentage of fines in newsprint is in the range of 30-40%.

The main contaminants of the deinking slurry are coatings and fillers (ash), such as latex, clay and calcium carbonate with particle sizes in the order of 1μm or less. The value of the fiber is four times that of the filler [3]. The other contaminants are: printing inks and adhesives which originate from bindings of books, labels, etc. An approximate percentage of ink on a newspaper is 1.5-2% [3].

A printing ink is generally made of pigments or dyes dispersed in a vehicle which serves as a carrier and binder with some other ingredients such as solvents, driers, wetting agents, waxes, etc. The vehicle helps transfer the pigment to the sheet and bind it. Vehicles are generally vegetable oils, mineral distillates, resins (natural and synthetic), polymers and volatile solvents [16]. A complete ink classification based on the chemical composition of the ink is not practical since the ink formulations in use are so numerous. The chemical nature of most commonly used inks is presented by Bassemir [19].

The strength of ink attachment to the fibers and, consequently, the difficulty of removal depends on physical properties such as: viscosity, tack (resistance to removal from the paper surface by pulling forces), uniformity of ink distribution on the sheet and drying [16]. In some cases ink particles may be released as large particles, called specks, that can be seen by the naked eye. The size of the specks can range from 40-400 μm. For the purpose of characterizing ink according to the probability of

producing specks, printed materials are classified by the type of printing surface and the state of the ink vehicle at the time of deinking [12], or the setting mechanism of the ink on the sheet [16]. Such characteristics determine the size of ink particles upon dispersion. McCool and Silveri [12] mentioned four categories of papers. Newsprint belongs to the first category. These are uncoated papers in which the ink vehicle does not dry but is adsorbed onto the fibers, when oil-based ink (80-90% mineral oil and 10-15% pigments) is used. In other cases of uncoated papers, ink is set onto the paper by evaporation when volatile solvents are used for the vehicle, or when water-based ink is used (65-80% water, 12-20% pigment and 5-15% binder). In these cases, it is relatively easy to disperse ink into small particles in the range of a few microns with no specks or large particles.

1.2.2. Deinking Techniques

The role of a deinking plant is to remove all non-cellulosic contaminants from fibers to produce a pulp with acceptable optical and mechanical properties. Since a considerable amount of the cellulosic material is lost during processing, the yield of a deinking operation may be lower than 60% [3]. Different deinking techniques are applied to achieve the desired separation such as screening, cleaning, flotation and washing; the choice of a certain technique depends mainly on the size of the ink particles. For coarse particles, screening and cleaning [20] are preferred while washing is used to remove small particles (less than 10 μm). For intermediate sizes, flotation cells are effective. Most of the ink fractions are removed by washing and flotation [17]

1.2.2.1. Washing

Washing is a mechanical process that rinses ink particles, ash and dirt particles from the recycled pulp [17,21,22]. Different types of washers are used, but in all of them the fibers are trapped on a mesh forming a cake, through which the ink particles pass with the filtrate. Horacek and Dewan [17] described several types of

washers and the advantages and disadvantages of each. This technique separates particles that are small enough to flow with the liquid stream through the formed fiber mat, i.e. the washer is similar to a filter except that it is desirable for the particles to flow through the fiber mat. Obviously, for larger ink particles mechanical entrapment of ink particles in the fiber matrix increases. On the other hand, as the ink particle size decreases, the probability of being entrapped on the fiber surface or within the individual fibers increases [6].

Washing removes up to 90% of the ash and a part of the fines along with the ink. Fiber loss depends on the size of the wire mesh covering the washer, and a substantial amount of fiber may be lost. Fiber loss as percentage of the fiber content of paper ranges from 24-42% for fine wire to 40-54% for coarse wire [3].

Washing is generally preferred for well dispersed ink (fine particles) or if substantial ash removal is desired from a filled or coated furnish, e.g., newsprint, ledgers, computer printouts, magazines, etc. Washing is ineffective for the removal of specks because they are caught in the fiber mat [12]. The major drawbacks of washing systems are that the yield is poorer and the water requirements are higher than flotation cells.

1.2.2.2. Flotation

Froth flotation is a chemimechanical process which selectively floats ink particles from a dilute deinking suspension through which air is bubbled. The surfaces of the ink particles and the bubbles are altered using chemicals to make the ink hydrophobic and to promote ink-bubble adhesion [23,24]. The process of flotation may be divided into three stages: collision between the ink particle and the air bubble, attachment of the particle to the bubble, and ascent of the particle-bubble complex to the surface. Each step is affected by particle size. Below a certain size, the rate of flotation decreases because the frequency of bubble-particle collisions decreases, and Brownian motion opposes the adhesion of particles to the bubble.

On the other hand, when the particle size exceeds a certain limit, the particle may not be captured by a bubble. As well, adhering large particles can reduce the buoyancy of the particle-bubble complex, thus reducing its rate of rise to the surface. Although flotation is considered to be a selective separation method, mill data indicate that fibers, fines and fillers are floated in addition to ink [25]. Turvey [25] stated that the loss from a floatation cell is between 5-12%. Furnishes containing both newsprint and magazines are usually deinked by flotation [16], however, experience indicates that deinking of 100% newsprint waste is difficult with flotation [6].

The efficiency of a flotation cell is controlled by the following factors: water hardness, pH, consistency, particle size, bubble size, the quantity of air, dwell time in the cell, temperature and the type and amount of chemicals added [23]. The consistency of the suspension in the cell is generally less than 1.2% in order to minimize fiber loss.

Because of the several different washing and flotation devices, each having different characteristics and operational parameters, generalized comparisons between the two processes are difficult to make. However, cost comparisons between washing and flotation processes appear to favor flotation. Ink and ash particles are removed together by washing, whereas flotation requires a separate washer for ash removal, thus flotation is preferred when ash retention is desired or for waste furnishes having chemically nondispersible inks (large specks that are visible to the naked eye) as encountered with foodboard or photocopier paper. Since a flotation cell removes ink selectively, it increases brightness [12]. The fibers that are lost in a flotation cell are long fibers, as these tend to float readily [25], whereas pulp lost from a washer is primary fines and debris [17]. In order to provide greater flexibility in handling various types of ink, some new deinking systems use both flotation and washing [7,9,10], particularly the modern newsprint system [9]. Usually the flotation cell is located before the washers [10].

1.3. Spouting

Spouting is the vertical injection of a fluid into a bed of particles through a centrally located orifice at the base of a conical, cylindrical or conical-cylindrical vessel. The resulting "spouted bed" consists of a centrally located dilute-phase, cocurrent-upward fluid/particle transport region, the spout, surrounded by a dense-phase downward moving packed bed annulus, with an upward percolation of fluid from the spout into the annulus. After rising to a certain height above the surface of the bed, the particles rain back as a fountain onto the annulus, resulting in a circulation between the two regions [26]. Figure 1.2 is a schematic representation of a conical spouted bed [27]. The vessel is a vertical, truncated cone with a smaller inside diameter d. Fluid enters through the nozzle, diameter D, located at the axis.

Spouting was developed as an alternative to fluidization for effective handling of coarse particulate solids which are difficult to fluidize. Since fine solids can also be spouted there is some overlap of the operating particle size for spouted beds and fluidized beds [26,28,29]. Spouted beds have been applied in several industrial areas for processes that involve heat and mass transfer, chemical reactions, as well as purely mechanical operations [26]. Most published studies involved gaseous spouting in conical-cylindrical columns. Less attention has been given to the conical spouted bed [27,30-35],despite of some attractive characteristics [27]. Conical spouted beds can handle solids that are difficult to treat, i.e. solids that are adherent and/or have a wide particle size distribution [30-33]. Liquid spouted beds have been the subject of only a few publications [36-40].

1.3.1. Mechanism of Spouting

A spouted bed operates over a limited range of fluid velocities, bracketed by a fixed bed at the lower end and by bubbling or slugging fluidized beds at the upper end [29]. The transition behavior of a bed of particles from a packed into a spouted bed is usually presented in a "phase diagram" of pressure drop against velocity, as

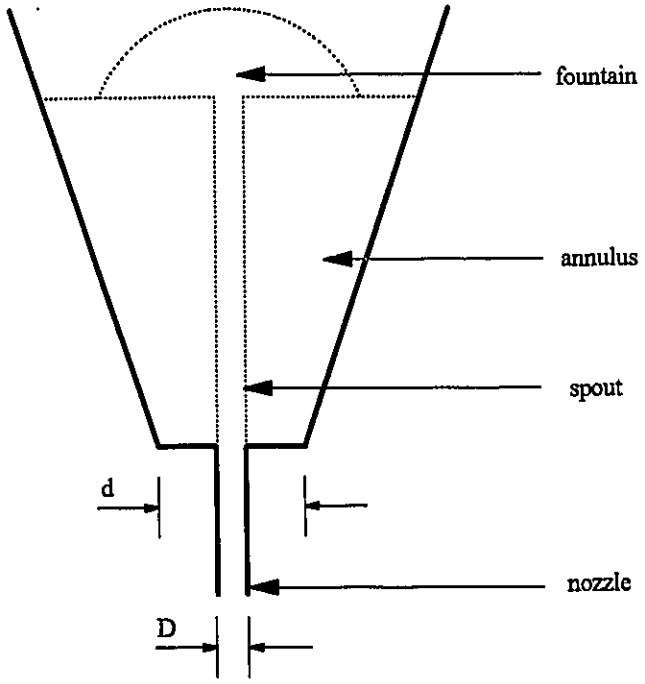

Figure 1.2: A schematic representation of a conical spouted bed

shown in Fig.1.3. At low velocities the fluid passes upward through a packed bed of particles which remain motionless. Increasing the fluid velocity increases the pressure drop, until a relatively empty cavity is formed at the fluid inlet. This cavity elongates with increasing velocity to form an internal spout. The pressure drop rises further with increasing velocity as the internal spout increases in height. When the height of the internal spout approaches the bed height, the pressure drop starts to decrease with increasing velocity, since the height of the packed section decreases. When the spout breaks through the bed surface, the pressure drop decreases sharply to a nearly constant value. For velocities above the spout breakthrough the bed is mobile and further increase in velocity causes the fountain to climb higher without significant additional pressure drop. If the gas flow is decreased slowly from the spouted condition, the bed remains spouted until at certain velocity, referred to as the minimum spouting velocity (U_{ms}), the spout collapses and the pressure drop rises suddenly. As the velocity is lowered further the pressure drop decreases slowly. The mechanism of formation of a spouted bed in a conical vessel is identical to that occurring in a cylindrical vessel [27].

1.3.1.1. Jet Spouted Bed

When particles are sticky and tend to agglomerate, they require flow fields with high velocities and enough shear to be fluidized or spouted. Such a regime is jet spouting [30-33, 41-45]. The jet spouted bed was first observed by Markowski and Kaminski [44] in a conical-cylindrical column when the fluid velocity was increased by a factor higher than 70% beyond the minimum spouting velocity. In jet spouting, the spout has a very high velocity and takes the shape of a cone that occupies a larger volume than in conventional spouting. The downward particle velocity and the solid circulation rate are an order of magnitude greater than in conventional spouted beds [43].

Jet spouting can also be obtained in a conical-cylindrical column by reducing the depth of the bed and increasing the fluid velocity [41]. The bed is a dilute fluid-solid

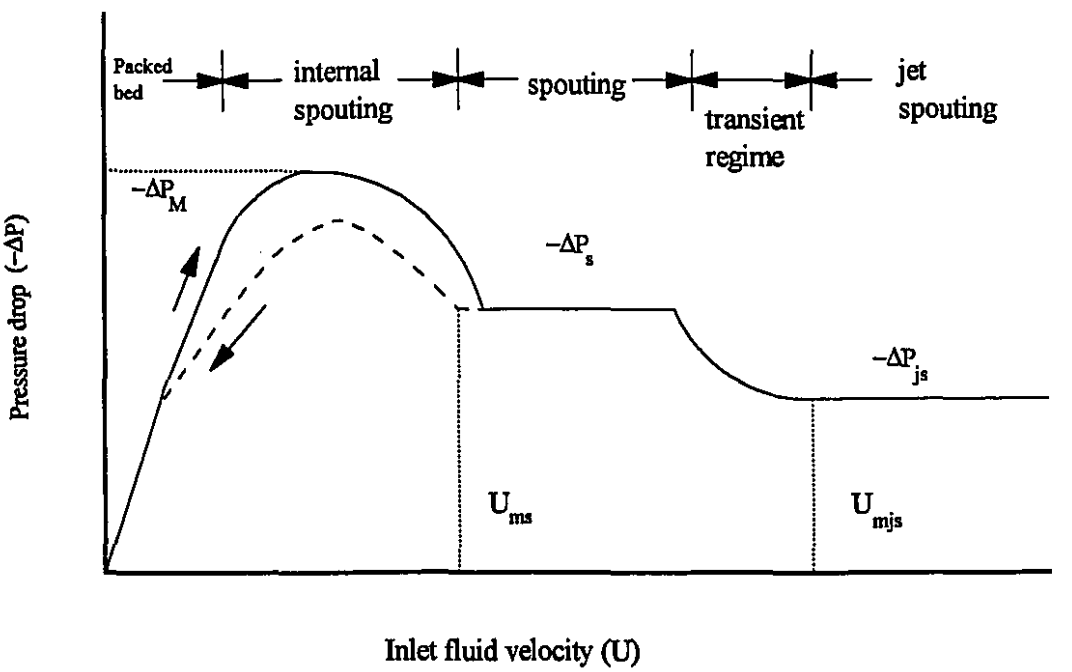

Figure 1.3: A schematic representation of pressure drop against inlet velocity for bed of solids. Solid curve: increasing flow; dashed curve: decreasing flow.

system with a global void fraction in the range of 0.85-0.99. There are conflicting findings related to the void fraction in the spout and annulus. Billo et al. [41] reported that the voidage is essentially the same in the spout and annulus while Uemaki and Tsuji [43] reported lower voidage in the spout than in the annulus. In conventional spouting the void fraction is larger in the spout than in the annulus.

Jet spouting in conical vessels has received some attention because it permits the handling of sticky particles [30-33]. The phase diagram was similar to Fig.1.3 with a maximum pressure drop followed by a constant value for stable spouting. At higher velocities the pressure drop decreases gradually until it reaches a new constant value ($-\Delta P_{js}$) for the jet spouting regime at velocities above U_{mjs}.

1.3.2. Characteristic Parameters

Spouting in a vessel of any shape is characterized by the following parameters: the minimum spouting velocity, the peak and the spouting pressure drop, limit(s) of spouting height, and stability. In the following sections, a brief review of these parameters for conical beds is presented. Most of the information comes from references 27 and 30-33.

1.3.2.1. Pressure Drop

Two pressure drops are important in characterizing the hydrodynamic behavior of a spouted bed: the maximum or peak pressure drop ($-\Delta P_M$) and the spouting pressure drop ($-\Delta P_s$) (see Fig.1.3). The occurrence of the peak pressure drop is attributed to the energy required by the fluid jet to penetrate the bed of solids during the expansion of the internal spout. This pressure drop is dependent on bed history.

The two pressure drops ($-\Delta P_M$ and $-\Delta P_s$) are usually expressed as a multiple of the weight of solid per unit cross-sectional area. For example, for the spouting

pressure drop:

$$\frac{-\Delta P_s}{(1-\epsilon)(\rho_p-\rho)gH} = K_s \qquad (1.1)$$

where ρ_p and ρ are the particle and fluid densities, respectively, ϵ is the voidage of the bed, g is the acceleration of gravity, H is the bed height, and K_s is the spouting pressure drop coefficient. Different expressions have been developed for the coefficient K_s [26, 31, 34]. It is a function of the vessel geometrical variables, the particle size, and the bed height. In these expressions, K_s increases with increasing bed height (H), and various correlations have been given. The mathematical analysis of Kmiec [44] showed that the coefficient K_s is linear with the bed height (H) at large bed heights and it is constant for the case of shallow beds. The maximum pressure drop is usually related to the spouting pressure drop. For conical beds, the ratio of $(-\Delta P_M/-\Delta P_s)$ normally falls between 1.5 and 2.0 [26, p.28, 31].

1.3.2.2. Minimum Spouting Velocity

The minimum spouting velocity is the inlet velocity at which the bed changes from the spouted state as the flow is decreased i.e. when the spout collapse (see Figs.1.2 and 1.3). This velocity depends upon solid and fluid properties as well as vessel geometry. Many theoretical and empirical relationships have been proposed for the minimum spouting velocity for both conical-cylindrical and conical vessels [26-29, 33-35]. However, the differences in these relations are very wide and no relation has been confirmed to be of general use. In most of the relations proposed for a conical spouted bed [see 27], the minimum spouting velocity varies as D^{-n}, with n between 1.8 and 2.2. Similarly, it increases with increasing initial static bed height or the mass of solids in the bed. Previous investigators [32, 34] observed an almost linear increase of minimum spouting velocity with bed height.

1.3.2.3. Limit(s) of Spoutable Height

The existence of an upper limit for spoutable bed height was first discovered by Mathur and Gishler [29] for a cylindrical bed. Mathur and Epstein [26] described three mechanisms through which spouting may become unstable at some height: fluidization of particles at the upper surface of the annular zone, choking of the spout, and growth of the surface instability (created at the base of the bed) causing the spout to break up before it reaches the surface of the bed.

For conical spouted beds, on the other hand, there is no maximum spoutable bed height [26,33,35],except for large particles [33] which exhibit a slugging instability. For large particles the maximum spoutable height increases with decreasing particle size, with decreasing ratio of the inlet diameter to the diameter of the vessel base (D/d), and with increasing cone angle. Olazar et al. [33] also reported a minimum spoutable height, below which the fluid velocity at the upper surface of the bed is higher than the minimum fluidization velocity, thus preventing the particles from falling back into the annulus. For the jet spouting regime they found neither a maximum nor a minimum height.

1.3.2.4. Stability

Instability of a spouted bed appears as bubbles or slugs in the spout [26] or as a rotational movement of the spout around the axis of the column [32]. Instability occurs in spouting and jet spouting, although jet spouting is more stable.

Spouting can be achieved only within certain ranges of solids properties. Whether a material with appropriate properties will produce stable spouting depends on the particle size the geometry of the column and the vessel inlet as well as the bed height.

Mathur and Epstein [26] reported that the cone angle should be less than 40°

and if the cone is too small, spouting becomes unstable because the entire bed tends to be lifted by the fluid jet. Olazar et al. [32] give a lower limit of 28° for the cone angle.

Povrenovic [27] studied the stability of spouting in a conical vessel by observing the appearance of bubbles and slugs in the spout through the flat wall of a half conical vessel. He concluded that the spouted bed in a conical vessel is stable if the inlet nozzle diameter (D) is less than 25 times the particle diameter (d_p). On the other hand, Olazar et al. [32] reported that when the ratio (D/d_p) was in the range of 2-60 a stable spouting was obtained.

The ratio of inlet diameter to vessel base diameter (D/d) (see Fig.1.2) as well as the design of the fluid inlet also play a role in stabilizing the spouting flow pattern. Olazar et al. [32] found that for D/d greater than about 0.8 the spout rotates. They also found that a pipe inlet gave more stable operation than other geometries they investigated.

Povrenovic [27] found that the height of the initial static bed did not affect the stability of the spout, however for relatively large heights in beds with large cone angles (e.g. H > 0.6m and cone angle of 60°) an annular ring of stationary particles was observed at the surface of the bed adjacent to the column wall. On the other hand, Olazar et al. [32] reported that the initial static height determines whether the bed can be spouted in a stable regime [see Fig.4 in ref. 32].

1.3.3. Liquid spouting

There are no major differences between liquid and gaseous spouting. For example, the theoretical model proposed by Grbavcic et al. [46] for predicting fluid flow patterns, minimum spouting velocity, maximum spoutable height and spouting pressure drop in a cylindrical column was verified with experimental data for both water and air spouted beds. One difference they reported was in the pressure drop

flow rate diagram, Fig.1.3. When the flow rate was decreased below U_{ms}, for a liquid spouted bed, the pressure drop decreased continuously, whereas in gaseous spouting a peak in the pressure was usually observed. They also found that liquid beds could be operated at heights greater than the maximum spoutable height to give a bed that consisted of a lower spouted bed of height equal to the maximum spoutable height and an upper fluidized bed.

Ogino et al. [38] measured fluid velocity profiles with a laser doppler anemometer in a water spouted bed of 2.6 mm glass beads. Their experiments were conducted in a cylindrical column with an inlet diameter of 0.6 cm, a column diameter of 49.2 cm and the height of the initial static bed height equal to the column diameter. Their spouted bed had a recirculating zone similar to that in the flow of a fluid through a sudden expansion. For a spouted bed the upward fluid velocity in the central region decreased more rapidly with height than in the same vessel at the same flowrate when no particles were present. Other investigators did not find circulating flows; the flow in the annulus was always considered to be upward with an increase in the upward fluid velocity with height as a result of fluid percolation from the spout into the annulus [47].

1.3.4. Particle Elutriation

Elutriation refers to the separation of small particles from a mixture of particles by means of an upward fluid flow. The separation is based mainly on the difference in the terminal settling velocity between the two particles, which may be due to differences in size and/or density. In an elutriation process, the fluid velocity is adjusted to be larger than the settling velocity of the small particles and smaller than the settling velocity of the large particles. In principle, this can be achieved in a number of geometries.

Elutriation was first used as a technique for grading particles in a series of vertical vessels, usually of conical-cylindrical shape and of successively increasing

diameters [48]. The fluid velocity decreased in each vessel so that the coarse particles were retained in the smallest vessel and finer particles in the subsequent larger vessels. In processes using fluidized or spouted beds for granulation, reaction, etc. elutriation of fines from the bed is undesirable, hence studies of elutriation have been carried out [49-55]. No publications were found concerning the use of elutriation from fluidized or spouted beds as a particle separation technique.

In fluidization, the fluid velocity must be above the minimum fluidization velocity and below the velocity at which solids are entrained by the exiting fluid. This upper limit is called the minimum elutriation velocity. For a binary mixture of particles, this velocity is usually approximated as the terminal settling velocity of the fine particles. Ganguly [51] reported that the minimum elutriation for a liquid fluidized bed is below the terminal settling of the fines. Gaseous conical-cylindrical spouted beds behave in a similar fashion [54]. The settling velocity of the fines was larger than the minimum elutriation velocity. This velocity is a function of the initial mass fraction of fines in the bed, but is little affected by the nozzle diameter and the cone angle. Elutriation from a conical cylindrical liquid spouted bed is similar to the gaseous case [40].

1.3.4.1. Elutriation Model

Elutriation from a fluidized bed has been described as a first order process [55]. As elutriation proceeds, the rate decreases as the concentration of fines in the bed decreases. Defining c as the concentration of fines in the bed and assuming that the bed is perfectly mixed the rate of change of concentration is given by:

$$\frac{dc}{dt} = -k_e\, c \qquad (1.2)$$

where t is the time and k_e is the elutriation constant. Initially the concentration is c_o, hence the initial condition for eqn.1.2 is

$$at\ t = 0,\ c = c_o \qquad (1.3)$$

The elutriation curve is determined by estimating the dimensionless concentration (C), nondimensionalized with respect to the initial concentration, by integrating eqn.1.2 with the initial condition in eqn.1.3. This leads to

$$C = e^{-k_e t} \qquad (1.4)$$

This model was first confirmed to fit results from fluidization in both gas and liquid phases [49-53,55]. It was then applied to gaseous spouting [54] and recently to liquid spouting [40] although the flow patterns in the bed are completely different. The value of the elutriation coefficient is nearly the same for both fluidized and spouted beds for relatively large bed heights. For small bed heights, however, spouted beds have a larger k_e-values than fluidized beds. The column and nozzle diameters as well as the total initial hold-up and initial fines concentration have little effect on k_e [40].

1.4. Objectives of the Thesis

The main objective of this work was to establish a hydrodynamic field in a certain vessel geometry that would allow the elutriation of small particles from pulp fibers by an upward liquid stream. After failure to fluidize pulp fibers due to their flocculation into a large mass, spouting was chosen since it would provide some mixing that would prevent large scale flocculation of fibers. Preliminary spouting experiments indicated that pulp spouting was possible and promising for separating small particles from fibers.

Hence, the major objectives of this thesis were as follows:

1) To spout pulp fibers in a certain geometry.

2) To elutriate small particles from a pulp suspension.
3) To demonstrate a continuous process of elutriation-spouting.

In order to achieve these objectives, some sub-objectives had to be achieved. The research went through the stages and the scheme illustrated in Fig.1.4.

1.5. Thesis Outline

Chapter 2 reports an experimental study of the hydrodynamics of a conical spouted bed of pulp fibers. Pulp spouting is compared with the conventional spouting of rigid spherical particles in the same vessel.

Chapter 3 deals with the characterization of liquid flow through the conical vessel used in Chapter 2. A model for predicting the minimum spouting velocity for pulp spouting is developed.

Chapter 4 deals with the separation of small particles from pulp fibers (particle elutriation) in the vessel characterized in Chapter 3.

Chapter 5 presents a mathematical model for the process of particle elutriation from a spouted bed of pulp suspension. The model is used to fit the experimental findings from Chapter 4.

Chapter 6 is an experimental demonstration of the extension of this principle to continuous operation.

The major conclusions and some recommendations for future research are summarized in Chapter 7.

Chapters 2-6 are written in the form of five papers which are suitable for submission to journals with minor changes. The thesis supervisors will be co-authors.

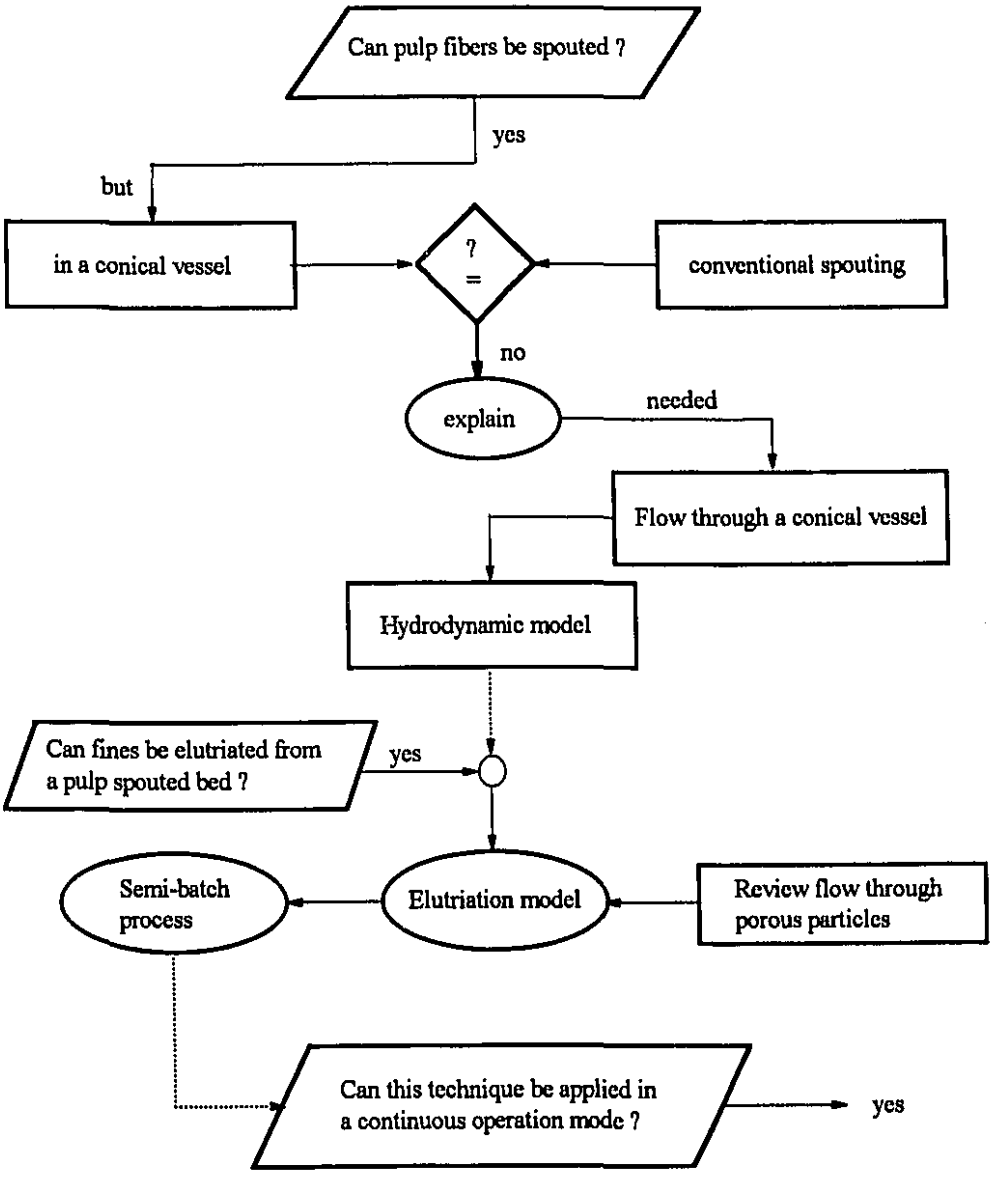

Figure 1.4: Stages of the Ph.D. Research.

Nomenclature

c	Concentration of fines (kg m^{-3}).
c_o	Initial concentration of fines (kg m^{-3}).
C	Dimensionless fines concentration.
D	Inlet diameter (m).
d	Diameter of vessel base (m).
d_p	Particle diameter (m).
H	Height of the bed (m).
g	Gravity acceleration (m s^{-2}).
k_e	Elutriation coefficient (s^{-1}).
K_s	Spouting pressure drop coefficient.
t	Time (s).
U_{ms}	Minimum spouting velocity (m s^{-1}).
U_{mjs}	Minimum jet spouting velocity (m s^{-1}).
$-\Delta P_M$	Maximum pressure drop (kg m^{-1} s^{-2}).
$-\Delta P_s$	Spouting pressure drop (kg m^{-1} s^{-2}).
ϵ	Void fraction in the bed.
ρ_p	Particle density (kg m^{-3}).
ρ	Fluid density (kg m^{-3}).

References

(1) J.H. Kleinau, "Secondary Fibers and Recycling", in *Pulp and Paper Manufacture, Vol. 3*, Secondary Fibers and Non-Wood Pulping, (M.J. Kocurek, Ed.), 127-131, The Joint Textbook Committee of the Paper Industry, TAPPI, Atlanta, U.S.A and CPPA Montreal, Canada (1987).

(2) J.H. Kleinau, "Processes and their equipments", in *Pulp and Paper Manufacture, Vol. 3*, Secondary Fibers and Non-Wood Pulping, (M.J. Kocurek, Ed.), 159-178, The Joint Textbook Committee of the Paper Industry, TAPPI, Atlanta, U.S.A and CPPA Montreal, Canada (1987).

(3) E.D. Clark, F. R. Hamilton and J. H. Kleinau, "Economics of secondary fiber", in *Pulp and Paper Manufacture, Vol. 3,* Secondary Fibers and Non-Wood Pulping, (M.J. Kocurek, Ed.), 151-158, The Joint Textbook Committee of the Paper Industry, TAPPI, Atlanta, U.S.A and CPPA Montreal, Canada (1987).

(4) D.G. Smith, "Secondary Fibers Sources", in *Pulp and Paper Manufacture, Vol.3,* Secondary Fibers and Non-Wood Pulping, (M.J. Kocurek, Ed.), 132-142, The Joint Textbook Committee of the Paper Industry, TAPPI, Atlanta, U.S.A and CPPA Montreal, Canada (1987).

(5) J.H. Kleinau, "Contaminants", in *Pulp and Paper Manufacture, in Pulp and Paper Manufacture, Vol. 3*, Secondary Fibers and Non-Wood Pulping, (M.J. Kocurek, Ed.), 136-142, The Joint Textbook Committee of the Paper Industry, TAPPI, Atlanta, U.S.A and CPPA Montreal, Canada (1987).

(6) J.M. Zabala and M.A. McCool, "Deinking at Papelera Peninsular and the philosophy of deinking system design", *Tappi, 71, 62* (1988).

(7) L. Pfalzer, "Deinking of secondary fibers, A comparison of washing and flotation", *Tappi, 63, 113-116* (1980).

(8) D.W. Duncan, " Wastepaper recycling. The production of fines and specialty papers", *Tappi, 62, 31-33* (1979).

(9) R.A. Koffinke, "Modern newsprint system combines flotation and washing deinking", *Tappi, 68, 61-63* (1985).

(10) D. R. Crow and R.F. Secor, "The ten steps of deinking", *Tappi, 70, 101-106*

(1987).

(11) L. Pfalzer, "Deinking of Xerographic and carbonless copy papers", *Tappi, 62, 27-30* (1979).

(12) M.A. McCool and L. Silveri, " Removal of specks and nondispersed ink from a deinking furnish", *Tappi, 70, 75-79* (1987).

(13) F.R. Hamilton, "Pulping Systems",, in *Pulp and Paper Manufacture, Vol. 3,* Secondary Fibers and Non-Wood Pulping, (M.J. Kocurek, Ed.), 170-188, The Joint Textbook Committee of the Paper Industry, TAPPI, Atlanta, U.S.A and CPPA Montreal, Canada(1987)

(14) L.L. Turai and C.H. Teng, "Ultrasonic deinking of waste paper", *Tappi, 61, 31-34* (1978).

(15) L.L. Turai and C.H. Teng, "Ultrasonic deinking of waste paper, A pilot plant study", *Tappi, 62, 45-47* (1979).

(16) A. Shrinath, J. T. Szewczak and I. J. Browen, "A review of ink-removal techniques in current deinking technology", *Tappi, 74, 85-93* (1991).

(17) R.G. Horacek and A. Dewan, "Getting the most out of washing", *Tappi, 65, 64-68* (1982).

(18) A. Swerin and L. Odberg, "Flocculation and floc strength in suspensions flocculated by retention aids", *Nord. Pulp Paper Res. J., 8, 141-147* (1993).

(19) R.W. Bassemir, "The chemical nature of modern printing inks and deinking", *Tappi, 62, 25-26* (1979).

(20) M.R. Doshi, J. H. Kleinau and F. R. Hamilton, "Cleaning and screening", in *Pulp and Paper Manufacture, Vol. 3,* Secondary Fibers and Non-Wood Pulping, (M.J. Kocurek, Ed.), 221-233, The Joint Textbook Committee of the Paper Industry, TAPPI, Atlanta, U.S.A and CPPA Montreal, Canada (1987).

(21) R.G. Horacek, "Washing ink from the pulp slurry", in *Pulp and Paper Manufacture, Vol. 3,* Secondary Fibers and Non-Wood Pulping, (M.J. Kocurek, Ed.), 179-188, The Joint Textbook Committee of the Paper Industry, TAPPI, Atlanta, U.S.A and CPPA Montreal, Canada (1987)

(22) R.G. Horacek, "Using less water in deinking, The increasing significance of high-consistency washing", *Tappi, 62, 39-42* (1979).

(23) W. K. Forester, "Deinking of UV-cured inks", *Tappi, 70, 127-130* (1987).

(24) H.E. Ortner, "Flotation deinking", in *Pulp and Paper Manufacture, Vol. 3,* Secondary Fibers and Non-Wood Pulping, (M.J. Kocurek Ed.), 206-220, The Joint Textbook Committee of the Paper Industry, TAPPI, Atlanta, U.S.A and CPPA Montreal, Canada (1987)

(25) R.W. Turvey, "Why do fibers float", *JPPS, 19, 52-57* (1993).

(26) K.B Mathur and N. Epstein, *"Spouted Beds"*, Academic Press, New york (1974).

(27) D. S. Pourenovic, Dz. E. Hadzismajlovic, Z. B. Grbavcic and D. V. Vukovic, "Minimum fluid flow rate, pressure drop and stability of a conical spouted bed", *Can. J. Chem. Eng., 70, 216-222* (1992).

(28) N. Epstein and J.R. Grace, "Spouting of particulate solids", In *"Handbook of Powder Science and Technology"*, (M.E. Fayed and L. Otten, Eds.) Van Nostrand Reinhold company, New York, USA (1984).

(29) K.B. Mathur and P.E. Gishler, "A technique for contacting gases with coarse solid particles", *AIChE J.,1, 157-164* (1955).

(30) M.J. San Jose, M. Olazar, A. T. Aguayo, J. M. Arandes and J. Bilbao, "Expansion of spouted beds in conical contactors", *Chem. Eng. J.,51, 45-52* (1993).

(31) M.Olazar, M. J. San Jose, A. T. Aguayo, J. M. Arandes and J. Bilboa, "Pressure drop in conical spouted beds", *Chem. Eng. J.,51,53-60* (1993).

(32) M. Olazar, M. J. San Jose, A. T. Aguayo, J. M. Arandes and J. Bilbao, "Stable operation conditions for gas-solid contact regimes in conical spouted beds", *Ind. Eng. Chem. Res., 31, 1784-11792* (1992).

(33) M. Olazar, M. J. San Jose, A. T. Aguago, J. M. Arandes and J. Bilbao, "Design factors of conical spouted beds and jet spouted beds", *Ind. Eng. Chem. Res., 32, 1245-1250* (1993).

(34) A. Kmiec, "The minimum spouting velocity in conical beds", *Can. J. Chem. Eng., 61, 274-280* (1983).

(35) Dz.E. Hadzimajlovic, Z. B. Grbavcic, D. V. Vukovic, D. S. Povrenovic and H. Littman, "A model for calculating the minimum fluid flowrate and pressure drop in a conical spouted bed", in *"Fluidization V"*, K. Osteraard and A. Sorensen, Eds., 241-248, Engineering Foundation, New York (1986).

(36) S.J. Kim and H. Littman, "Flow in the annulus of a bed of fine particles spouted with water", *Can. J. Chem. Eng., 65, 723-729* (1987).

(37) S.J. Kim and J. H. Ha, "Flow in the annulus of a water spouted bed of small glass particles at minimum spouting", *J. Chem. Eng. Japan, 19, 319-325* (1986).

(38) Ogino, Fumimaru, Kamata, Masahiro, Shimokawa and Keishi, "Measurement of velocity profiles of fluid in a liquid spouted bed by using a laser doppler velocimeter", *Kagaku Kogaku Ronbunshu, 18, 510-514* (1992).

(39) H. Littman, D. V. Vukovic, F. K. Zdanski and Z. B. Grbavcic, "Pressure drop and flow rate characteristics of a liquid phase spouted-fluid bed at the minimum spout-fluid flow rate", *Can. J. Chem. Eng., 52, 174-179* (1971).

(40) T.Ishikura and I. Tanaka, "Behaviour and removal of fine particles in liquid-solid spouted bed consisting of binary mixtures", *Can. Chem. Eng. J., 70, 880-886* (1992).

(41) J.Bilbao, M. Olazar, A. Romero and J. M. Arandes, "Design and operation of jet spouted bed reactor with continuous catalyst feed in the benzyl alcohol polymerization", *Ind. Eng. Chem. Res., 26, 1297-1304* (1987).

(42) M.H. Morgan, H. Littman and B. Sastri, " Jet penetration and pressure drops in water spouted beds of fine particles", *Can. J. Chem. Eng. 66, 735-738* (1988).

(43) O. Uemaki and T. Tsuji, "Particle velocity and solid circulation rate in a jet-spouted bed", *Can. J. Chem. Eng., 70, 925-929* (1992).

(44) A. Markowski and W. Kaminski, "Hydrodynamic characteristics of jet-spouted beds", *Can. J. Chem. Eng., 61, 377-381* (1983).

(45) A. Kmiec, "Expansion of solid-liquid spouted beds", *Chem. Eng. J., 10, 219-223* (1975).

(46) Z.B. Grbavcic, d. V. Vukovic and F. K. Zdanski, "Fluid flow pattern, minimum spouting velocity and pressure drop in spouted beds", *Can. J. Chem. Eng., 54, 33-42* (1976).

(47) G. Rovero, C. M. H. Brereton, N. Epstein, J. R. Grace, L. Casalegno and Piccinini, "Gas flow distribution in conical-base spouted beds", *Can. J. Chem. Eng., 61, 289-296* (1983).

(48) T. Allen, "Particle Size Measurement", 110-119 Chapman & Hall, London

(1968).

(49) I. Tanaka, H. Shinohara, H. Hirosue and Y. Tanaka, "Elutriation of fines from fluidized bed", *J. Chem. Eng. Japan, 5, 51-56* (1972).

(50) I. Tanaka and H. Shinohara, "Elutriation of fines from fluidized bed-Study of transport disengaging height", *J. Chem. Eng. Japan, 5, 57-61* (1972).

(51) U.P. Ganguly, "Elutriation of solids from liquid fluidized bed systems, Part I: Onset of elutriation", *Can. J. Chem. Eng., 60, 466-469* (1982).

(52) U.P. Ganguly, "Elutriation of solids from liquid fluidized bed systems, Part II: Prediction of equilibrium bed concentration", *Can. J. Chem. Eng., 60, 470-474* (1982).

(53) U.P. Ganguly, "Elutriation of solids from liquid fluidized bed systems, Part III: A study of the possible cases of non-linearity in the elutriation of fine particles from fluidized beds", *Can. J. Chem. Eng., 64, 171-174* (1982).

(54) T. Ishikura, H. Shinohara and I. Tanaka, " Behaviour of fine particles in a spouted bed consisting of fine and coarse particles", *Can. J. Chem. Eng., 61, 317-324* (1983).

(55) M. Leva, "Elutriation of fines from fluidized systems". *Chem. Eng. Progr.,47, 39-45* (1951).

Chapter Two

Spouting of Pulp Fibers in a Conical Vessel

Abstract

Pulp fibers can be spouted in water in a conical vessel. Liquid spouting of pulp fibers, as well as various rigid spherical particles, in a conical bed was investigated experimentally. Spouting mechanisms and stability were studied and compared. The minimum spouting velocity and the pressure drop were measured as functions of mass of solids in the bed and the diameter of the vessel inlet. Liquid spouting of rigid spherical particles is similar to gaseous spouting behavior.

A comparison of spouted beds of pulp fibers and rigid particles shows that the only similarity is in the direction of solid flow, which is upward in the central region (spout) and downward in the annular region. In all other respects, they are different, due to the different flow fields, relative densities and tendencies to form aggregates.

2.1. Introduction

Pulp fibers are hollow cellulosic particles of a roughly cylindrical shape. The density of the cylindrical wall is about 1.5 g/cm^3. They are present in suspension in water as flocs which contain a number of entangled fibers. It is impossible to fluidize pulp fibers in water in a cylindrical vessel, since they flocculate into a large mass which moves upward with the flow. On the other hand, the spouted bed technique provides mixing and a circulating motion of fibers which prevents the formation of a large mass of fibers.

In spouting, the vertical injection of the fluid entering into a particle suspension through a centrally located orifice at the base of the vessel produces two regions: a centrally located dilute-phase, cocurrent upward fluid/particle transport region, called the spout, surrounded by a dense-phase downward moving packed bed, or annulus, with countercurrent percolation of fluid from the spout into the annulus. After rising to a certain height above the surface of the bed, the particles rain back as a fountain onto the annulus, thus resulting in a circulation between the two regions [1-5] (see sec.1.3.). These flow phenomena can be achieved with either a gas or a liquid [6-11]. When the column is operated at relatively high velocity ($U > 1.7U_{ms}$), the bed expands, the solid content decreases, and the motion of solids between the central and the annular region has different characteristics. This process is called jet spouting [12-17] (sec.1.3.1.1.).

Both gas and liquid spouting technology has been investigated and applied in several industrial applications. Such applications involve heat and mass transfer and chemical reaction processing, as well as some mechanical applications like solid blending [1]. Although conical-cylindrical spouted beds are more popular in applications, conical spouted beds [16-22] have some advantages in handling light and sticky particles [16-19]. Studies concerning spouting in conical vessels have dealt with gas/solid spouting only.

Although investigating the feasibility of liquid spouting of pulp fibers in a conical vessel was the basic goal of this work, rigid particles were spouted for comparison, since no data were found in the literature dealing with liquid spouting in a conical column. In this chapter, the minimum spouting velocity (MSV) is reported as a function of mass of solids and column inlet size for pulp fibers and rigid particles. Also, the pressure drop across the vessel was measured for both types of particles. Differences in spouting behavior and stability are reported as well.

2.2. Experimental

Spouting experiments were carried out in the acrylic conical vessel shown in Fig.2.1. The lower cone had an angle of 31°, with 8.5 mm and 12.7 cm as its smallest and largest diameters (i.e. d=8.5 mm). The upper converging cone had a 60° angle and 8.5 mm outlet tube; the total height of the vessel was 33 cm. The inlet of the vessel consisted of a circular plate with a central orifice, placed between the column and the inlet tube of 6 mm diameter. The plate was changed to obtain the required inlet diameter (orifice with D in the range of 1-4 mm). When the plate was removed, a tube inlet geometry was obtained with D= 6 mm. The orifice and tube inlets are shown in the insets in Fig.2.1.

The experimental set-up is shown in Fig.2.2. Distilled water was pumped from a main reservoir to an overhead vessel using a centrifugal pump which kept the level in the overhead vessel constant by recycling the overflow back to the main reservoir. The constant pressure feed passed through a control valve and a flowmeter (Omega FL-1808). A three-way valve was used to switch the flow to the pulp suspension vessel to fill the column with fibers while they were suspended, in order to prevent fiber settling and the accumulation of fiber mass at the bottom of the vessel during the filling stage. When rigid particles were used, the upper cone was removed and the solids were placed directly in the lower cone and then covered. Two pressure taps were connected to the inlet and outlet tubes for measuring the pressure drop across the vessel. The types of solids used in this work are listed in Table 2-1.

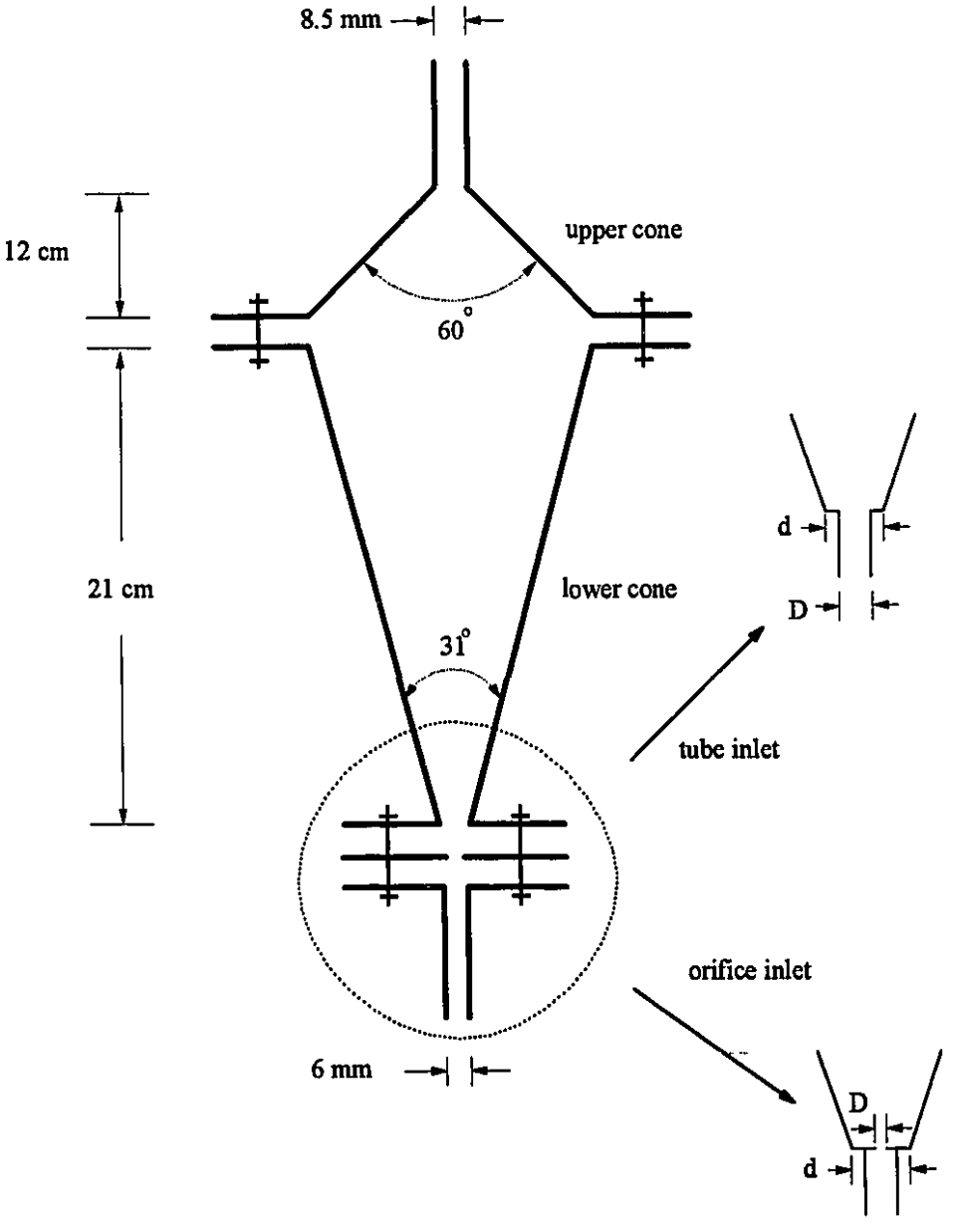

Figure 2.1: A schematic representation of the conical vessel used in the experiments

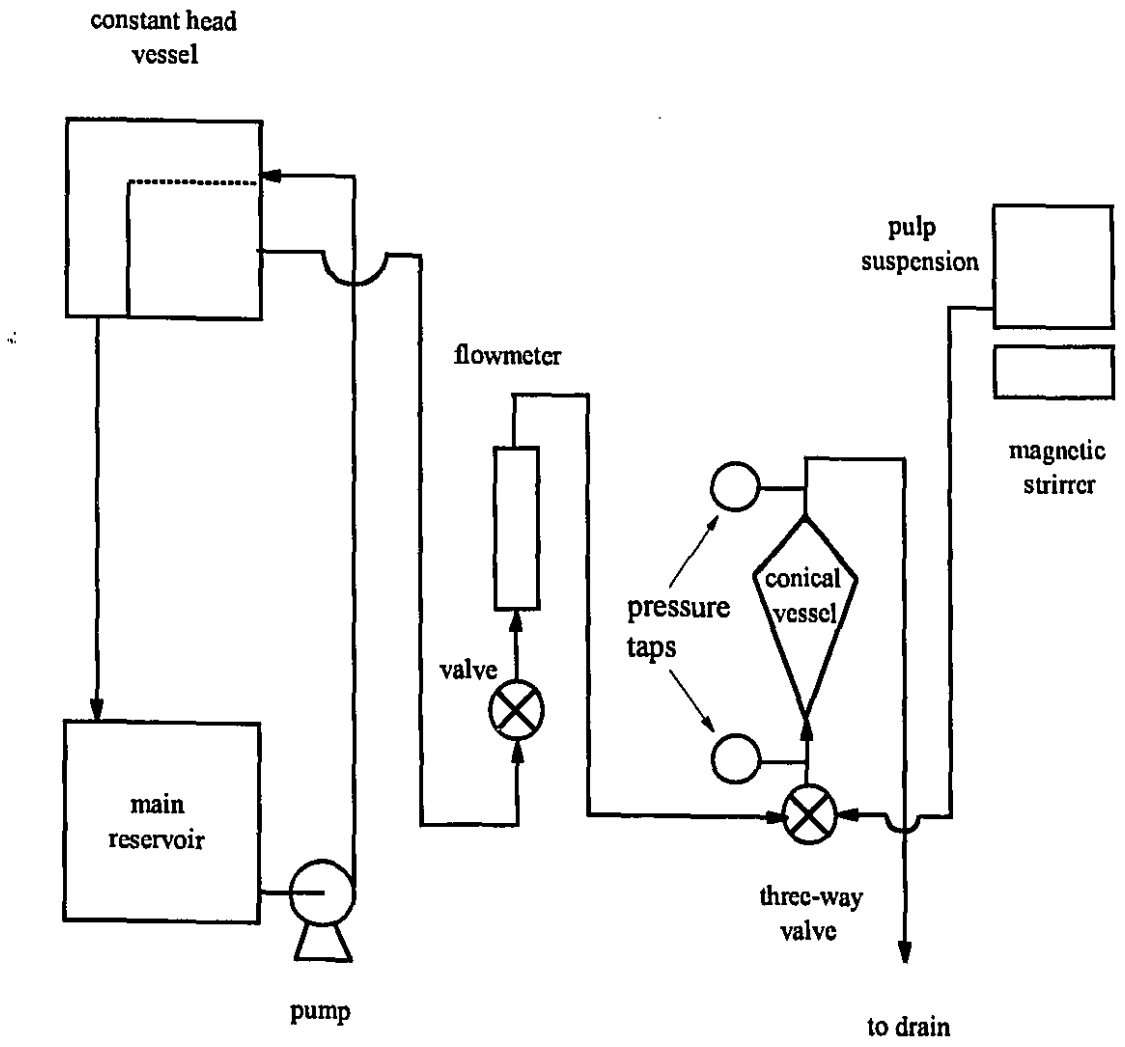

Figure 2.2: Experimental set-up

Table 2-1: Solid particles used in the experiments

Solids	Shape	Approximate Size	Specific Gravity
Pulp fibers: • Hardwood • Softwood	Long, flexible cylinders forming flocs	1 mm x 20 μm 4 mm x 40 μm	1.5
Zinc Particles	Spherical	0.6 mm	7.1
Iron Particles	Spherical	0.4-0.5 mm	7.9
Glass Particles	Spherical	0.6-0.9 mm	2.5
Glass Fibers	Cylindrical	1 mm x 10 μm	2.5
Nylon Fibers	Cylindrical	1.5 mm x 20 μm	1.1
Carbon Fibers	Cylindrical	0.5 mm x 10 μm	2.2

For every group of experiments with pulp, a stock suspension of fibers was prepared by disintegrating a few grams of pulp in a standard British disintegrator for 15 minutes after immersing the pulp in water for about 15 minutes. The required amount of pulp was placed in the suspension vessel which was kept under magnetic stirring (see Fig.2.2). After filling the column and all dead volumes with water, the flow was switched to the suspension line. The suspension flowed into the column by gravity, and the flow rate was adjusted so that fibers neither escaped with the outlet water nor settled at the bottom. Then the flow was switched back to the water line and the flow rate was adjusted to allow pulp spouting. Subsequently, the flow rate was decreased incrementally, waiting at least 5 minutes at each increment, to ensure that steady spouting occurred. At a certain critical flow rate, a growing mass of fibers was observed to form at the bottom of the bed within 1 or 2 minutes after the flow adjustment at that particular flow rate. This critical flow rate was divided by the

inlet area, to obtain the minimum spouting velocity.

2.3. Results and Discussion

2.3.1. Spouting Pulp Fibers

Figure 2.3 is a photograph of a spouted bed of pulp fibers. Similar to conventional spouting, pulp fibers were raised by the liquid up to a certain height, then they fell back onto an annular region. Due to the different nature of pulp fibers as well as the low solids concentration in the bed, the spout, the fountain and the annulus are not as well defined as in the case of conventional spouting. Pulp fibers tend to flocculate and the operating consistency in the pulp spouting experiments was in the range of 0.1-0.3%. At these consistencies fibers form non-coherent flocs whose size is of the order of fiber length [23]. The "particles" spouted were actually fiber flocs rather than single fibers. Single fibers do not have a settling velocity that is sufficiently high to sediment back into the annulus of the spouted bed. Thus, below a certain mass of pulp (which was about 0.4 g in the vessel shown in Fig. 2.1) pulp fibers could not be spouted because two little flocculation of fibers occurred.

Generally, the minimum spouting velocity is determined experimentally either by visual observation of the disappearance of the fountain or from the pressure drop flow rate diagram (see sec.1.3.1). For pulp spouting, however there was no significant pressure drop due to the presence of pulp in the column (as discussed below) and, at most of the investigated conditions, the top of the bed did not have a clear fountain in the middle of a flat top surface as in the case of conventional spouted beds. The criterion used for determining the MSV was the formation of a fiber plug at the bottom of the column which propagated and resulted in the termination of the circulating motion of fibers between the spout and the annulus. This difference in the criterion of minimum spouting is due to the different flow fields. In the case of pulp spouting (which occurs at relatively low Re), the flow field is an expanding jet with a surrounding circulating zone (as will be shown in Chapter

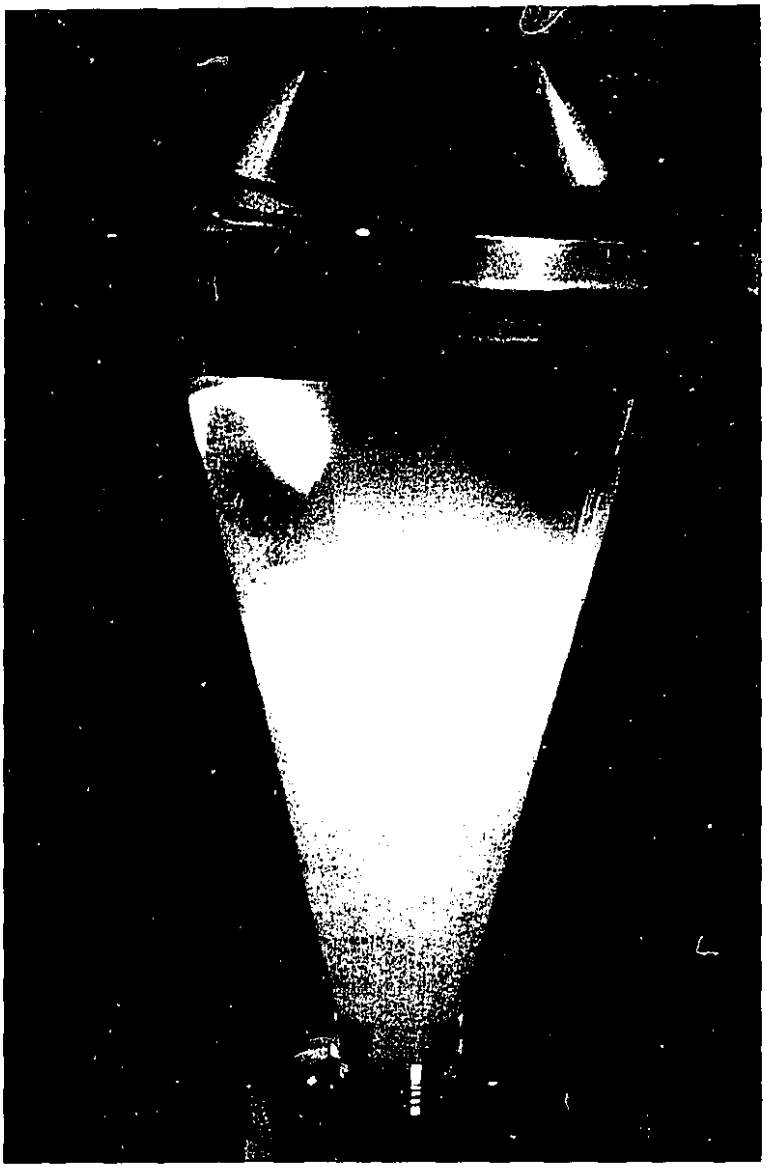

Figure 2.3: Photograph of a spouted bed of pulp fibers. Mass of fibers was 1.0 g, the inlet size was 1 mm and the flow rate was 32 mL/minute.

3); the fibers do not cause noticeable changes in this field since their density is close to that of the water and they do not form a packed bed in the annular region. In conventional spouting, the upward fluid flow in the spout causes fluid percolation from the spout into the annulus which creates an upward flow in the annulus itself [1,6,7]. The fluid velocity field in a conventional spouted bed is controlled by the presence of the particles, while in pulp spouting, the motion of solids is controlled by the flow field itself; the central flow region (expanding jet) determines the characteristics of the "spout" and the "fountain". The behavior of pulp spouting is more like to jet-spouting; since the bed is more dilute than a conventional spouted bed and since their is no distinct boundary between the spout and the annulus.

The instability of the expanding jet flow resulted in a continuous movement of the "fountain" at a relatively high speed. Hence, the upper surface of the bed looked like a dome, especially for large inlet diameters (where the jet was less stable). With 1 or 2 mm inlet orifices at flow rates just above the minimum spouting flow rate, the flow field was more stable, and a clear central fountain was observed. With a slight decrease in flow rate, the fountain pulsed in the center of the top flat surface of the bed. A further decrease resulted in internal spouting. With a further small decrease, a mass of settled fibers formed near the inlet of the vessel, terminating the spouting behavior. The change from internal spouting to a settled mass of fibers occurred over a very small range of velocity. Similar behavior was observed with larger inlet diameters for both orifice and tube inlets (see Fig.2.1). For large inlet diameters, no clear central fountain or internal spouting were observed. For these cases, the upper surface of the bed was like a dome due to jet instability.

For the purpose of comparison, attempts were made to spout nylon, carbon and glass fibers having sizes close to that of pulp fibers. None of these fibers behaved like pulp fibers. Some circulation of fibers between a central and an annular flow region was observed, but the bed was much more dilute than the pulp bed because these fibers behaved mainly as single fibers and thus rose to a higher height (since the settling velocity of a single fiber is less than that of a floc). Also, a large portion

of the fibers adhered to the wall of the lower cone. At a low flow rate, fibers settled near the inlet forming a small ring-like mass. When the flow rate was increased to break this mass and re-suspend the fibers, fibers escaped with the exiting liquid since the liquid velocity exceeded the fiber settling velocity at the upper surface of the bed. Kerekes et al. [23] found that a suspension of nylon fibers of low aspect ratio (i.e. length to diameter) tended to remain uniform, while at a similar consistency, pulp fibers formed non-coherent flocs, in agreement with the present observation. Consequently, for single fibers, the two criteria of having sufficient velocity at the bottom and a velocity less than fiber settling velocity at the top cannot be met simultaneously in the conical vessel used in this work.

2.3.2.Spouting of Rigid Particles

Experiments with rigid particles were performed to investigate liquid spouting in a conical vessel in order to make a clear comparison between spouting of pulp fibers and conventional spouting of rigid particles. Figure 2.4 shows photographs of a bed of zinc particles at different flow rates. The appearance of the bed is similar to that reported in the literature for gaseous spouting. At very low flow rates no solid motion occurred; the solid formed a packed bed. As the flow rate increased to a certain value, an internal spout formed while the surface remained flat (Fig. 2.4 a). With a further increase in the flow rate a fountain was formed above the surface of the bed (Fig. 2.4 b), and its height increased with increasing flow rate (Fig. 2.4 c).

These features were not observed in pulp spouting since a packed bed of pulp fibers could not be transformed into a spouted bed because settled fibers formed a network which could not be disrupted without using high flow rates which caused fiber elutriation from the vessel.

A conventional spouted bed is considered to be unstable either when bubbles and slugs appear in the spout [1,20] or when the spout rotates around the axis of the vessel [19] (see sec.1.3.2.4.). In this work, a spouted bed is considered unstable

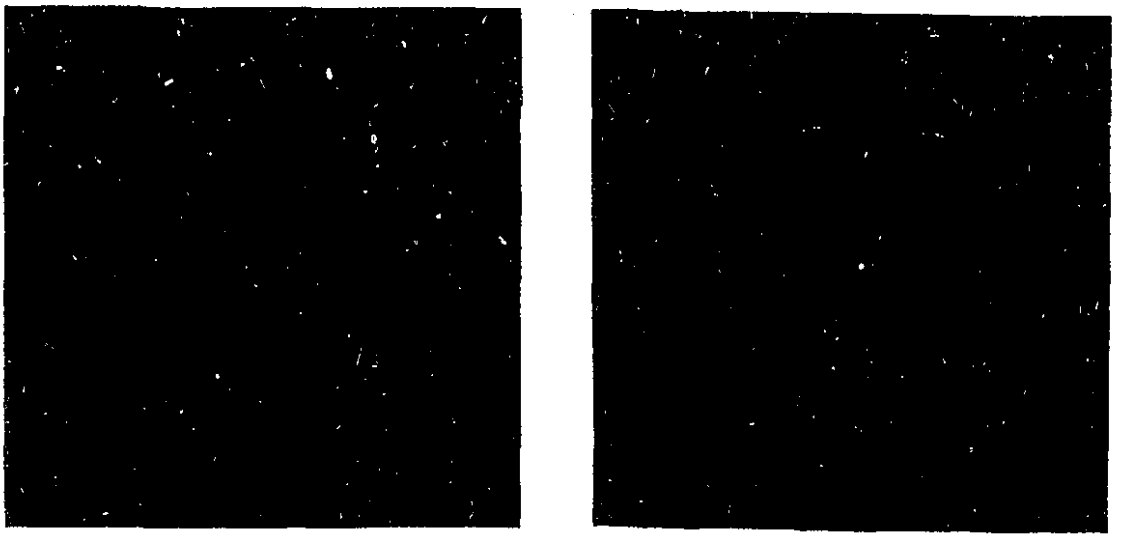

(a) (b)

(c)

Figure 2.4: Photographs of bed of zinc particles illustrating the transition from a packed bed into a spouted bed for the case of D = 2 mm and m = 150 g. (a) internal spouting with $U<U_{ms}$ (Q = 275 mL/min), (b) spouting with $U>U_{ms}$ (Q = 510 mL/min) and (c) spouting at high flow rate (Q = 590 mL/min).

when the spout rotates around the axis of the vessel or when the spout adheres to the vessel wall. The inlet size has a major effect on the stability of spouting of rigid particles. For the largest inlet, D=6 mm, which was the tube inlet, the spout adheres to the wall of the conical vessel, while for D=3 or 4 mm, with an orifice inlet, the fountain rotates around the axis of the vessel. The top view of the path of spout rotation forms a circle with a diameter which is proportional to the inlet size. Despite this instability, a flat surface still exist in spouting rigid particles. At small inlet size (D=1 or 2 mm), the spout is much more stable and it keeps its position centered at the axis of the vessel.

Two criteria are usually used to characterize the stability of a conventional spouted bed: the ratio of inlet diameter to vessel base diameter (D/d) and the ratio of inlet diameter to particle diameter (D/d_p) [9,19]. Olazar et al. [19] found that for gaseous spouting in a conical vessel, the spout rotates when D/d is larger than 0.8. The present results suggest that the upper limit is about 0.3. This difference in the upper limit of D/d may be due to the different inlet designs and/or due to different spouting fluids. Pourenovic et al. [9] found that for a conical vessel having a cone angle greater than 10°, a gaseous spouted bed was unstable if the ratio of inlet diameter to particle diameter (D/d_p) was greater than 25. In this work, the conventional spouted bed was unstable at large inlet diameters although the mentioned limit of D/d_p was not exceeded. Instability was observed for cases of $D/d_p \approx 3\text{-}6$. This difference in the range of the operating conditions for stable spouting might be due to the spouting occurring in a liquid rather than a gas or, more probably, due to the different criteria for considering instability in this work. Pourenovic et al. [9] considered the bed to be unstable if slugs or bubbles were observed, while in this work, no slugs or bubbles were observed for any conditions. Spout-rotational instability, observed in this work and in Olazar et al. [19], might not depend on the ratio D/d_p, but rather on the ratio D/d as concluded by Olazar et al.

2.3.3. Minimum Spouting Velocity

Two types of pulp fibers were spouted: hardwood and softwood fibers. The properties of the two fibers are given in Table 2-1. The measured MSV (U_{ms}) of the two fibers is plotted in Fig.2.5 as a function of the mass of pulp (m) for an orifice inlet diameter of 2 mm. Some duplicated points are shown indicating the reproducibility of these results. The points represented by triangles are for TMP fibers (i.e. thermomechanical hardwood pulp, which is used in newsprint applications), the rest are for bleached kraft pulp. These results indicate that the MSV increases linearly with the mass of pulp. This is attributed to the increase in the viscosity of the suspension with the concentration of fibers as explained in Chapter 3. The MSV for softwood fibers is larger than that for hardwood fibers since softwood fibers are larger (see Table 3-1) and thus form larger flocs containing more fibers. No difference between the TMP and kraft fibers is observed. Figure 2.6 shows the MSV for kraft hardwood fibers as a function of the mass of pulp for different inlet diameters. The linearity of U_{ms} against m is clear at all inlet diameters. The slopes decrease with increasing diameter (a model is presented in Chapter 3).

The MSV of rigid particles was measured in the same conical vessel as a function of both the inlet diameter and the mass of particles. Figure 2.7 shows the effect of the inlet diameter (D) on the MSV (U_{ms}) for zinc, iron and glass particles. The solid curves were obtained by fitting the measured MSV to the following relationship.

$$U_{ms} = \frac{K_{ms}}{D^n} \qquad (2.1)$$

where K_{ms} is a constant and n was fixed at 2, which provided a good fit. Most of the previous correlations for gaseous spouting in conical vessels had n between 1.8 and 2.2 [see ref. 21]. Thus liquid and gaseous spouting have the same dependence of MSV on the inlet diameter.

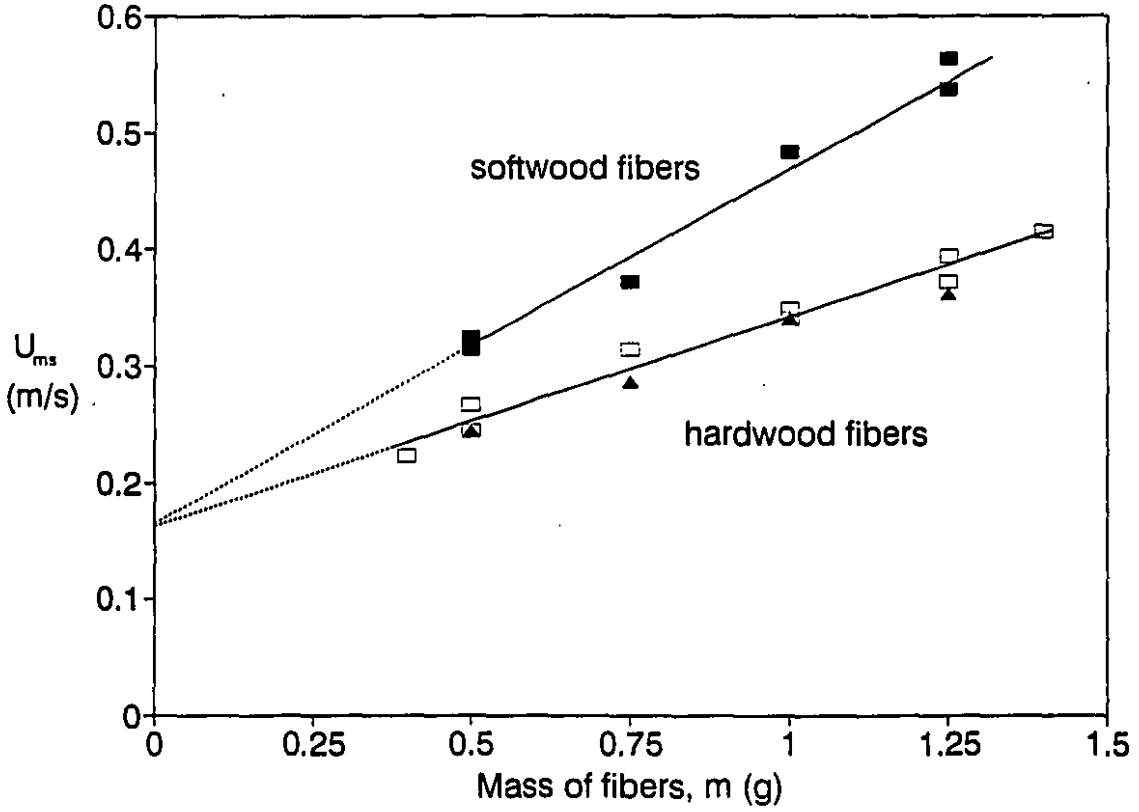

Figure 2.5: The MSV (U_{ms}) for softwood and hardwood fibers as a function of the mass of fibers (m); inlet diameter D = 2 mm. The empty squares are for kraft hardwood fibers, the triangles are for TMP fibers and the filled squares are for kraft softwood fibers.

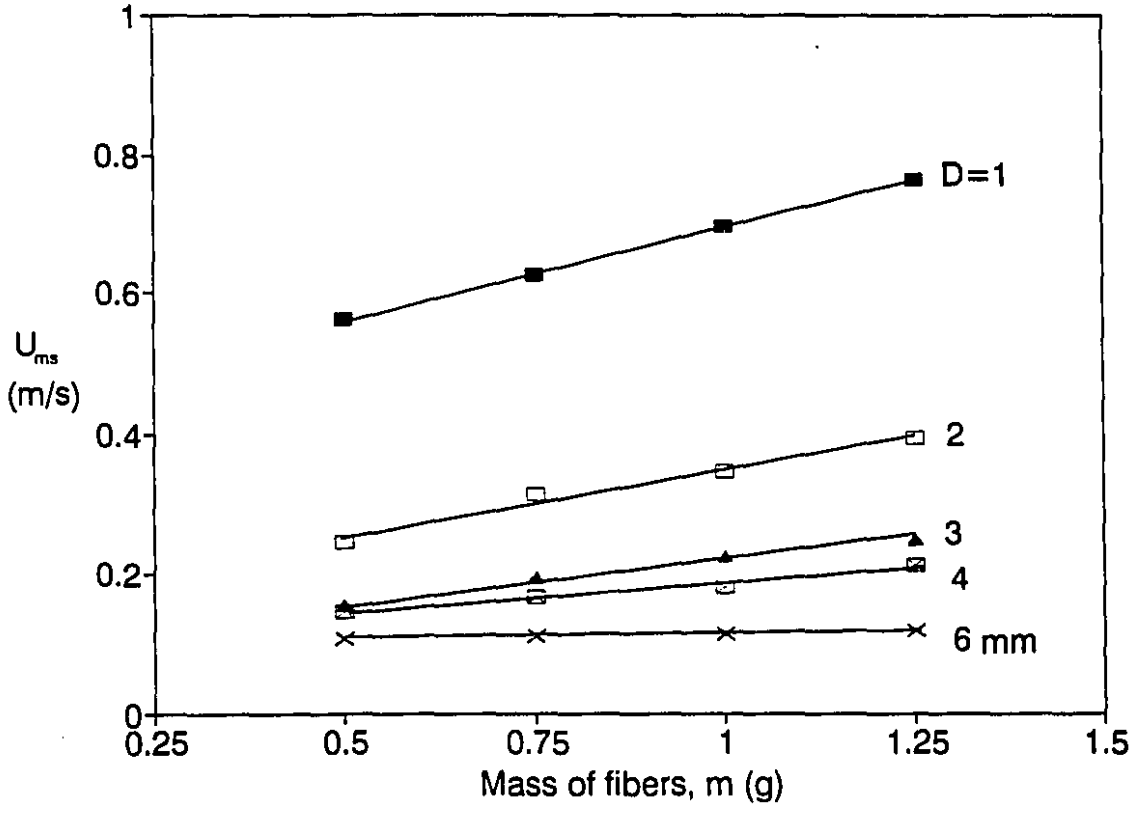

Figure 2.6: The MSV (U_{ms}) for hardwood fibers as a function of mass of fibers, for different inlet diameters (D = 1-4 mm with orifice inlet and D = 6 mm with tube inlet).

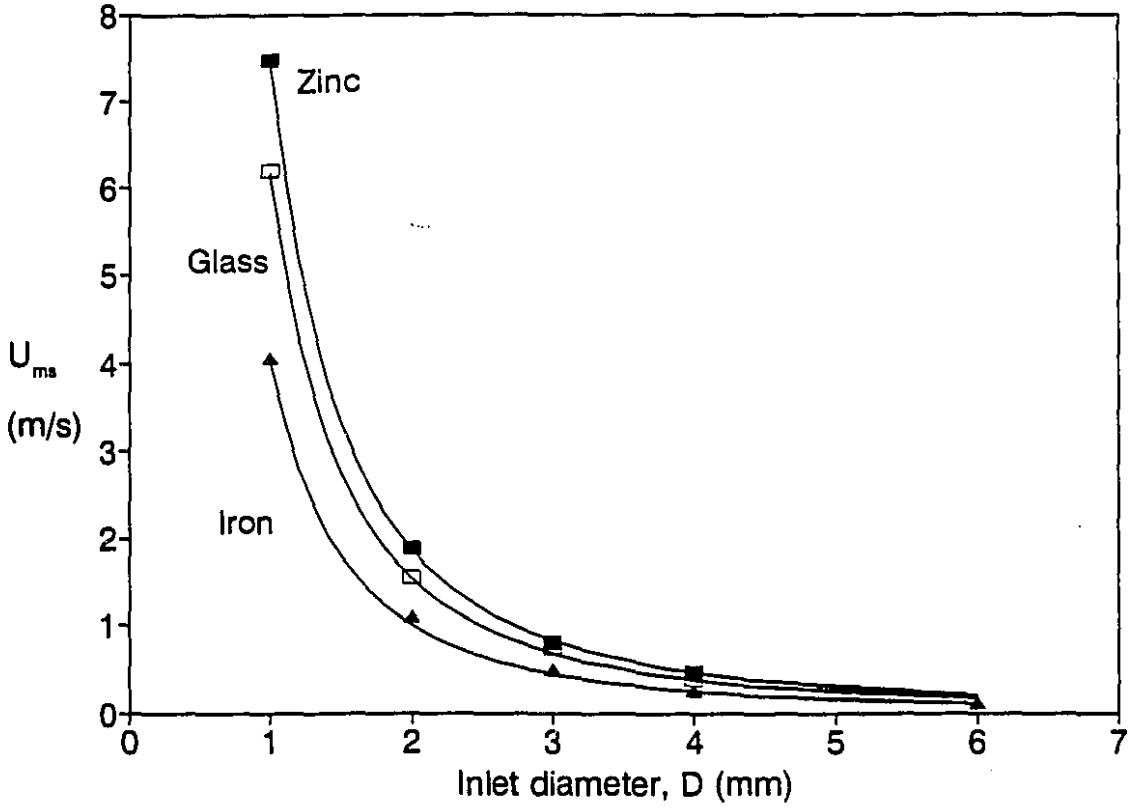

Figure 2.7: The MSV (U_{ms}) as function of inlet diameter (D). The filled squares are for zinc particles with m = 242 g, the empty squares are for glass particles with m = 55 g and the triangles are for iron particles with m = 55 g.

The difference in the dependence of the minimum spouting velocity on the inlet size (D) between conventional and pulp spouting emphasises that they have different flow fields. In both cases the flow is cocurrent upward in the central region, but the flow in the annular region is different. For conventional spouting there is countercurrent fluid flow through downward moving packed bed accomplished with fluid percolation from the spout into the annulus, while for pulp spouting the resulting circulating liquid flow causes cocurrent downward flow of pulp and water in most of the annular region.

Figure 2.8 shows the effect of the mass (figure a) and the height of the bed (figure b) of zinc, iron and glass particles on the minimum spouting velocities. Packed beds of different masses of particles had different heights while the concentration of particles (or void fraction) remained unchanged. Upon spouting, very little increase in the bed height compared to a packed bed height was observed experimentally. This resulted from the decrease in solid content in the central region (spout). This indicates that the void fraction in the annulus of a liquid spouted bed of rigid particles is almost the same as that for a packed bed and it is not a function of the mass of particles. Consequently, the increase in the minimum spouting velocity with the mass of particles resulted from the increase in the height of the bed (not particle concentration as in pulp spouting) and thus in the pressure drop across the column. Previous studies of conical spouted beds [13, 19] showed an almost linear increase of MSV with bed height similar to the plot of U_{ms} against bed height shown in Fig.2.8b.

2.3.4. Pressure Drop

The pressure drop behavior of a liquid spouted bed of zinc particles in a conical vessel is shown in Fig. 2.9. Liquid velocity (U) is taken at the inlet orifice. Curve A represents the measured points at various inlet velocities. These measured pressure drops have two components, one coming from the bed of the solids and the other coming from the effect of the inlet orifice. Following previous investigators,

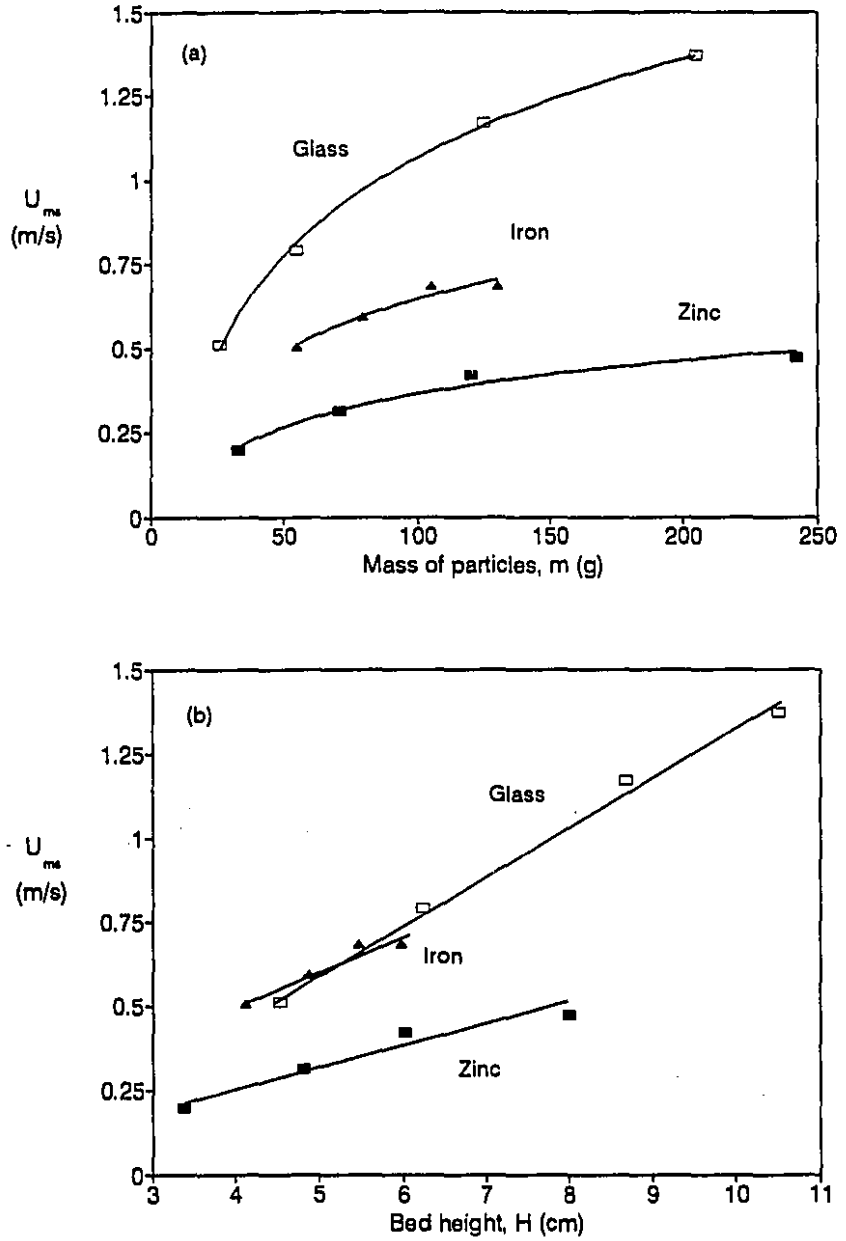

Figure 2.8: The MSV (U_{ms}) as function of mass of particles (a) and bed height (b). The filled squares are for zinc particles with D = 4 mm, the empty squares are for glass particles with D = 3 mm, and the triangles are for iron particles with D = 3 mm.

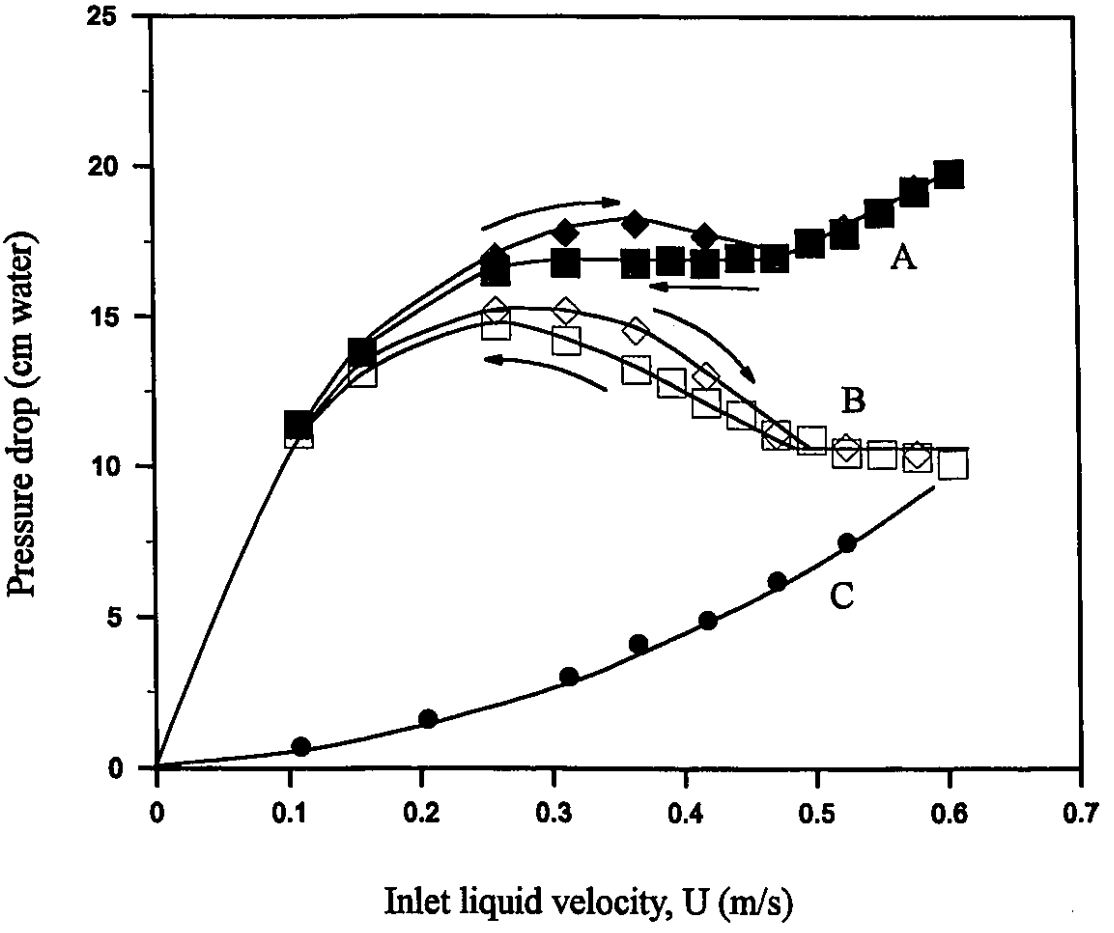

Figure 2.9: The pressure drop across the conical vessel as a function of inlet velocity (U) with an orifice inlet of 4 mm diameter and m = 120 g. Curve A shows the measured pressure drop in the presence of solids, curve C shows the measured pressure drop for a solid-free vessel, and curve B shows the corresponding phase diagram (i.e. curve A - curve c). In curves A and B, the diamonds represent the pressure drop obtained when the flow rate was increased while the sqaures represent the pressure drops obtained when the flow rate was decreased.

the effect of inlet orifice is taken into account by subtracting the pressure drop for fluid flow through the solid-free vessel (curve C) from the measured curve (A) to obtain the phase diagram (B). In curves A and B, the diamonds represent the pressure drop obtained when the flow rate was increased while the squares represent the pressure drops obtained when the flow rate was decreased. With increasing inlet liquid velocity, curve B passed through a maximum value associated with the energy required by the jet to rupture the structure of the bed. With further increase in the inlet velocity, the pressure drop decreased to a constant value for steady spouting, in the same way as gaseous beds behave. When the velocity was decreased, the pressure drop was below that for increasing flow, since the energy required by the liquid jet to penetrate the solids is no longer expended during the collapse of the spout [1]. This agrees with the results of Olazar et al. [18] for gaseous spouted beds in conical columns.

In Fig. 2.10 the phase diagrams for beds having different masses of zinc particles are presented. The maximum and spouting pressure drops increase with increasing mass of particles. Maximum and spouting pressure drops are usually related to the weight of the bed per unit area, (H (ρ_p - ρ) g). Several correlations have been proposed in the literature for estimating these two pressure drops [1,18,20,21]. For example, the spouting pressure drop ($-\Delta P_s$) is often correlated by

$$\frac{-\Delta P_s}{(1-\epsilon)\,(\rho_p-\rho)\,gH} = K_s \qquad (2.2)$$

where ρ_p and ρ are the particle and fluid densities, respectively, ϵ is the voidage of the bed, g is the acceleration of gravity, H is the bed height, and K_s is the spouting pressure drop coefficient. Table 2.2 shows the values of K_s as a function of mass (or bed height H); the measured value of ϵ was 0.46 ± 0.02. The spouting pressure drop coefficient (K_s) is essentially constant, in agreement with the conclusion of Kmiec [13] from his mathematical model for shallow beds although the value determined here is higher than the value from his analysis (K_s= 1.0). Table 2-2 shows also the

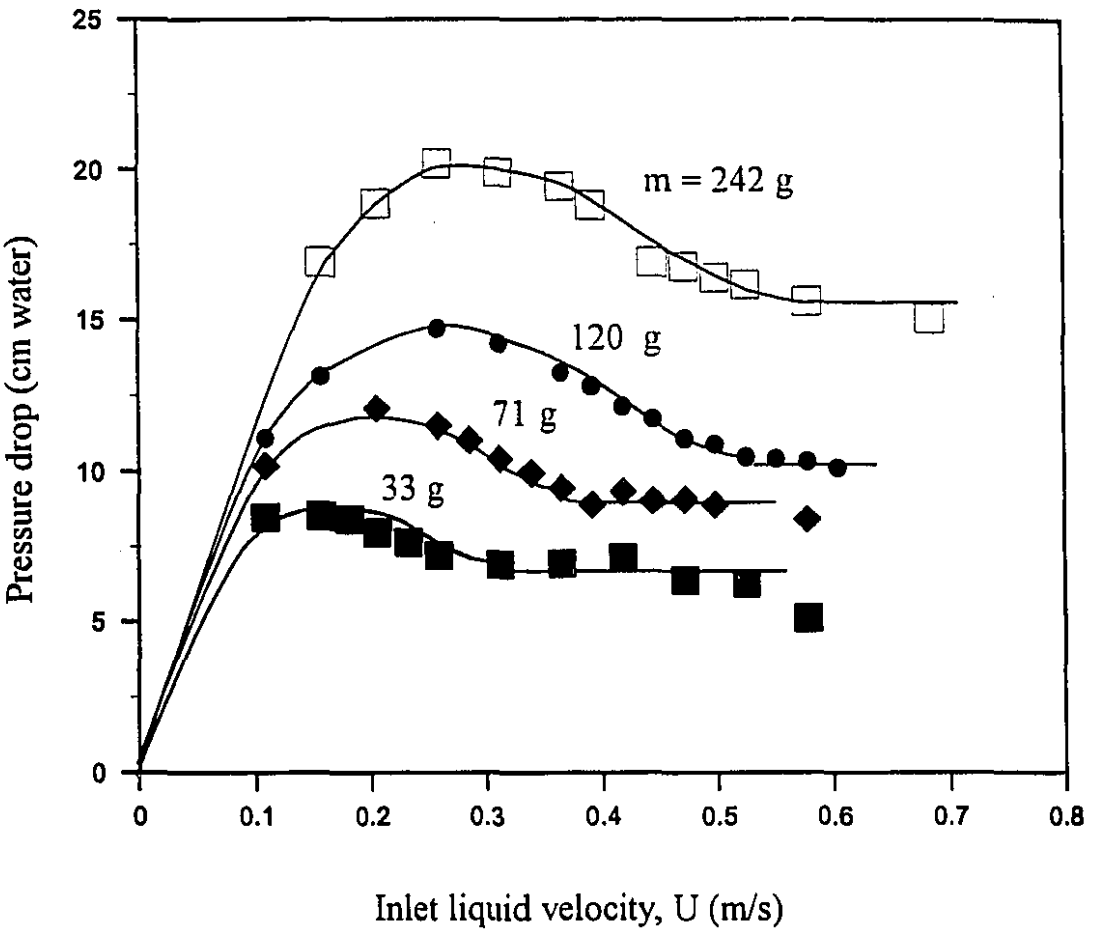

Figure 2.10: Phase diagrams for different masses of zinc particles with an orifice inlet of 4 mm diameter. The points are for experiments with decreasing flow rate.

ratio of the maximum to the spouting pressure drop ($-\Delta P_M/-\Delta P_s$) for increasing flowrate and for decreasing flowrate. The average value of ($-\Delta P_M/-\Delta P_s$) from our experiments agrees well with the results of Olazar et al. for gaseous spouting in a conical vessel [18]. In their two figures of phase diagrams (for different inlet diameters and bed heights); it was found that the average value of ($-\Delta P_M/-\Delta P_s$) was about 1.3. In general, these findings show that gaseous spouting in a conical vessel is similar to liquid spouting of rigid particles.

Table 2-2: Results of pressure drop

Mass (g)	H (cm)	K_s	$(-\Delta P_M/-\Delta P_s)_{dec.}$	$(-\Delta P_M/-\Delta P_s)_{inc.}$
33	3.3	6.1	1.32	1.36
71	4.6	6.0	1.31	1.43
120	5.8	5.7	1.42	1.45
240	7.7	6.2	1.34	1.36
average		6.0	1.34	1.40

Figure 2.11 shows the pressure drop against inlet liquid velocity for beds of pulp fibers. The solid curve is the fit of the measured pressure drop across a solid-free vessel (i.e. with no pulp, triangles) to a second order polynomial. In all pulp experiments, the mass of fibers was so small that its effect on the pressure drop was negligible and could not be detected experimentally; the points with pulp lay on the same curve obtained for the solid-free vessel. In contrast, for the case of spouting rigid particles, the mass of particles was at least 30 times larger and for most data 60-200 times larger than the mass of pulp. This fact, as well as the fibers being suspended (no packed annulus), explains the differences in the reported pressure drops in both cases.

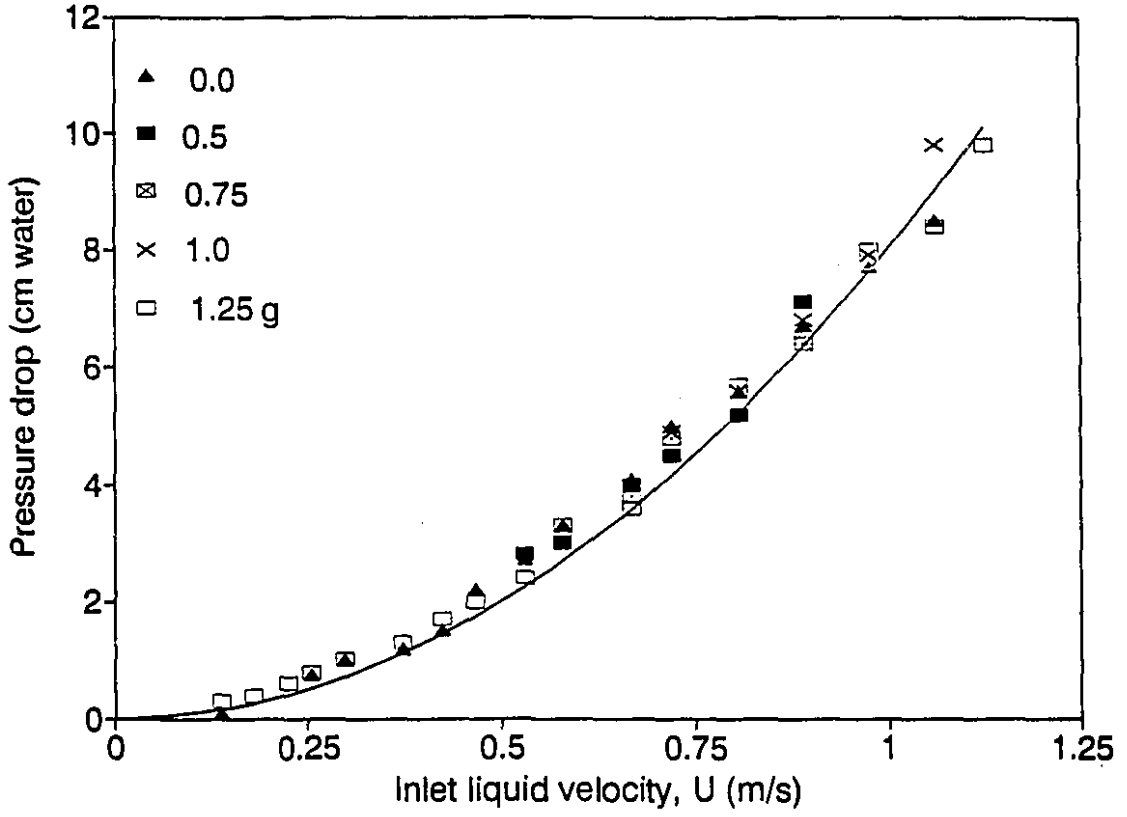

Figure 2.11: The drop across the vessel in the case of pulp spouting as function of inlet velocity U for different masses of pulp, shown in the figure. The inlet diameter, D=1 mm.

2.3.5. Comparison Between Conventional and Pulp Spouting

The main similarity between spouting of pulp fibers and that of rigid particles is the solid circulating motion between a central and an annular region ("spout" and "annulus"). Hence the same name is used for the system of pulp fibers although the hydrodynamics are different. However, since the bed is more diluted than conventional spouted beds and since there is no distinct boundary between the spout and the annulus, the term "jet-spouting" is a better representation of the observed hydrodynamics. While the experimental work was in progress, a few papers appeared dealing with gaseous jet-spouting in conical vessels and proposed this technique for handling sticky and light particles [16-19]. Their recommendation agrees with the choice of conical vessel in this work, since pulp fibers have a low density and they can be considered "sticky" because of fiber-fiber entanglements. Table 2-3 shows a comparison between the two cases studied in this chapter. It is obvious that liquid spouting of pulp fibers does not belong to the category of conventional spouting. The main difference can be summarized as follows: pulp spouting is controlled mainly by the jet flow characteristics, while in conventional spouting, the presence of the solids in the annulus as packed bed controls the flow field.

2.4. Conclusions

Liquid spouting of rigid particles in a conical vessel was found to be similar to gaseous spouting. Pulp fibers can be spouted in water in a conical vessel. Both softwood and hardwood fibers can be spouted, but with different minimum spouting velocities. Fibers that exist in a water suspension as single particles could not be spouted in the same way as flocculating fibers, showing that the formation of flocs is essential for fiber spouting.

Table 2-3: Comparison between liquid spouting of pulp fibers and rigid particles

Criteria	Spouting Rigid Particles	Spouting Pulp Fibers
Solids	single particles	flocs
Relative Density:		
$(\rho_p-\rho)/\rho$	> 1	< 1
Particle permeability	zero	high
Flocculation	nil	form flocs
Liquid flow field in the vessel	Upward; with liquid percolation from the spout into the annulus	Unstable jet-expansion; with separated zone and appreciable downward liquid flow
State of the annulus	Packed bed moving downward with countercurrent liquid flow	Dilute suspension cocurrent movement with circulating liquid
Pressure drop	Caused by liquid expansion and the presence of solids	Only from liquid expansion
MSV	decreases as D^{-2} non-linear with mass	decreases as D^{-1} linear with mass
Stability	Rotation of the spout around the axis of vessel.	Unstable jet expansion causes dome-shape top surface.
Occurs at	Large inlet diameters	Large inlet diameters and/or high flow rate for small diameters

Nomenclature

D	Inlet diameter (m).
d	Vessel base diameter (m)
d_p	Particle diameter (m).
g	Gravity acceleration constant (m s^{-2}).
H	Height of the bed (m).
K_{ms}	A fitting coefficient in the correlation defined in eqn.2.1 (m^3 s^{-1}).
K_s	Spouting pressure drop coefficient.
m	Mass of solids in the bed (kg).
n	Constant value
U	Inlet liquid velocity (m s^{-1}).
U_{ms}	Minimum spouting velocity (m s^{-1}).
$-\Delta P_M$	Maximum pressure drop (cm water).
$-\Delta P_s$	Spouting pressure drop (cm water).
ϵ	Void fraction in the bed.
ρ_p	Particle density (kg m^{-3}).
ρ	Fluid density (kg m^{-3}).

References:

(1) K.B Mathur and N. Epstein, *"Spouted Beds"*, Academic Press, New York (1974).

(2) N. Epstein and J.R. Grace, "Spouting of particulate solids", In *"Handbook of Powder Science and Technology"*, edited by M.E. Fayed and L. Otten, Van Nostrand Reinhold, New York (1984).

(3) K.B. Mathur and P.E. Gishler, "A technique for contacting gases with coarse solid particles", *AIChE J., 1, 157-164* (1955).

(4) Z.B. Grbavcic, D. V. Vukovic and F. K. Zdanski, "Fluid flow pattern, minimum spouting velocity and pressure drop in spouted beds", *Can. J. Chem. Eng., 54, 33-42* (1976).

(5) G. Rovero, C. M. H. Brereton, N. Epstein, J. R. Grace, L. Casalegno and N. Piccinini, "Gas flow distribution in conical-base spouted beds", *Can. J. Chem. Eng., 61, 289-296* (1983).

(6) S.J. Kim and H. Littman, "Flow in the annulus of a bed of fine particles spouted with water", *Can. J. Chem. Eng., 65, 723-729,* (1987).

(7) S.J. Kim and J. H. Ha, "Flow in the annulus of a water spouted bed of small glass particles at minimum spouting", *J. Chem. Eng. Japan, 19, 319-325,* (1986).

(8) Ogino, Fumimaru, Kamata, Masahiro, Shimokawa and Keishi, "Measurement of velocity profiles of fluid in a liquid spouted bed by using a laser doppler velocimeter", *Kagaku Kogaku Ronbunshu, 18, 510-514* (1992).

(9) H. Littman, D. V. Vukovic, F. K. Zdanski and Z. B. Grbavcic, "Pressure drop and flow rate characteristics of a liquid phase spouted-fluid bed at the minimum spout-fluid flow rate", *Can. J. Chem. Eng., 52, 174-179* (1971).

(10) T.Ishikura and I. Tanaka, "Behaviour and removal of fine particles in liquid-solid spouted bed consisting of binary mixtures", *Can. Chem. Eng. J., 70, 880-886,* (1992).

(11) M.H. Morgan, K. Littman and B. Sastri, "Jet Penetration and pressure drops in water spouted beds of fine particles", *Can. J. Chem. Eng. 66, 735-738,* (1988).

(12) A. Markowski and W. Kaminski, "Hydrodynamic characteristics of jet-spouted beds", *Can. J. Chem. Eng., 61, 377-381,* (1983).

(13) A. Kmiec, "Expansion of solid-liquid spouted beds", *Chem. Eng. J.,10, 219-223,* (1975).

(14) J.Bilbao, M. Olazar, A. Romero and J. M. Arandes, "Design and operation of jet spouted bed reactor with continuous catalyst feed in the benzyl alcohol polymerization", *Ind. Eng. Chem. Res., 26, 1297-1304* (1987).

(15) O. Uemaki and T. Tsuji, "Particle velocity and solid circulation rate in a jet-spouted bed", *Can. J. Chem. Eng., 70, 925-929,* (1992).

(16) M.J. San Jose, M. Olazar, A. T. Aguayo, J. M. Arandes and J. Bilbao, "Expansion of spouted beds in conical contactors", *Chem. Eng. J.,51, 45-52* (1993).

(17) M. Olazar, M. J. San Jose, A. T. Aguago, J. M. Arandes and J. Bilbao, "Design factors of conical spouted beds and jet spouted beds", *Ind. Eng. Chem. Res.,32, 1245-1250* (1993).

(18) M.Olazar, M. J. San Jose, A. T. Aguayo, J. M. Arandes and J. Bilboa, "Pressure drop in conical spouted beds", *Chem. Eng. J.,51,53-60* (1993).

(19) M. Olazar, M. J. San Jose, A. T. Aguayo, J. M. Arandes and J. Bilbao, "Stable operation conditions for gas-solid contact regimes in conical spouted beds", *Ind. Eng. Chem. Res., 31, 1784-11792* (1992).

(20) D. S. Pourenovic, Dz. E. Hadzismajlovic, Z. B. Grbavcic and D. V. Vukovic, "Minimum fluid flow rate, pressure drop and stability of a conical spouted bed", *Can. J. Chem. Eng., 70, 216-222* (1992).

(21) A. Kmiec, "The minimum spouting velocity in conical beds", *Can. J. Chem. Eng., 61, 274-280,* (1983).

(22) Dz.E. Hadzimajlovic, Z. B. Grbavcic, D. V. Vukovic, D. S. Povrenovic and H. Littman, "A model for calculating the minimum fluid flow rate and pressure drop in a conical spouted bed", in *"Fluidization V"*, K. Osteraard and A. Sorensen, Eds., 241-248, Engineering Foundation, New York (1986).

(23) R.J. Kerekes and C.J. Schell, "Characterization of fiber flocculation regimes by a crowding factor", *J.Pulp. Paper Sci., 18, p.32* (1992)

Chapter Three

A Model for the Minimum Spouting Velocity of Pulp Fibers in a Conical Vessel

Abstract

The flow patterns for jet flow through a conical vessel with Reynolds number (Re) in the range of 100-1000 were visualized and photographed by injecting a dye into the vessel. There are two types of flow pattern: (a) At low Re, a straight narrow jet passes from the vessel inlet to the outlet without mixing with the liquid bulk in the surrounding circulating zone, (b) At higher Re, an expanding jet with unsteady mixing and a back flow region surrounding the jet with an unstable and wavy boundary between the two regions. The transition from pattern (a) to pattern (b) occurs at a critical Reynolds number (Re_c) that depends on the shape of the vessel inlet. The approximate value of Re_c was 600 with an orifice inlet and 450 with a tube inlet.

Based on these experimental observations, a model for predicting the minimum spouting velocity for pulp spouting was developed. It shows a very good agreement with the experimental findings reported in Chapter 2.

3.1. Introduction

Flow through expanding conical vessels, sometimes called conical diffusors, has received great attention in airspace and aircraft engineering research, especially for high Reynolds numbers ($Re \approx 10^4$-10^5). In such diverging vessels, the kinetic energy is converted into pressure energy [1-6]. Due to the divergence of the vessel, there is a decrease in the axial velocity. The consequent increase in the pressure is superimposed on the frictional pressure in such a manner that the direction of flow will reverse itself when the resultant pressure gradient becomes negative [7]. Some effort has been devoted to predict the conditions at which the flow will separate in order to avoid operation at such conditions in practical designs [6].

In addition to the single phase applications, conical vessels are used as solid contactors in both fluidization and spouting [8-11]. Although the presence of the solid changes the flow patterns of the fluid, it is useful to analyze the flow patterns of the solid free vessel. This analysis helps in understanding the general behavior of fluid flow in the case of solid handling. Ogino et. al. [12] found that the liquid flow patterns in both spouted and solid-free columns of cylindrical geometry were qualitatively comparable. However, a conical spouted bed was found to be the best geometry for spouting adhesive and light particles [11], due to the large reduction in the axial fluid velocity with height.

Modeling the flow through vessels of varying cross sectional area was investigated by several authors since the beginning of this century. In this field, two types of geometries were considered: two and three dimensional channels, i.e. wedge-like vessels (2D) and conical vessels (3D). The steady flow 2D problem has an analytical solution [7,13], which can be found in textbooks. The 3D problem is more complicated since the model describing such flow consists of a system of partial differential equations. However, the limiting case of one dimensional creeping flow does have an analytical solution since the problem can be simplified into a boundary value problem similar to the 2D case. This problem was solved by Gibson [14] (in

1909), Harrison [15] (in 1919) and by Bond [16] (in 1925). The velocity in the 3D diverging channel decreases with the square of the distance from the tip of the cone similar to the general behavior of free 3D jets. On the other hand, in the case of a 2D channel the velocity decreases with the inverse of distance from inlet [7]. This is an important effect, since in some applications (such as handling light materials in a spouted bed) a large reduction in velocity is required within a short distance from the inlet of the vessel, as e.g. in the case of spouting pulp fibers. Obviously, the 3D jet flow in a diverging channel should be chosen for such an application.

The field of the streamlines in a conical vessel with a geometry that is the same as the one used in this study, was obtained numerically by Kuhn [17], who solved the governing equations of momentum and mass balance together with the required boundary conditions for the case of a two dimensional (axisymmetric) flow field.

In Chapter 2, it was demonstrated experimentally that pulp fibers can be spouted in water in a conical vessel. The hydrodynamics of pulp spouting has been found to be different from that of a conventional spouted bed. In this chapter, the flow patterns for water flow through the column used in pulp spouting are determined. A model for predicting the minimum spouting velocity (MSV) is developed based on the experimentally observed flow patterns.

3.2. Experimental Apparatus and Procedure

The conical column described in Chapter 2 was used (Fig.2.1). The experimental set-up is shown in Fig.3.1. Two main vessels were used for water and dye solution (Methylene Blue), the exit from each was connected to a three-way valve used to switch the flow from water to dye. The liquid levels in the two vessels were higher than the level of exit from the conical vessel; the liquid flowed by gravity. After filling the column and the tubing system with clean water, the flow rate was fixed. When steady state was achieved, the flow was switched to the dye solution and the vessel was photographed. The flow transition condition was detected by changing

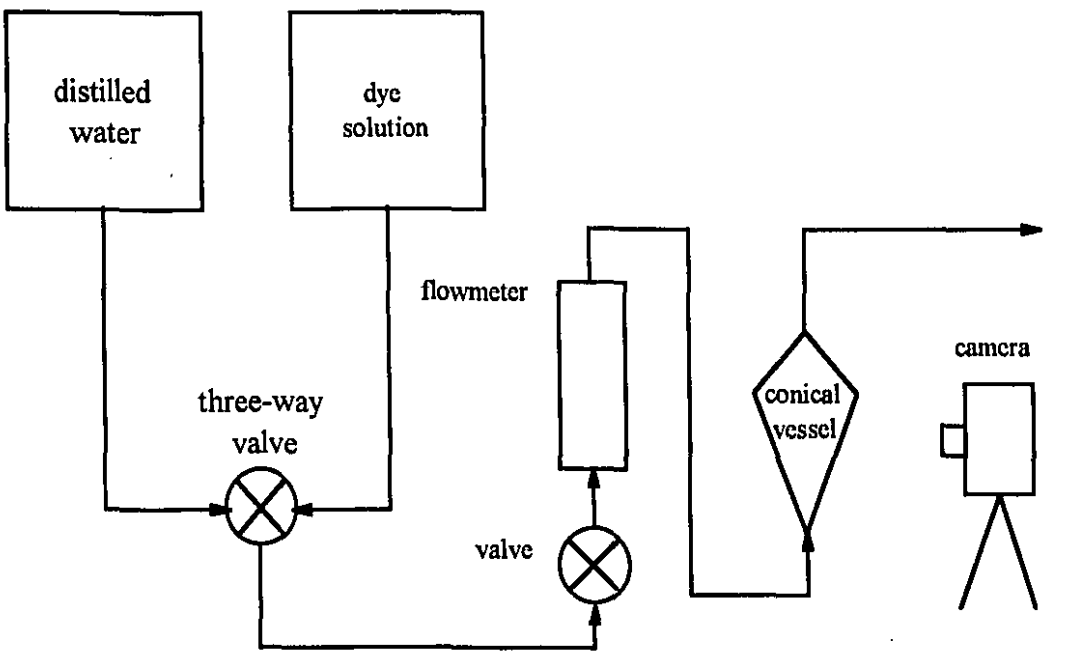

Figure 3.1: Experimental set-up

the inlet flow rate.

3.3. Results and Discussion

3.3.1. Flow Patterns in a Conical Vessel

The flow visualization experiments show that the flow field is of one of two main types; (a) a straight narrow jet separated from the rest of the liquid in the vessel with a smooth and steady boundary, and (b) an expanding jet with an unsteady wavy boundary. The first type is shown in Fig.3.2 for an inlet size D= mm and a flow rate Q = 28 mL/min, which is equivalent to a low inlet Reynolds number of 300. The straight jet passed through the vessel without mixing. The upward jet flow created a circulating flow of closed stream lines in the region surrounding the central jet and filling the rest of the column volume. The width of the jet increased very little with the axial position from the inlet of the column. The jet was very sensitive to vibrations which made it discontinuous or wavy. Also, any displacement of the inlet orifice plate produced an asymmetric jet.

Figure 3.3 shows the theoretical streamlines from the numerical solution of Kuhn [17] for Re=300. Two types of streamlines were obtained: open streamlines going from the inlet to the outlet of the vessel and closed streamlines in the circulating zone. The flow pattern shown in Fig.3.2 is similar.

Above a critical flow rate, the jet became discontinuous and expanded into an unsteady conical shape after a certain length of straight jet as shown in Fig.3.4. The central upward flow region was surrounded by a circulating flow region. The jet region occupied a larger volume and the length of the initial straight part of the jet decreased as the flow rate increased. Figures 3.4 and 3.5 compare the flow rates Q = 60 and 90 mL/min. respectively. At higher flow rates, the upward flow filled the vessel and there was no backflow region.

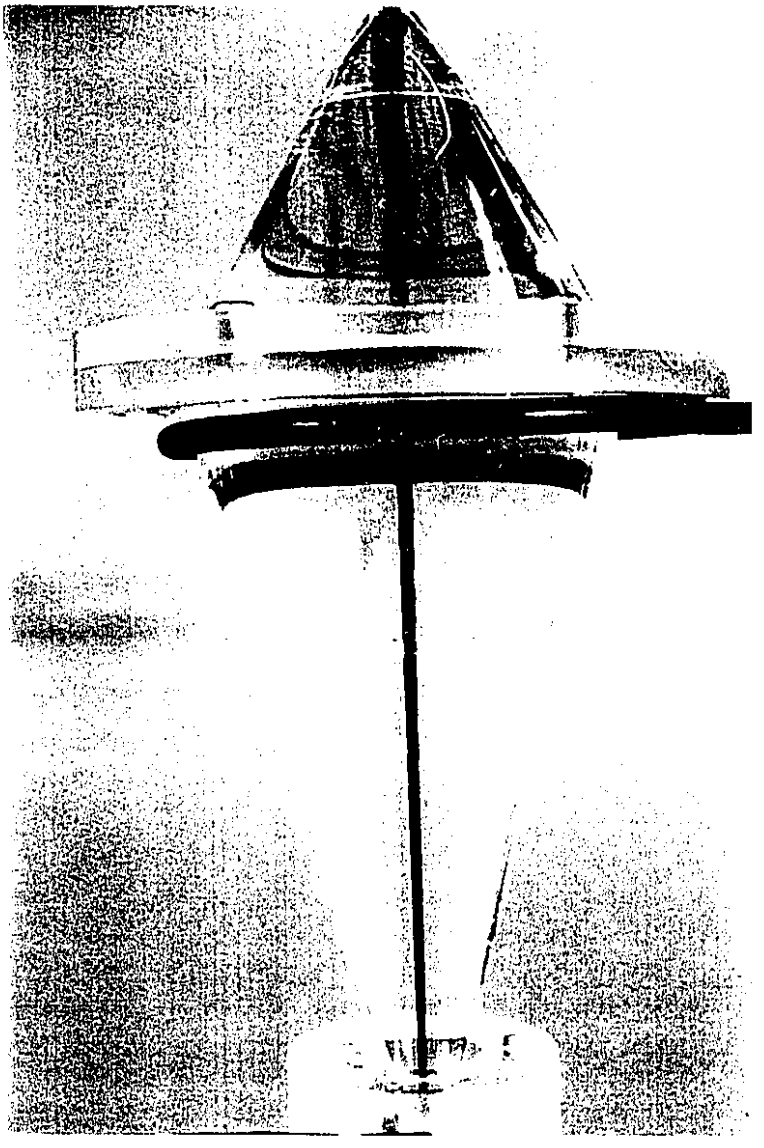

Figure 3.2: A steady jet pattern for the conical vessel with an orifice inlet. For the case of D = 2 mm and Q = 28 mL/min (inlet Re = 300).

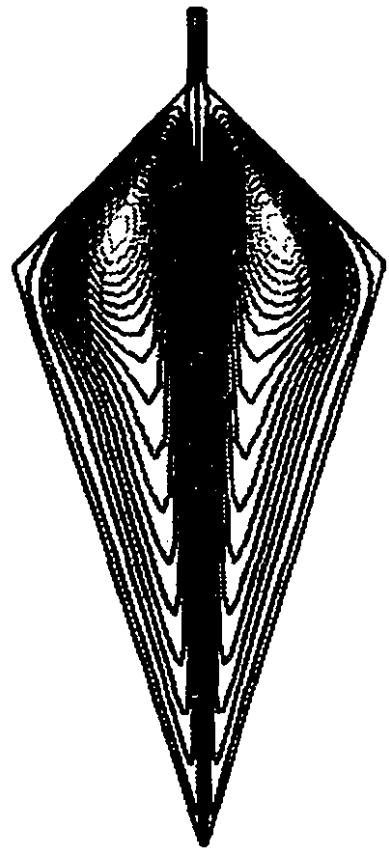

Figure 3.3: The theoretical field of the streamlines obtained from the numerical code [17] for conical vessel at inlet Re = 300. [Courtesy of Dr. D.C.S. Kuhn]

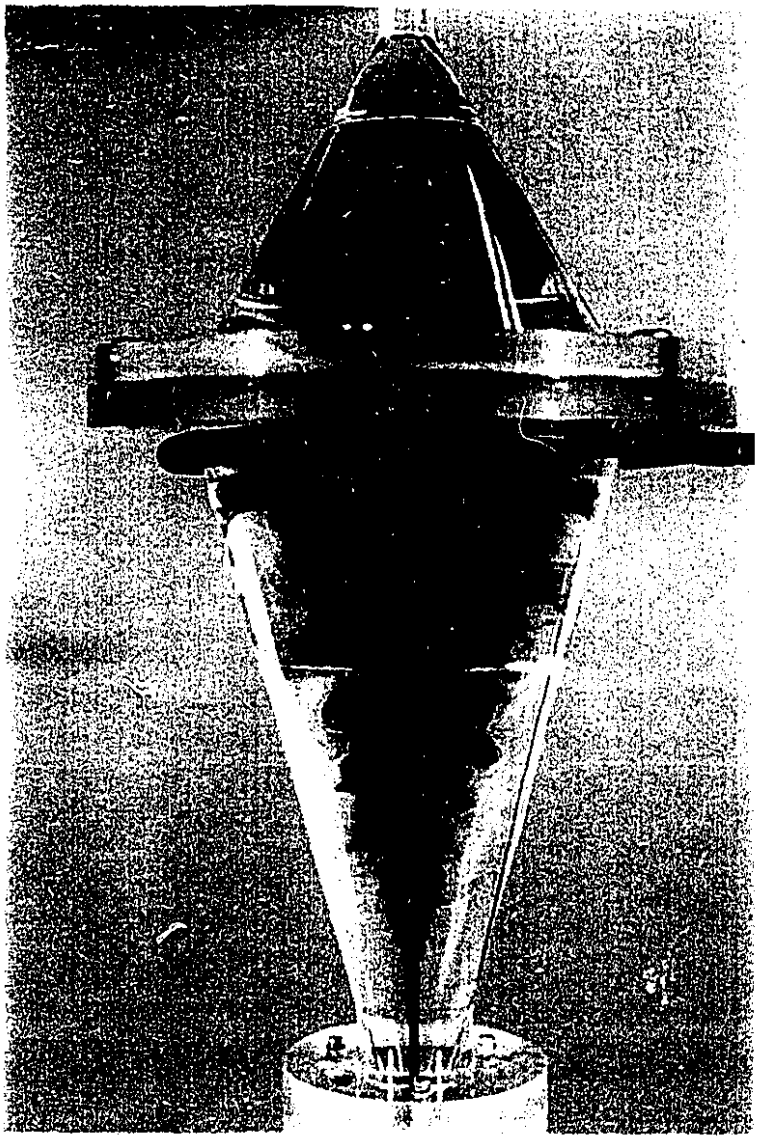

Figure 3.4: An expanding jet pattern for the conical vessel with orifice inlet. For the case of D = 2 mm and Q = 60 mL/min (inlet Re = 650).

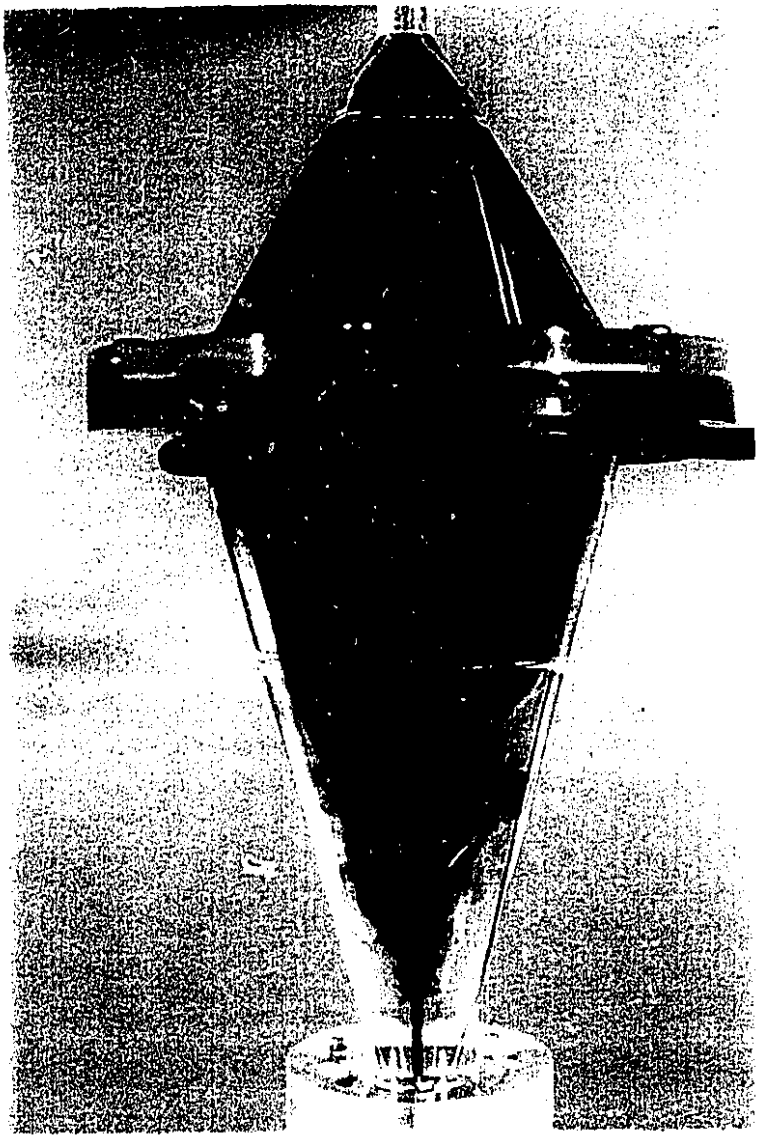

Figure 3.5: An expanding jet pattern for the conical vessel with orifice inlet. For the case of D = 2 mm and Q = 90 mL/min (inlet Re = 960).

This qualitative behavior does not depend on the size or the shape of the inlet orifice; similar flow patterns were obtained with different inlet diameters with both orifice and tube inlets (see Fig.2.1 for inlet shape).

The flow transition from a straight steady jet to an unsteady expanding jet occurred at a critical flow rate which depended on inlet size and shape. The critical value of the flow rate was determined experimentally by observing the flow rate at which the straight jet started to become discontinuous and expanded. The critical inlet velocity (U_c), which was based on the inlet area, is shown as function of the inlet size in Fig.3.6. The region below the curve represents the condition for obtaining a flow with a straight jet and no-mixing, while the region above the curve represents the condition for obtaining an unsteady expanding jet. The critical Reynolds number at which the flow transition occurs is defined as

$$Re_c = \frac{\rho_o U_c D}{\mu_o} \tag{3.1}$$

where ρ_o and μ_o are the density and viscosity of the water, respectively, and D is the inlet diameter. The values of Re_c are tabulated in Table 3-1. For the four orifice inlets almost the same Re_c is obtained ($Re_c \approx 600$), while for the tube inlet a lower value of Re_c is obtained ($Re_c \approx 450$).

3.3.2. Model for Predicting the Minimum Spouting Velocity

Since pulp fibers swell, they usually form beds that are dilute in solid content; packed beds of pulp fibers typically have a solid/liquid ratio of less than 10% [18]. A spouted bed of pulp fibers is much more dilute; its consistency (g pulp/100 mL water) is in the range of 0.1%-0.3% (see Chapter 2). Although such values do not reflect the true void fraction of the bed since pulp fibers flocculate into three dimensional networks, the bed is still dilute compared to a conventional spouted bed

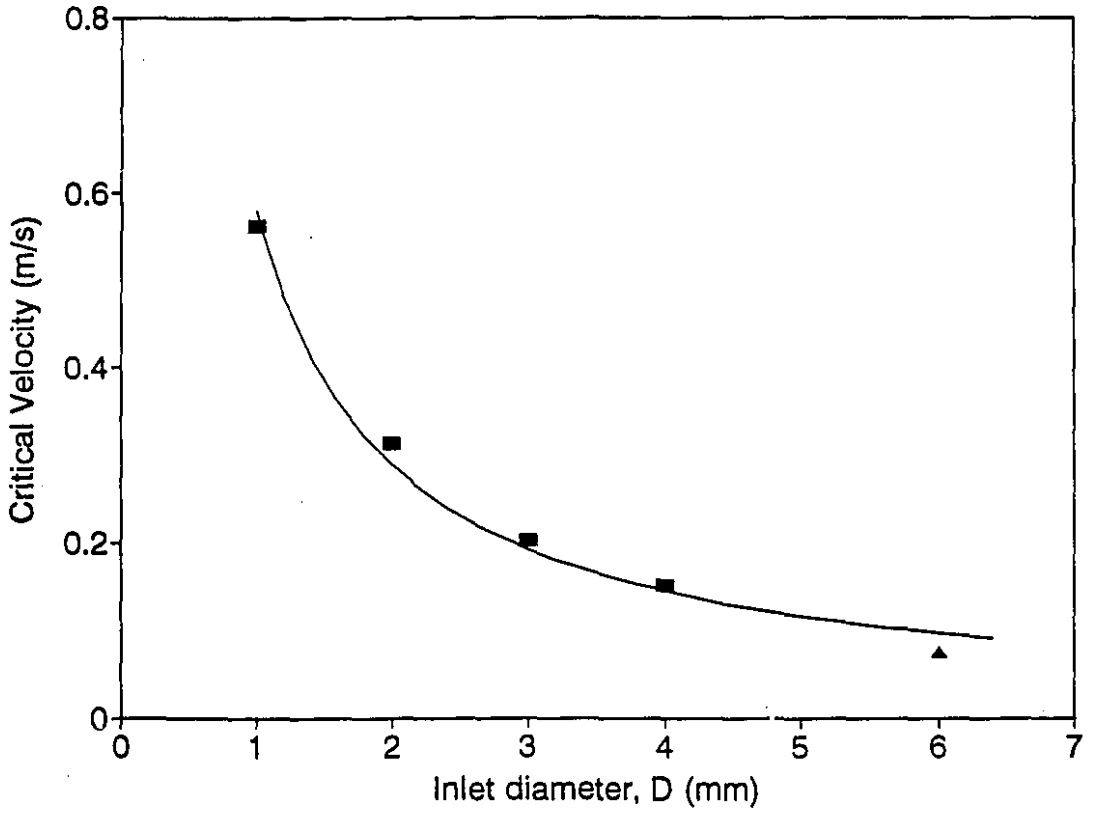

Figure 3.6: The critical velocity (U_c) for the flow transition between the two patterns (a and b) as a function of inlet diameter of the conical vessel with an orifice inlet (square) and a tube inlet (triangle).

of rigid particles. In conventional spouting, a packed bed having a void fraction of about 0.5 is established in the annular region; in pulp spouting, the whole bed is in a dilute state. The presence of fibers does not change the flow patterns qualitatively, and consequently, the hydrodynamics of the pulp spouting is determined by the flow characteristics of jet flow through the conical vessel.

Table 3-1: Jet Transition (Re_c)

Inlet Geometry	Inlet Diameter D (mm)	Re_c
Orifice	1	560
Orifice	2	630
Orifice	3	610
Orifice	4	610
(Average)		600
Tube	6	450

In order to spout pulp fibers two criteria must be satisfied by the flow patterns: first, there must be a mixing effect (resulting from the unsteadiness of the flow patterns) with a shear rate at the bottom of the vessel that is high enough to prevent the accumulation of pulp mass at the bottom; secondly, the liquid velocity must drop dramatically with the axial dimension of the vessel in order to allow fiber settling at some height within the diverging section of the vessel, so that fibers rain back into the annulus, creating a circulating motion between the annulus and the spout. These requirements are achieved simultaneously by the expanding jet shown in Fig.3.4. The straight jet does not allow fiber spouting because the liquid velocity in the jet does not decrease with height. Also, the straight jet creates a steady flow which does not prevent large scale flocculation of fibers. Some flocculation of fibers is required in order to form flocs that have a larger settling velocity than a single fibers, so that the

flocs settle at a reasonable height within the vessel (see Chapter 2).

The minimum spouting velocity for pulp fibers occurs at the condition where the straight jet changes into an expanding jet i.e. the minimum spouting condition is equivalent to the flow transition condition shown in Fig.3.6. Thus, the minimum spouting velocity (U_{ms}) can be given by the following relation:

$$\frac{\rho\ U_{ms}\ D}{\mu} = Re_c \qquad (3.2)$$

where U_{ms} is the minimum spouting velocity at the inlet orifice and ρ and μ are the density and the viscosity of the suspension, respectively. The flow transition Reynolds number (Re_c) was determined from liquid flow experiments (as presented in the previous section). In this relation, ρ and μ are the density and the viscosity of the medium in the vessel, i.e. the pulp suspension. For a dilute suspension of fibers, the density does not change significantly with the presence of fibers since their specific gravity is only about 1.5 and more than 99% of the suspension is water (i.e. $\rho = \rho_o$). The viscosity of a dilute suspension of particles (μ) varies linearly with their volume fraction (ϕ) [19]

$$\mu = \mu_o\ (\ 1 + k_i\ \phi\ ) \qquad (3.3)$$

where μ_o is the viscosity of the particle-free liquid and k_i is the intrinsic viscosity [19]. The intrinsic viscosity of a dilute suspension of porous spherical aggregates is given by the following expression [20]:

$$k_i = \frac{5}{2}\ \frac{\varphi_o(\xi_1) - 3\ \varphi_1\ (\xi_1)}{10\ \varphi_2\ (\xi_1) + \varphi_o(\xi_1)} \qquad (3.4)$$

where

$$\varphi_n(\xi_1) = \left(\frac{1}{\xi_1}\frac{d}{d\xi_1}\right)^n \frac{\sinh \xi_1}{\xi_1} \tag{3.5}$$

in which n is 0, 1 or 2. The dimensionless parameter ξ_1 is

$$\xi_1 = \frac{a}{k_p^{1/2}} \tag{3.6}$$

where a is the radius of the porous sphere and k_p is its permeability.

In this analysis fibers are assumed to aggregate into spherical flocs with radius a. The value of ϕ in eqn.3.3 represents the volume fraction of fiber flocs, not individual fibers. Each floc is an effective porous sphere composed of a loose network of fibers containing a volume of liquid. Defining v_e as the ratio of the volume of a floc to the volume of the fibers composing it, the volume fraction of the flocs in the bed is

$$\phi = \frac{v_e\, m}{\rho_f\, V} \tag{3.7}$$

where m and ρ_f are the mass and density of fibers, respectively, and V is the total volume occupied by the pulp suspension.

In order to obtain an expression for the minimum spouting velocity, eqns.3.3 and 3.7 are substituted into eqn.3.2:

$$U_{ms} = \frac{\mu_o\, Re_c}{\rho_o\, D}\left(1 + \frac{k_i\, v_e}{\rho_f\, V}\, m\right) \tag{3.8}$$

Since Re_c is constant for the same inlet shape, the MSV varies linearly with the mass of pulp (m) and inversely with the inlet diameter (D). This agrees with the experimental findings shown in Fig.2.3. Equation 3.8 differs from the correlations for conventional spouted beds, for which the MSV is generally proportional to D^{-2} and directly to height, i.e. to $m^{1/3}$ (see sec. 2.3.3.).

Equation 3.8 can be written in terms of the ratio of the minimum spouting Reynolds number calculated using liquid properties, $(Re_{ms})_o$, to Re_c as follows:

$$\frac{(Re_{ms})_o}{Re_c} = \left(1 + \frac{k_i \nu_e}{\rho_f V} m\right) \tag{3.9}$$

Equation 3.9 suggests that a plot of $(Re_{ms})_o$ against m is linear and that the value of the intrinsic viscosity (k_i) can be obtained from its slope. The value of the parameter (ξ_1) which characterizes the fiber floc, may then be estimated by solving the algebraic-nonlinear eqns. 3.4 and 3.5. The intercept of the line with the vertical axis, where $m = 0$, can be used to obtain Re_c.

The size of a floc and the number of fibers per floc depend on the shear force exerted by the flow field as well as the nature of the fibers, their surface properties, pulp consistency, etc. The magnitude of the shear force depends on the position in the spouted bed; it varies considerably between the annulus and the spout. Thus, the volume ratio ν_e and the floc size cannot be determined precisely. In the range of the operating consistency (0.1 to 0.3%), the size of a floc is usually of the order of the fiber length, and the number of fibers can be approximated to 6 ± 3 (for short fibers) [21]. Considering the floc as a sphere, with its diameter equal the length of a fiber, ν_e is given by

$$v_e = \frac{2\ L_f^2}{3\ d_f^2\ N_f} \qquad (3.10)$$

where L_f and d_f are the length and the diameter of a pulp fiber, and N_f is the number of fibers per a floc. For hardwood fibers, v_e is approximately 300.

3.3.3. Comparison of the Experimental Findings with the Model

Figure 3.7 shows a plot of $(Re_{ms})_o$ against pulp mass (m) for the data shown in Fig.2.4. The data for D=6 mm are excluded because the inlet geometry is a tube rather than an orifice.

In order to determine the value of the intrinsic viscosity from the slope of the lines, the values of v_e and V are needed. The volume occupied by the suspension (V) could not be determined precisely because of the instability in the central flow region which produced dome-shaped surface. For small inlet sizes a better defined surface was observed, but the height of the bed was not constant, preventing its precise measurement. Nevertheless, the suspension volume at minimum spouting was about 400 mL $\pm$ 20%. This approximation, together with the approximate value of v_e, indicates that the intrinsic viscosity k_i (from the slope of the line) is around 1.9. This estimate of k_i is less than the theoretical value for rigid spheres, $k_i = 2.5$. Equations 3.4-6 indicate that k_i is less than 2.5 for permeable particles and that it approaches 2.5 as the value of ξ_1 increases i.e. as the particle permeability decrease. The estimated value of the intrinsic viscosity is used to estimate the parameter ξ_1 from eqns. 3.4 and 5. This approximation yields $\xi_1 \approx 12$.

Figure 3.8 shows the results obtained for softwood and hardwood fibers with an inlet diameter of 2 mm. The relationships between $(Re_{ms})_o$ and m are linear, but the slope for softwood fibers is larger than that for hardwood fibers since softwood fibers are larger than the hardwood fibers (see table 2.1). The increase in fiber length for

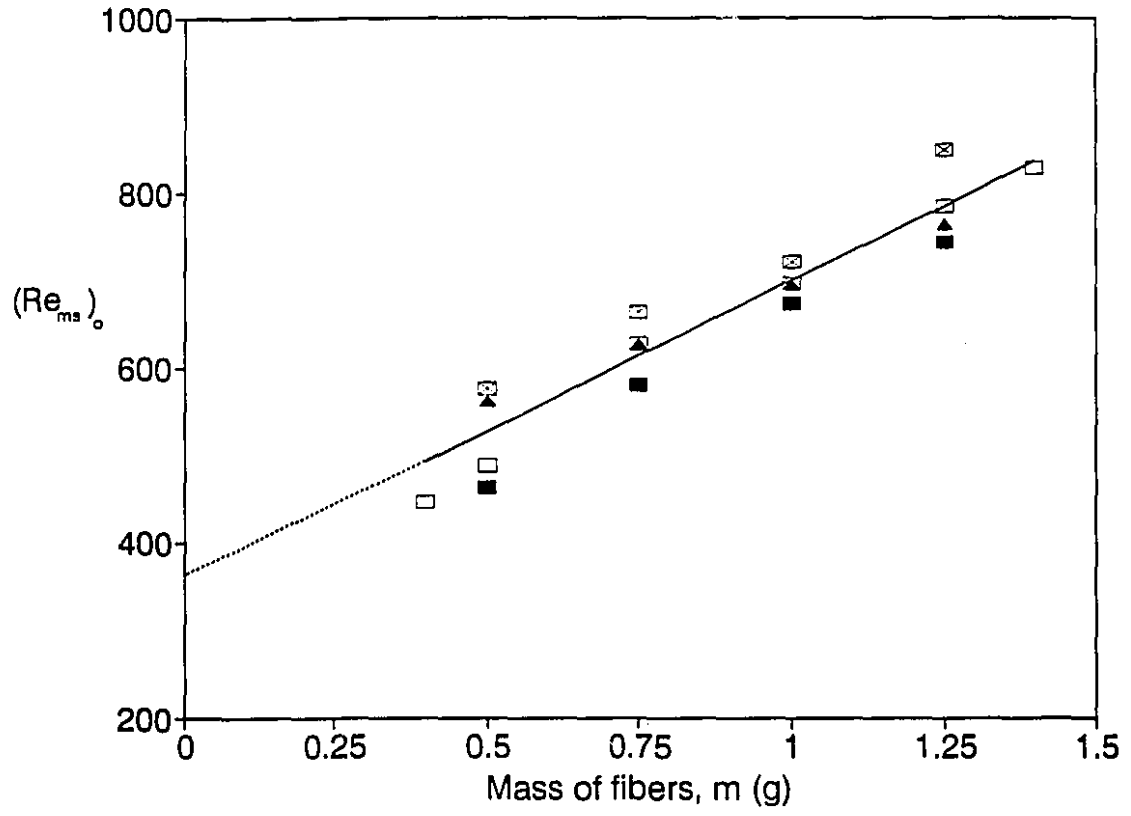

Figure 3.7: Minimum spouting Reynolds number $(Re_{ms})_o$ against m for hardwood fibers at different inlet diameters (for an orifice) D = 1 mm (filled square), 2 mm (empty square), 3 mm (triangle) and 4 mm (square with X).

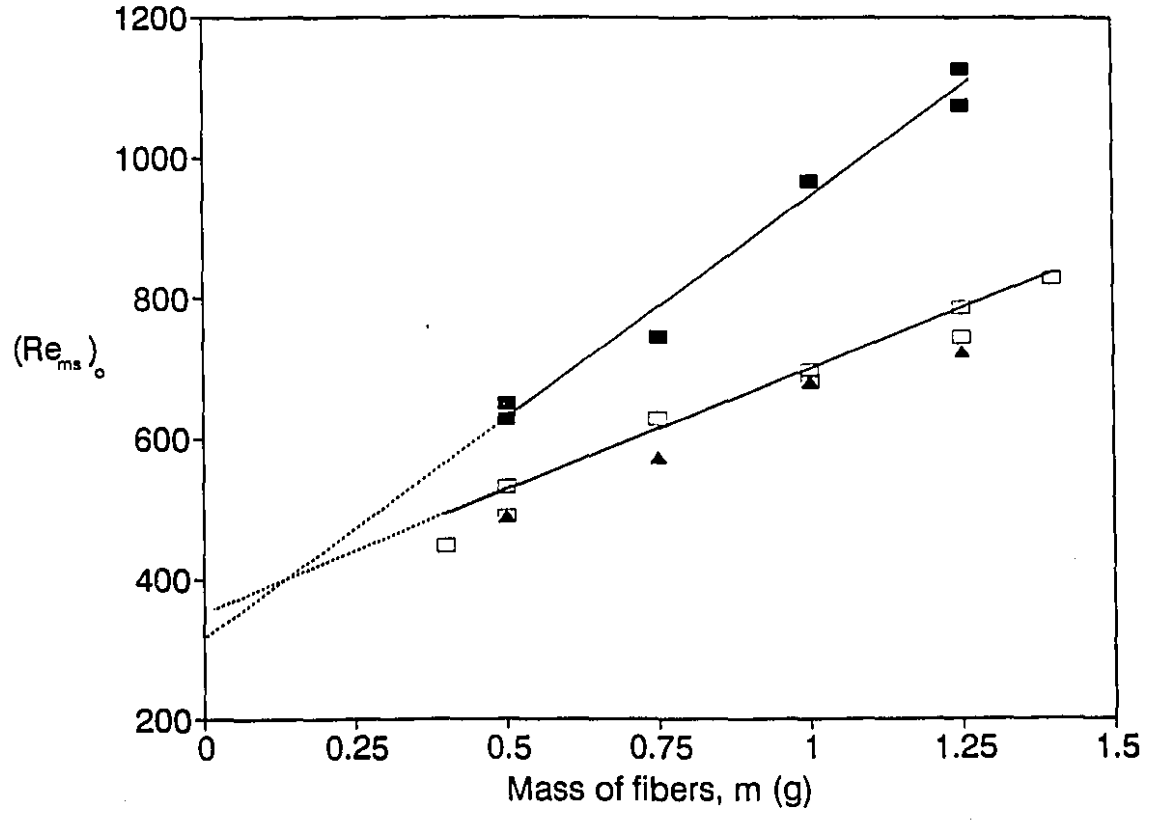

Figure 3.8: Minimum spouting Reynolds number $(Re_{ms})_o$ against m for hardwood and softwood fibers for an orifice inlet with 2 mm diameter. The empty squares are for kraft hardwood fibers, the triangles are for TMP fibers and the filled squares are for kraft softwood fibers.

softwood fibers increases the dimensionless floc radius ξ_1, which in turn increases the intrinsic viscosity (k_i) as predicted by eqn. 3.4 and 3.5. The value of v_e is expected to be the same for both fibers since the increase in the ratio of L_f/d_f for softwood fibers is compensated by an increase in the number of fibers per floc, N_f [21].

The intercept with the vertical axis should represent the value of Re_c for transition from a steady straight jet to an expanding jet, see eqn. 3.9 for m = 0. This intercept is the same for different fibers, since this critical value depends only on the geometry of the system; consequently, the lines have almost the same intercept. The estimated value of Re_c from Fig.3.7or 3.8 is close to 360. The value of Re_c determined from dye tracer experiments was 600 for orifice inlets - see Table 3-1. In view of the fact that the determination of Re_{ms} and Re_c depend on visual observations of different phenomena, these two estimated values are in fair agreement.

3.4. Conclusions

Two flow patterns have been observed for the flow of a liquid jet through a conical vessel: a smooth straight jet, and an unsteady expanding jet with circulating flow regions surrounding the jet in both cases. This qualitative behavior does not depend on the size or the type of the inlet, but the flow transition occurs at a critical value of Reynolds number which depends on the inlet shape.

Pulp fibers can be spouted in a conical vessel with an expanding jet flow. The minimum spouting occurs near the flow transition. The MSV increases with increasing mass of fibers and decreases with increasing inlet diameter. The model presented in this chapter shows a good agreement with experimental findings.

Nomenclature

a	Radius of a porous spherical particle (or a fiber floc) (m).
D	Inlet diameter (m).
d_f	Diameter of fiber (m).
k_i	Intrinsic viscosity.
k_p	Permeability of a porous particle (or fiber floc) (m^2).
L_f	Length of fiber (m).
m	Mass of solids in the bed (kg).
N_f	Number of fibers in one floc.
Q	Inlet flow rate ($m^3\ s^{-1}$).
Re	Reynolds number.
Re_c	Critical value of Re for jet flow transition.
$(Re_{ms})_o$	Minimum spouting Re calculated with water properties.
U	Inlet liquid velocity ($m\ s^{-1}$).
U_c	Critical value of U for jet flow transition ($m\ s^{-1}$).
U_{ms}	Minimum spouting velocity ($m\ s^{-1}$).
V	Total volume occupied by pulp suspension (m^3).
v_e	Ratio of the volume of a fiber floc to the volume of fibers composing it.
ρ	Density of suspension ($kg\ m^{-3}$).
ρ_f	Density of fibers ($kg\ m^{-3}$).
ρ_o	Density of water ($kg\ m^{-3}$).
μ	Viscosity of suspension ($kg\ m^{-1}\ s^{-1}$).
μ_o	Viscosity of water.
ξ_1	Dimensionless radius of a porous particle (defined in eqn.3.6).
φ_n	Function defined in eqn3.5, n is a number between 0 and 2.
ϕ	Volume fraction of solids in suspension.

References:

(1) D.J. Cochrell, A.F.R.Ae.S., M.I.A.S., and E. Markland, "A review of incompressible diffusor flow",*Aircr. Eng., 35, 286-292* (1963).

(2) P.A.C. Okwuobi and R.S. Azad, "Turbulence in a conical diffuser with fully developed flow at entry", *J. Fluid Mech., 57, 603-622* (1973).

(3) A.T. McDonald and R.W. Fox, "An experimental investigation of incompressible flow in conical diffusers", *Int. J. Mech. Sci., 8, 125-139* (1966).

(4) K. Ishikawa and I. Nakamura, "Performance chart and optimum geometries of conical diffusors with uniform inlet flow and free discharge", *JSME Int. J.,series II, 32, 559-567* (1989).

(5) A.C. Trupp, R.S. Azad and S.Z. Kassab, "Near-wall velocity distributions within a straight conical diffuser", *Experiments Fluids, 4, 319-331* (1986).

(6) J. M. Robertson and H. R. Fraser, "Separation prediction for conical diffusers", *Trans. A.S.M.E., 82, Series D, p. 201-209* (1960).

(7) M. Abramowitz, "On backflow of a viscous fluid in a diverging channel", *J. Math. Phys., 28, 1-21* (1949).

(8) M.J. San Jose, M. Olazar, A. T. Aguayo, J. M. Arandes and J. Bilbao, "Expansion of spouted beds in conical contactors", *Chem. Eng. J.,51, 45-52* (1993).

(9) .Olazar, M. J. San Jose, A. T. Aguayo, J. M. Arandes and J. Bilboa, "Pressure drop in conical spouted beds", *Chem. Eng. J.,51,53-60* (1993).

(10) Olazar, M. J. San Jose, A. T. Aguayo, J. M. Arandes and J. Bilbao, "Stable operation conditions for gas-solid contact regimes in conical spouted beds", *Ind. Eng. Chem. Res., 31, 1784-11792* (1992).

(11) M. Olazar, M. J. San Jose, A. T. Aguago, J. M. Arandes and J. Bilbao, "Design factors of conical spouted beds and jet spouted beds", *Ind. Eng. Chem. Res., 32, 1245-1250* (1993).

(12) Ogino, Fumimaru, Kamata, Masahiro, Shimokawa and Keishi, "Measurement of velocity profiles of fluid in a liquid spouted bed by using a laser doppler velocimeter", *Kagaku Kogaku Ronbunshu, 18, 510-514* (1992).

(13) K. Millsaps and K. Pohlhausen, "Thermal distribution in Jeffery-Hamel flows

between nonparallel plane walls", *J. Aero. Sci., 187-196* (1953)

(14) A. H. Gibson, "On the steady flow of an incompressible viscous fluid through a circular tube with uniformly converging boundaries", *Phil. Mag., 18, 35-39* (1909).

(15) W.J. Harrison, "The pressure in a viscous liquid moving through a channel with diverging boundaries", *Proc. Camb. Phil. Soc., 19, 307-312* (1919).

(16) W.N. Bond, "Viscous flow through wide-angled cones", *Phil.Mag.,50, 1058-1066* (1925).

(17) D. Kuhn, personal communication, March, 1993

(18) M. Al-Jabari A.R.P. van Heiningen and van de Ven, "Experimental study of deposition of clay particles in packed beds of pulp fibers", JPPS (to appear), october, 1994

(19) T.G.M. van de Ven, *"Colloidal Hydrodynamics"*, Academic Press, London (1989)

(20) P.M. Alder and P.M. Mills, "Motion and rupture of a porous Sphere in a Linear flow field", *J. of Rheol., 23, 25-37* (1979)

(21) R.J. Kerekes and C.J. Schell, "Characterization of fiber flocculation regimes by a crowding factor", *J. Pulp. Paper Sci., 18, p.32* (1992)

Chapter Four

Particle Elutriation
from
a Spouted Bed of Recycled Pulp Fibers

Abstract

Elutriation of small particles from a conical spouted bed of a recycled pulp suspension, called elutriation-spouting, was demonstrated experimentally. Both ink particles and pulp fines are removed by an upward liquid stream with little fiber loss (about 2%). Elutriation-spouting can be applied for deinking and/or fines-fiber separation purposes.

The concentration of particles in the exit stream was measured continuously as a function of time using a spectrophotometer connected to a personal computer. The resulting elutriation curve exhibited an approximate exponential decay. The elutriation coefficient, estimated using a first order model, was mainly dependent on the flow rate. Increasing the flow rate, by increasing the ratio of flow rate to minimum spouting flow rate (Q/Q_{ms}) at the same inlet size and initial solids hold-up or by operating at larger inlet diameter or larger initial solids hold-up at the same Q/Q_{ms}, increased the elutriation coefficient. Operation at larger Q/Q_{ms} resulted in more fiber loss.

4.1. Introduction

Elutriation is the separation of small particles from a suspension by an upward fluid flow which exceeds the settling velocity of the small particles. Elutriation can be highly efficient as long as the fluid velocity is greater than the settling velocity of the small particles and less than that of the coarse particles. This behavior can be achieved in several types of flow fields such as simple tube flow[13], fluidized [14-19] and spouted beds [20-21] [see sect.1.4.4]. Elutriation was proposed first as a grading technique for particle mixtures in tube flow [13], then it was investigated for the purpose of controlling the enviromental and/or economic problems that are encountered in some applications of fluidized and spouted beds of particles with wide size distributions [14-21]. None of the previous work has considered elutriation in such beds as a separation technique.

In this chapter, elutriation of small particles from a spouted bed of deinking slurry is investigated for possible applications in deinking and/or in fines-fiber separation. As described in Chapters 2 and 3, pulp fibers can be spouted in a conical vessel if the inlet Reynolds number exceeds a critical value, which depends on the vessel geometry and the mass of pulp. The flow rate required for pulp spouting results in an upward velocity that is higher than the terminal settling velocities of the ink and fines. Hence, the particles which are elutriated include pulp fines and ink. This chapter describes the experimental aspects of the elutriation process from a conical spouted bed and utilizes an existing empirical model to determine an elutriation coefficient.

4.2. Experimental

4.2.1. Set-up

The set-up shown in Fig.4.1,is identical to that described in Chapter 2 with small changes in tube connections and with the addition of a spectrophotometer and data

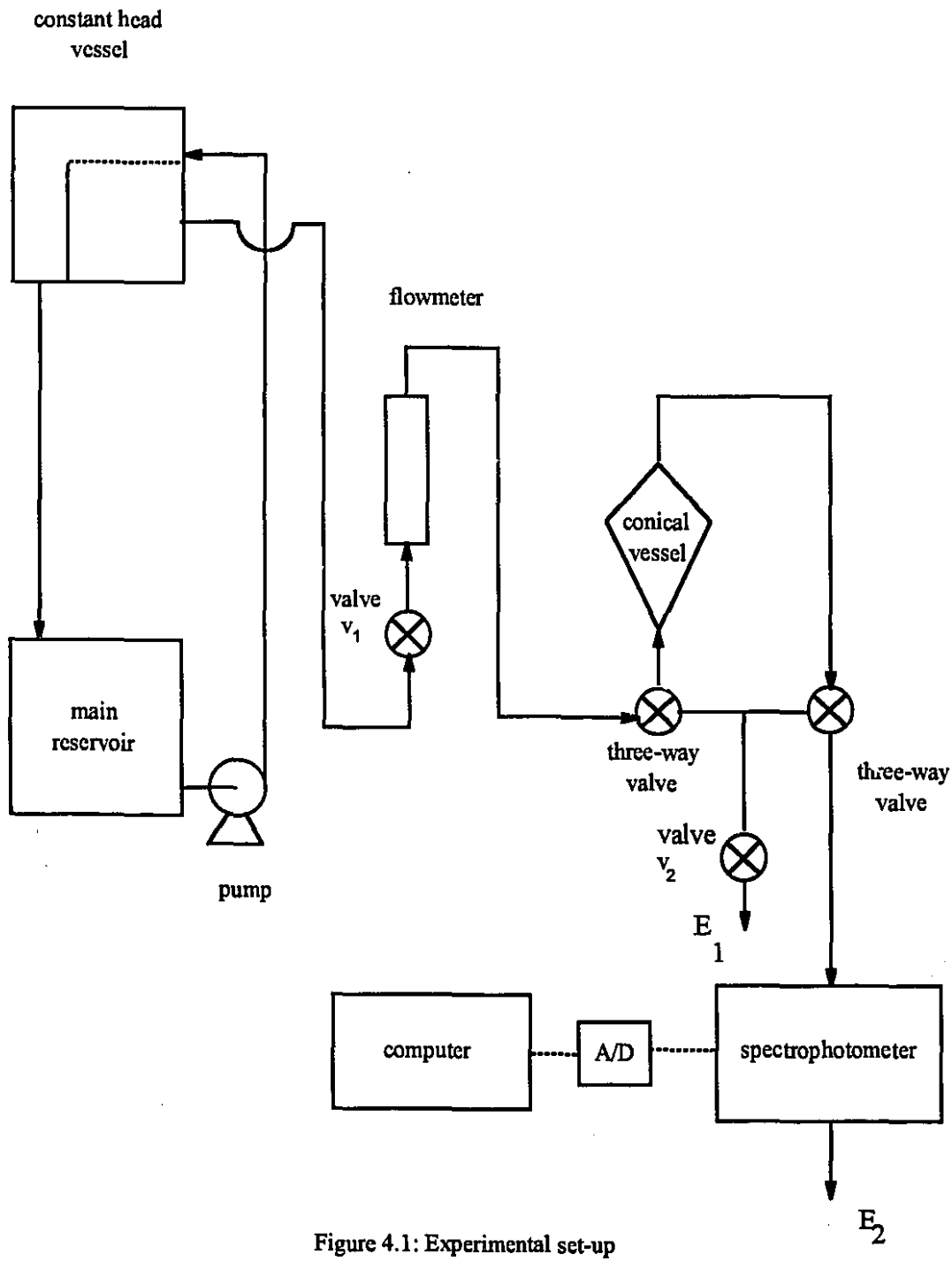

Figure 4.1: Experimental set-up

acquisition system. The exit suspension passes through a spectrophotometer (Spectronic 20, Milton Roy Inc.) which measures its transmittance at a wavelength of 500 nm and converts it into a voltage signal in the range 0-1.0 V. The signal is fed continuously to an XT personal computer through an analog to digital converter. The transmittance of the exit suspension is displayed on the computer screen in the real time.

4.2.2. Preparation of Suspensions

Different types of pulp suspensions were used including recycled pulp from a newspaper, fines-free hardwood fibers including both kraft and thermomechanical pulp (TMP) and mixtures of these fibers with a cellulosic particle suspension. These cellulosic particles were Avicel PH-105 (FMC Corp.) of 20 μm mean particle size.

Fiber suspensions were prepared by mechanical disintegration as described in Chapter 2. Avicel particle suspensions were prepared by immersing the required amount of Avicel powder into about 1 L of distilled water and mixing it in a blender (Waring 205-2/24) for about 40 minutes at 50 rpm. Avicel-fiber mixtures were prepared by mixing the required amounts of Avicel and fibers suspensions. The source of recycled papers used in this research was a newsprint from the McGill Daily newspaper. The fiber length and fines content were measured in a Kajaani FS-200 fiber analyzer. The average fiber length was 1.3 mm (L weighted average) and the fines content was about 33%. The deinking suspension was prepared by one of the following methods in order to investigate the effect of paper disintegration and cooking conditions (see section 1.2.1.).

(a) Mechanical Treatment

A few grams of newspaper flakes were suspended in 1 L of distilled water for several minutes before disintegration in a blender (Waring Blender 205-2/24) for about 15 minutes at 50 rpm. This suspension was diluted to the required consistency. For the purpose of comparison, some pulp samples were prepared using a British

standard disintegrator after being immersed in water for 24 hours. Subsequently, disintegration refers to the use of the blender unless otherwise specified.

(b) Thermomechanical Treatment

The newspaper flakes were suspended in 1 L of distilled water and heated to a temperature of 50-70 °C for 15 minutes. The flakes were then disintegrated as described above in one of the two disintegrators.

(c) Chemi-thermo-mechanical Treatment

Ten grams of newspaper flakes were disintegrated in a British standard disintegrator after immersion in water for 24 hours. The resulting slurry was mixed with a solution containing the chemicals and their amounts listed in Table 4-1. Since sodium hydroxide causes yellowing effects [7], some samples were prepared without its addition to compare the two cases. The slurry was then heated and held at 50-70 °C for about one hour. Finally, the slurry was diluted to the required consistency.

Table 4-1: Deinking chemicals for Chemi-Thermo-Mechanical Treatment

Chemical	Amount (mg/g newspaper)
sodium silicate	40
sodium carbonate	40
sodium oleate	16
potassium phosphates	6
hydrogen peroxide	40
sodium hydroxide*	20

* some samples were prepared without NaOH.

In order to compare the effectiveness of the different methods for ink dispersion, handsheets were made from the stock pulp suspensions following the standard handsheet preparation procedure [22].

4.2.3. Elutriation Procedure

The required volume of the suspension was placed in the lower conical part of the vessel (see Fig.2.1). The upper cone was attached and the empty volume was filled rapidly with upward water flow until the liquid level reached the outlet E_1 while the outlet E_2 was closed (see Fig.4.1). The flow was then stopped for about one minute to allow the fibers that were transported into the top section (during the filling step) to sediment back into the lower part of the vessel where spouting took place. Meanwhile, the three-way valves were adjusted so that the effluent from the vessel would pass through the spectrophotometer. The tubing system and the cell of the spectrophotometer were filled with distilled water by adjusting valves V_1 and V_2. During this step, the spectrophotometer was pre-set to read 100% transmittance (i.e. 1.0 V) which is equivalent to a particle-free liquid.

The elutriation experiment was started by directing the flow at the required rate ($Q \geq Q_{ms}$ determined from Chapter 2) to the vessel and simultaneously activating the data-acquisition system. The transmittance was recorded by the computer as a voltage signal (with 1 V equivalent to 100%) and shown on the screen in the real time. When the transmittance approached the value of 1 V, the experiment was stopped. An example of the time variation of the measured transmittance signal for an elutriation experiment of a recycled pulp suspension prepared by the thermomechanical treatment is shown in Fig.4.2. Two replicates are shown to illustrate the reproducibility of these curves.

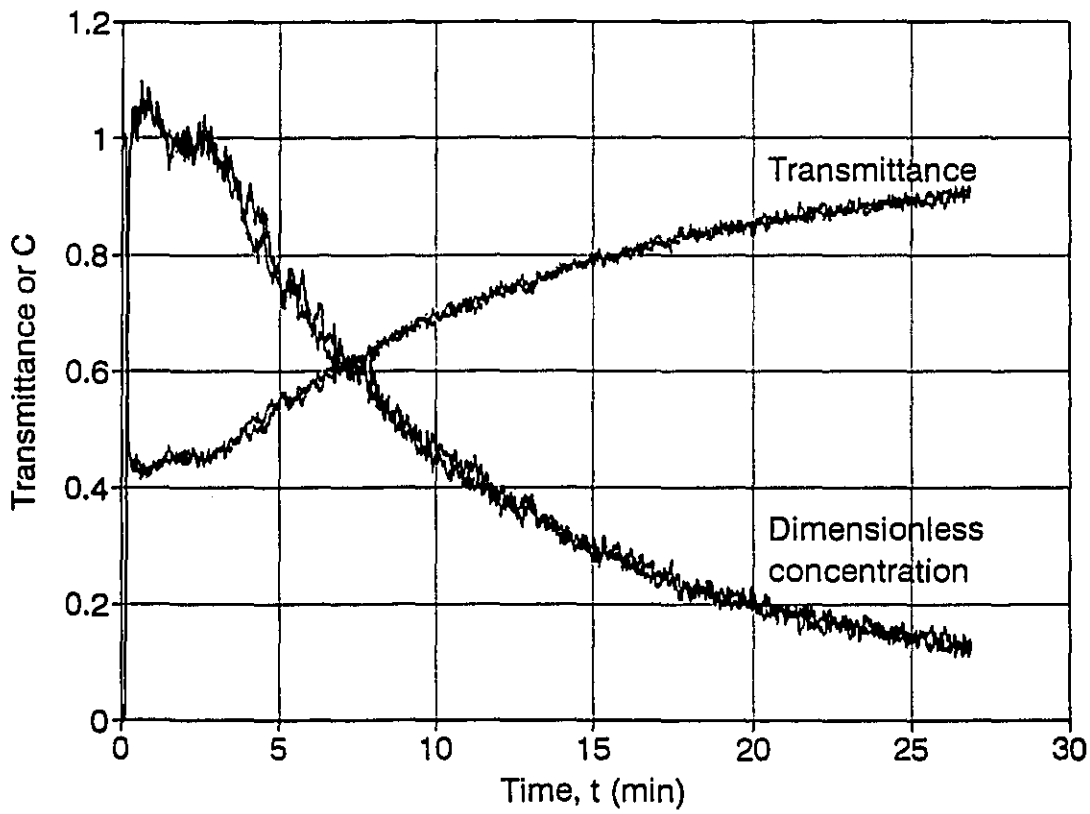

Figure 4.2: The measured transmittance and the calculated dimensionless exit concentration (C) versus time. Two replicates are shown for experiments done with recycled pulp prepared by thermomechanical treatment (British standard disintegrator) for D = 4 mm, m = 1.4 g and Q = 160 mL/min.

4.3. Analysis

The transmittance (T in volts) is related to the concentration of particles (c) by the Beer-Lambert law as follows:

$$c = \frac{1}{A\,b} \ln\left(\frac{1}{T}\right) \qquad (4.1)$$

where A and b are the absorptivity and the pathlength, respectively. The dimensionless exit concentration (C) is given by:

$$C = \frac{c}{c_o} = \frac{\ln(1/T)}{\ln(1/T_o)} \qquad (4.2)$$

where c_o is the initial particle concentration and T_o is the corresponding transmittance in volts. The value of T_o is given by the average recorded transmittance at the initial period of constant transmittance. Figure 4.2 shows the dimensionless exit concentration calculated from the transmittance (T) curve and eqn.4.2. The C-curve is called the elutriation curve.

The concentration of particles jumps from zero to 1 in the short time required for the liquid to flow from the vessel to the sensor of the spectrophotometer. Then it passes through a period of constant concentration which represents the time required to replace the liquid in the top section of the vessel that contained particles which were carried by the filling liquid. The filling stage caused the small particles to be distributed "equally" in the whole vessel i.e. in the bottom and the top sections, while the fibers sediment back into the bottom section during the waiting period.

The particle concentration in the falling period of Fig.4.2is similar to elutriation curves obtained in conventional spouted beds [20,21]. Previous investigators used

a first order empirical model to describe such curves (see sec. 1.3.4.1.) [14-21] which is given by eqn.1.4

$$C = e^{-k_e t} \qquad (4.3)$$

where k_e is the elutriation coefficient and t is the time. This equation is used in this chapter to determine the elutriation coefficient. A more detailed model for elutriation is presented in Chapter 5.

Substitution of eqn.4.1 into eqn.4.3 gives

$$\ln [\ln (\frac{1}{T})] = - k_e t + \ln [\ln (\frac{1}{T_o})] \qquad (4.4)$$

The plot of ln [ln(1/T)] against time was found linear up to a certain critical value. The elutriation coefficient (k_e) was determined from the linear fit of ln [ln(1/T)] against t in the initial period (excluding the initial period of constant exit transmittance). The square of the correlation coefficient was always larger than 0.98.

The percentage total solids removal was determined from a mass balance performed on the suspension in the vessel between the start and the end of the elutriation experiment. The residual suspension was filtreted through a 150 mesh screen. The filtration was done twice over the same mesh to reduce the possibility of fiber loss. In addition, the percentage fiber loss for experiments with fines-free suspensions as well as Avicel-fiber mixtures was determined by passing the exit stream through the mesh and collecting the retained fibers. The collected fiber mass in both cases was dried in an oven for sufficient time and then placed in a desiccator to cool to room temperature. The retained mass was then weighed. The accuracy of this filtration procedure for pulp recovery was tested by filtering a suspension of known solid content and measuring the mass of the dried retained solids (with both recycled pulp and fines-free pulp). The error was between 1 and 3 %.

The particle removal for Avicel-fiber mixtures was also determined from a mass balance on particles in the exit stream. A transmittance-concentration calibration curve was prepared for the Avicel suspension from which the product Ab in eqn.4.1 was found to be 0.55 L/g. The mass of particles removed by the exit stream (Δm) is given by

$$\Delta m = \int_o^{t_f} Qc\, dt = \frac{Q}{Ab} \int_o^{t_f} \ln\left(\frac{1}{T}\right)\, dt \qquad (4.5)$$

where t_f is the total elutriation time period and Q is the flow rate. The value of Δm was determined by numerical integration using Simpson's rule.

4.4. Results

The pulp preparation method, including disintegration and cooking, affected the degree of ink dispersion i.e. the size and the number of the dispersed ink particles. Figures 4.3 and 4.4 show photographs of handsheets made from a recycled pulp prepared by the different deinking treatments.

Figure 4.3 shows the effect of cooking conditions on the size of ink particles for pulps disintegrated in the standard disintegrator. Recycled pulp suspension prepared by mechanical treatment in the standard British disintegrator resulted in the largest ink specks. Their size was in the order of fiber length as shown in Fig.4.3a. When the pulp was pre-heated (thermomechanical treatment) better ink dispersion was obtained as shown in Fig.4.3b, this represents the common industrial conditions of simultaneous repulping and cooking (i.e. both carried out in the same vessel). The addition of chemicals and heating after repulping represents the case of consecutive repulping-cooking (see sec.1.2.1). This consecutive cooking step resulted in breaking the large ink specks produced by mechanical disintegration into smaller ones as shown in Fig.4.3c. The addition of sodium hydroxide resulted in yellowing effects with no noticeable improvement compared to the other chemical recipe (Fig.4.3d).

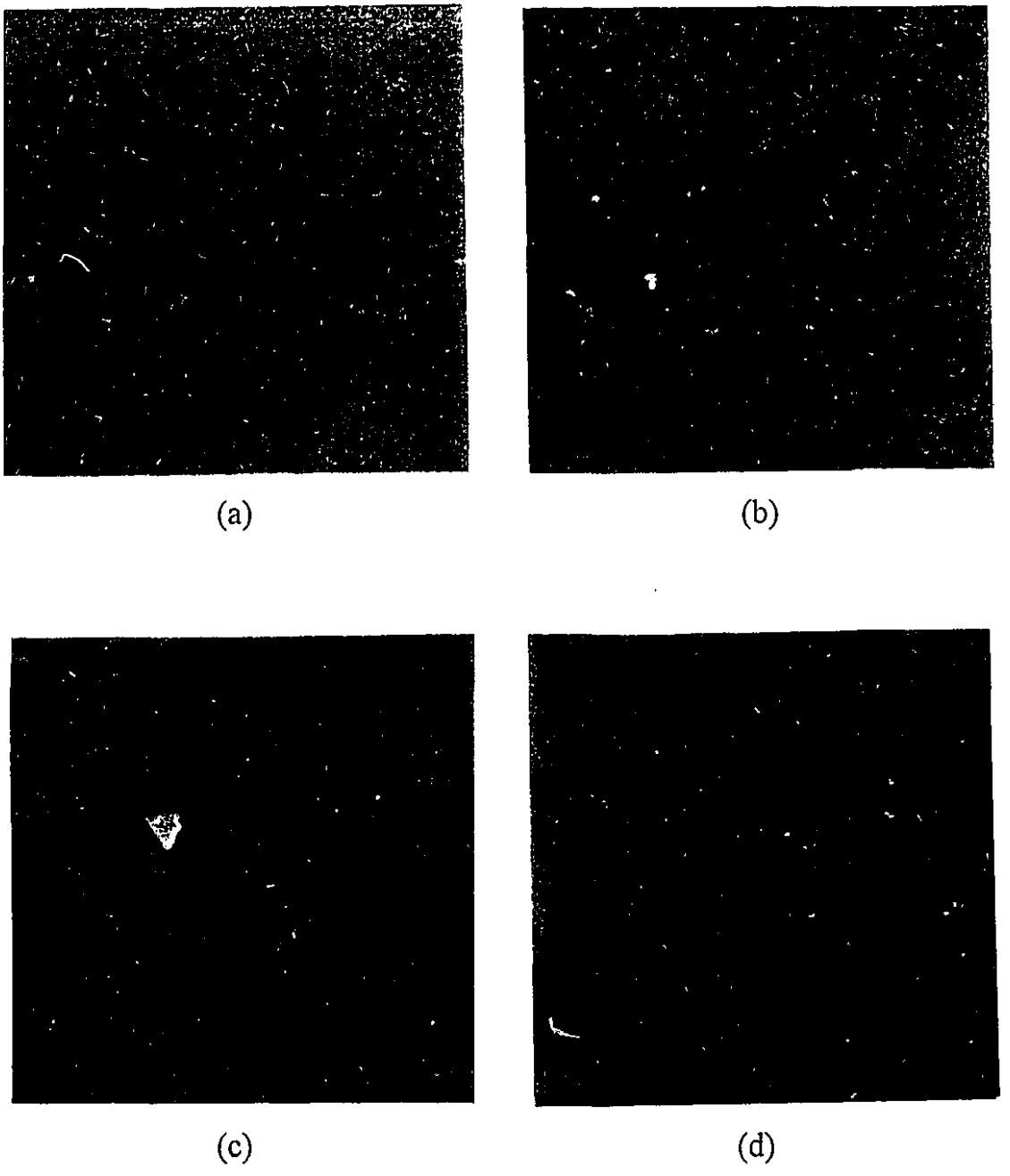

Figure 4.3: Photographs of handsheets made from recycled pulp disintegrated using the standard British disintegrator comparing the effect of treatments on the size of ink particles: (a) mechanical, (b) thermomechanical, (c) chemi-thermomechanical without sodium hydroxide and (d) chemi-themomechanical with sodium hydroxide.

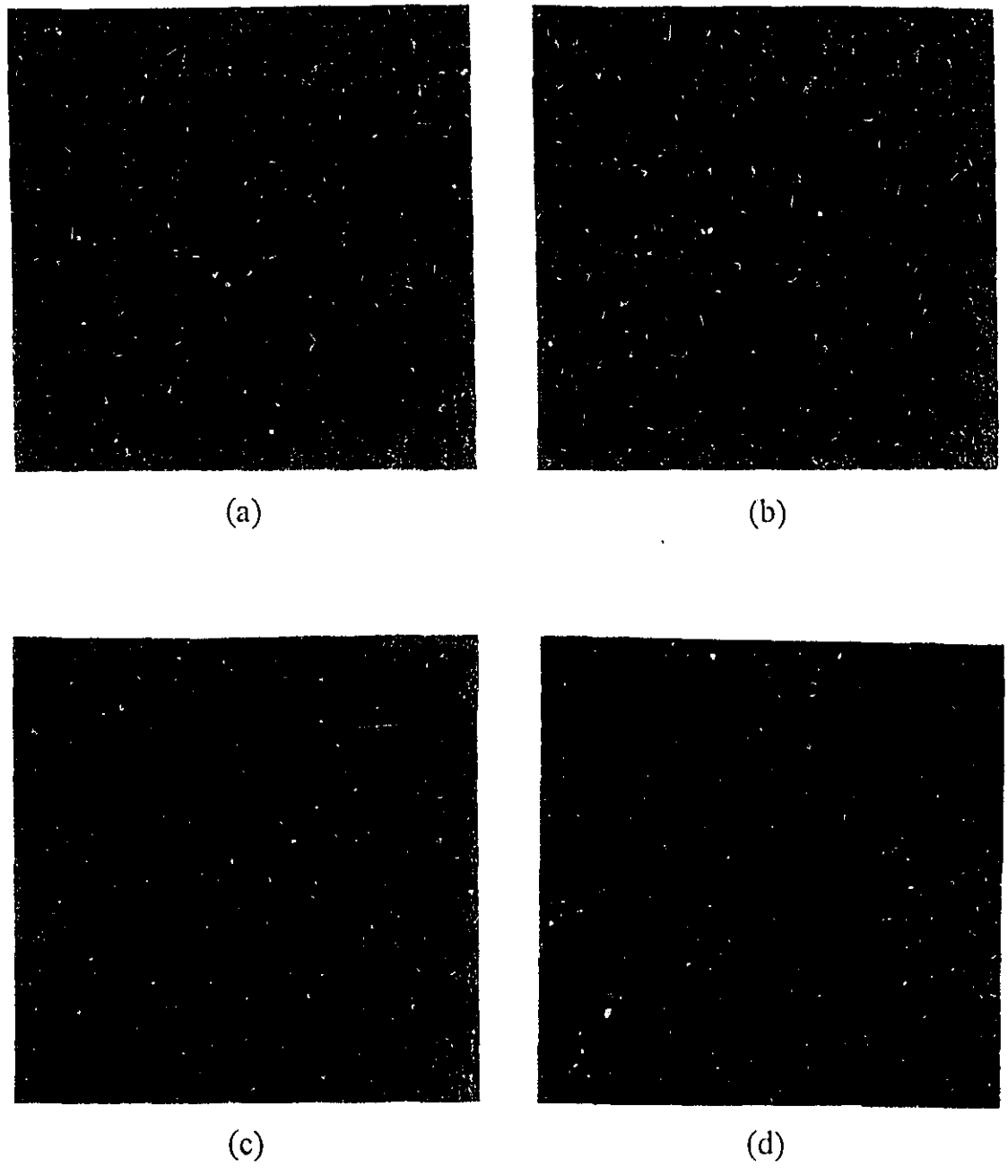

Figure 4.4: Photographs of handsheets made from recycled pulp comparing the effect of method of disintegration on the size of ink particles: (a) mechanical treatment with the blender, (b) mechanical treatment with the standard British disintegrator, (c) thermomechanical treatement with the blender and (d) themomechanical treatment with the standard British disintegrator.

Figure 4.4 shows the effect of the method of disintegration on the size of the ink particles. However, with or without cooking, disintegration in the blender resulted in better ink dispersion - compare Figs.4.4 b and d, (for mechanical and thermomechanical treatments in the standard disintegrator, respectively) with Figs.4.4 a and c (for mechanical and thermomechanical treatments in the blender, respectively). The best deinking treatment was the thermomechanical method with the blender (Fig.4.4 d).

The effects of the deinking pretreatment, flow rate, inlet diameter and initial solids hold-up on the elutriation curves are presented in Figures 4.5 to 4.8. In these figures the quantity ln [ln(1/T)] is plotted against time (t) as suggested by eqn.4.4.

Figure 4.5 shows the effect of pulp preparation method, including disintegration (Fig.4.5 a) and cooking (Fig.4.5 b), on the elutriation curves. The inlet size was 4 mm, the flow rate was 200 mL/min and the initial solids hold-up was 1.4 g. Figure 4.5 a shows that the disintegration method (i.e. using the blender or the standard British disintegrator) had little effect on the elutriation curve when the pulp was cooked (i.e. thermomechanical treatment). Both curves have an initial linear period with the same slope. At large times, the elutriation curve for pulp prepared in the standard disintegrator departed from linearity earlier than the curve for pulp prepared in the blender (more obvious with mechanical treatment). The method of disintegration would affect the state of the resulting fiber floc as well as the degree of ink dispersion (see Fig.4.4). Both factors have important effects on the elutriation behavior. The size of the ink particles will determine whether or not the particle can be elutriated by the upward liquid, while the state of the fiber floc determines the ease of fines release from inside the floc.

Figure 4.5 b compares the elutriation curves for recycled pulp with different cooking conditions (thermomechanical and chemi-thermomechanical with and without sodium hydroxide) and no-cooking treatments for pulps disintegrated in the standard disintegrator. The type of cooking affected the initial transmittance (T_o in eqn.4.1) since it affects the degree of ink dispersion. Experiments with chemi -

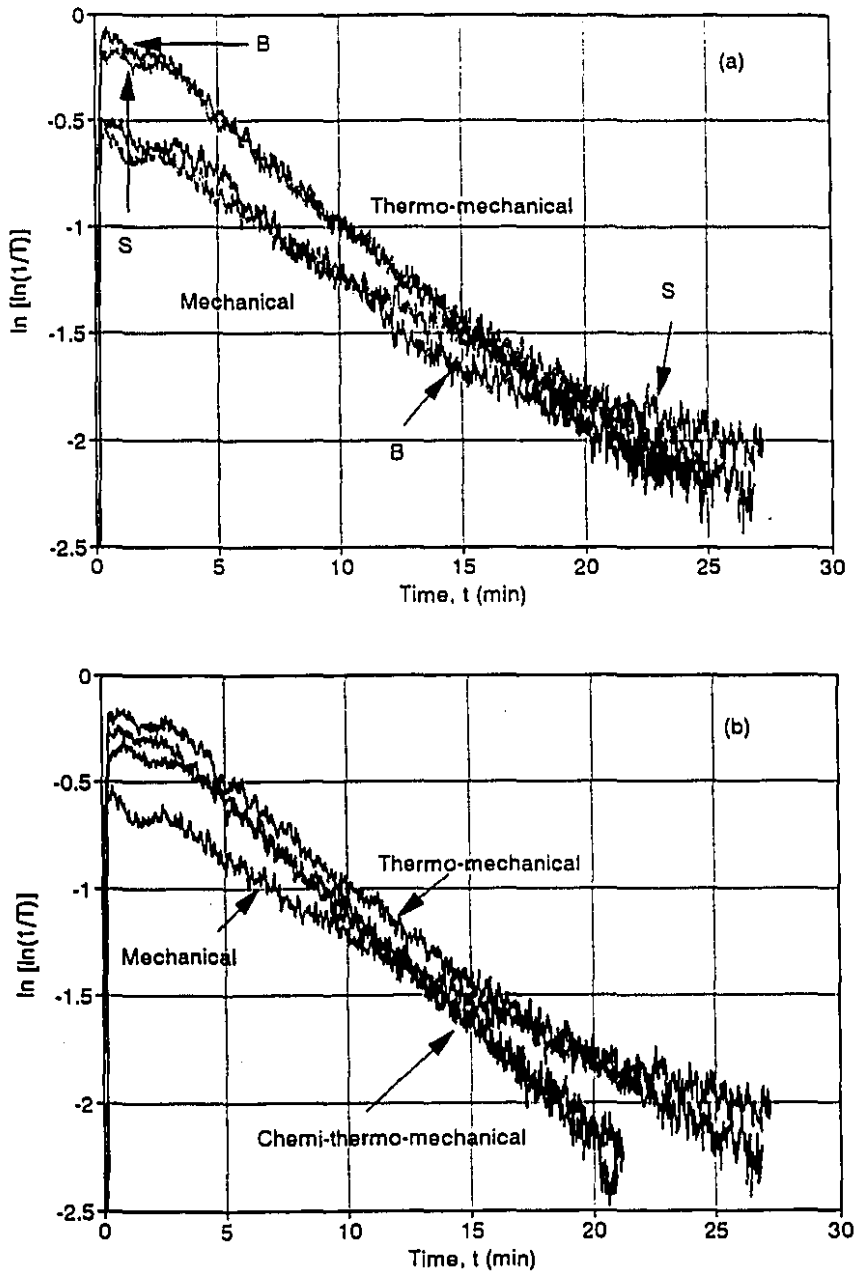

Figure 4.5: The effect of pretreatment on the elutriation curves. (a) Effect of the method of disintegration, S refers for the standard British disintegrator and B for the blender. (b) Effect of cooking treatment for pulp disintegrated with the standard disintegrator. The inlet diameter was 4 mm, the initial solids hold-up was 1.4 g and the flow rate was 200 mL/minute.

thermomechanical treatments resulted in a slight decrease in $\ln[\ln(1/T_o)]$ compared to that with thermomechanically treated pulp since a small improvement in ink dispersion was acheived by simultaneous cooking-disintegration. Pulp prepared by the mechanical treatment resulted in a large decrease in $\ln[\ln(1/T_o)]$ due to the presence of the large specks that were non-elutriable. The slopes of the linear portions of the curves in Fig.4.5 b are essentially the same since the elutriation coefficient does not depend on the initial particle (fines) concentration.

The pre-treatment method is not a major variable in elutriation behavior. In a practical application, the deinking treatment is chosen according to the effectiveness in ink dispersion. For the rest of this study, pulp was prepared by thermomechanical treatment with disintegration in the blender because it produced no specks.

Figure 4.6 shows the effect of flow rate on the elutriation curve. The initial solids hold-up was 1.0 g and the inlet size was 4 mm. Elutriation was more rapid at higher flow rates.

Figure 4.7 shows the effect of inlet diameter on the elutriation curves for a constant ratio of flow rate to minimum spouting flow rate ($Q/Q_{ms} = 1.05$) and an initial solids hold-up of 1.0 g. The elutriation rates were larger for larger inlet diameters.

The effect of the initial solids hold up on the elutriation curve was studied at two flow conditions: constant flowrate ($Q = 160$ mL/min) and constant ratio of flowrate to minimum spouting flowrate ($Q/Q_{ms} = 1.26$) for the case of $D = 4$ mm. The results are shown in Figure 4.8, a and b. Other than the shifts in the elutriation curves resulting from the differences in the initial particle concentrations, the initial solids hold-up had little effect on the elutriation curves.

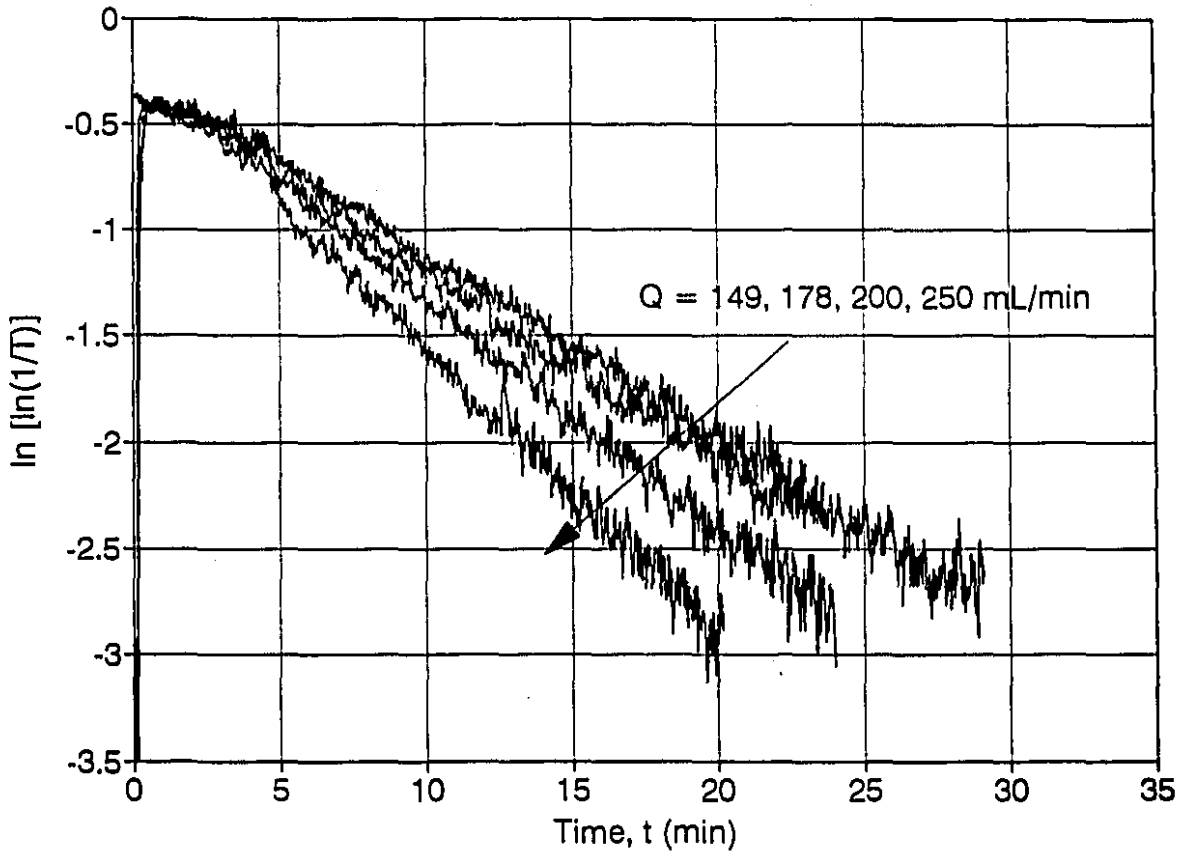

Figure 4.6: The effect of flow rate (Q) on the elutriation curves. The initial solids hold-up was 1.0 g and the inlet size was 4 mm.

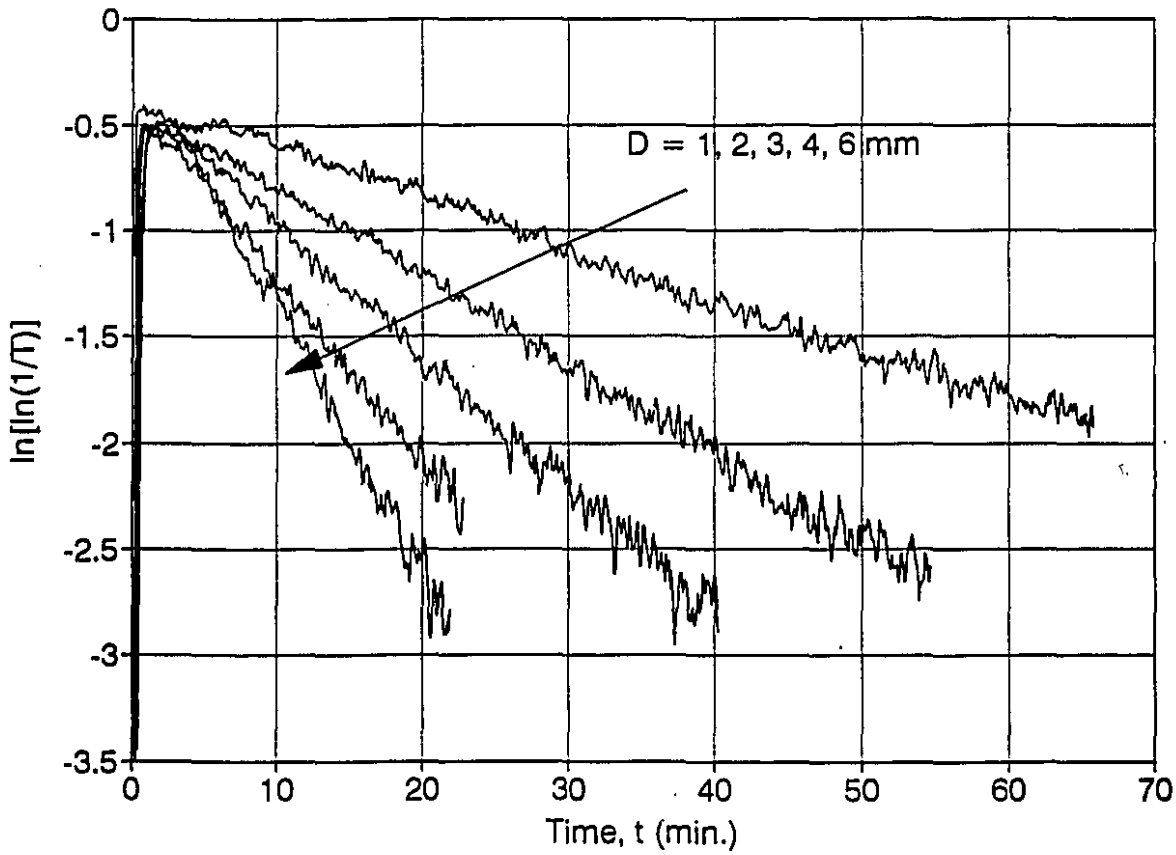

Figure 4.7: The effect of inlet diameter (D) on the elutriation curves for a constant ratio of flow rate to minimum spouting flow rate ($Q/Q_{ms}=1.05$) and an initial solids hold-up of 1.0 g.

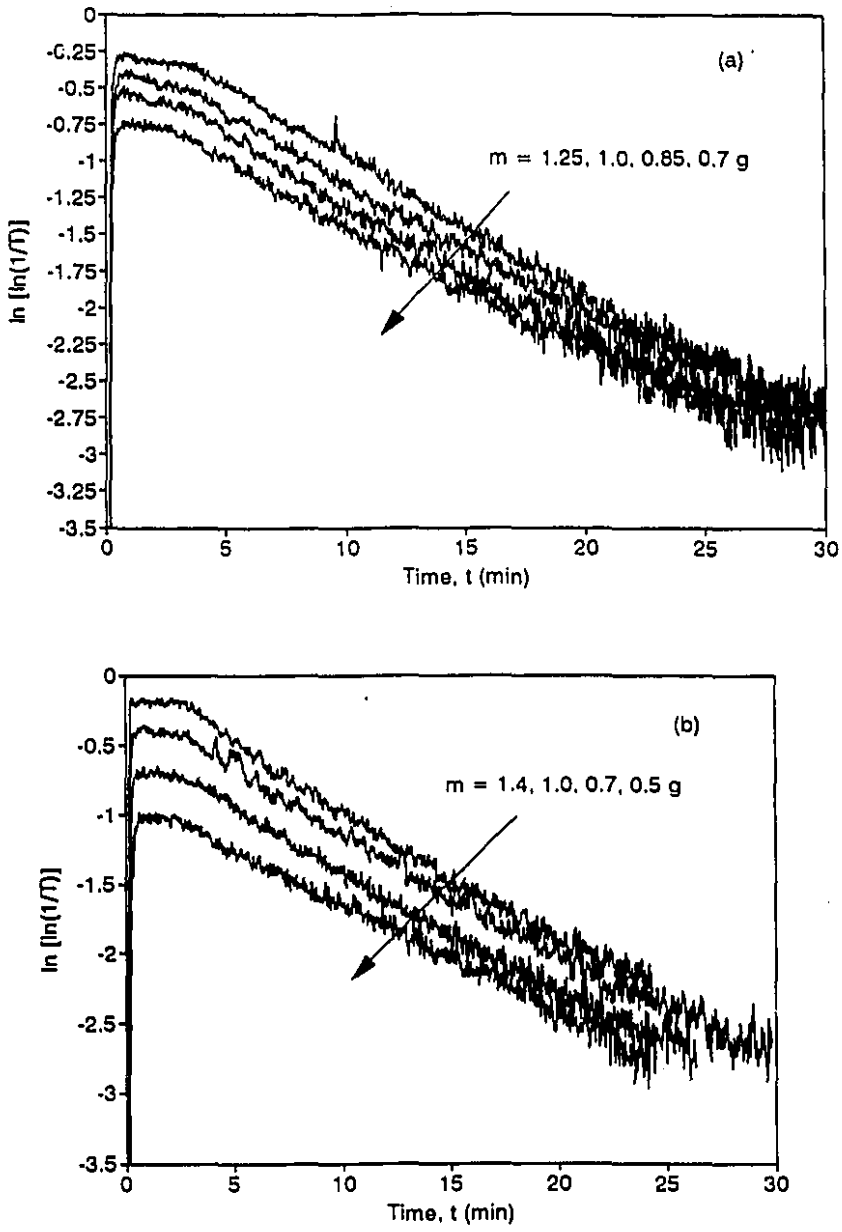

Figure 4.8: The effect of the initial solids hold up (m) on the elutriation curves at constant flow rate (Q = 160 mL/minute), figure a, and constant ratio of flow rate to minimum spouting flowrate (Q/Q_{ms} = 1.26), figure b. The inlet diameter was 4 mm.

4.5. Discussion

4.5.1 Feasibility of Particle Separation by Elutriation-Spouting

The elutriation-spouting mechanism is feasible for particle separation if most of the small particles present in the initial suspension are removed by the upward liquid stream and most of the large particles (fibers) are retained within the vessel. Both the percentage fiber loss in the exit stream and the percentage solids removal from the total initial solids hold-up are important. These quantities have been measured with suspensions of fines-free fiber with and without Avicel particles.

The results of fiber loss tests are reported in Table 4-2. The first two groups (1 and 2) are for suspensions of fines-free fibers. The third group of experiments (3) is for Avicel-fiber mixtures. In this case, only the fibers were retained by the mesh since Avicel particles are very small (20 μm) and no fiber cake formed since the quantity of retained fibers was too small. These results show that the average fiber loss was 2.4%. This loss is attributed to the presence of short fibers as well as non-flocculating fibers that escape in the exit liquid. Relatively short fibers are present in fiber suspensions since fibers usually have a wide size distributions.

The percentage solids removed was measured using Avicel-fiber mixtures. The elutriation experiments were run until the exit transmittance (T) reached 0.97 (1.0 is for distilled water). Results with both kraft and TMP fibers are listed in Table 4-3. For group (2), the values of solids removal given in parentheses were estimated using eqn.4.5. The two mass balances (on the retained solids and on the removed particles in the exit stream) gave close values. These results show that the major part of the particles was removed by the upward stream.

Consequently, elutriation-spouting is an efficient mechanism for the separation of small particles from fiber flocs. Most of the fibers present in the suspension in the form of flocs will be retained.

Table 4-2: Percentage fiber loss

Fiber / Q/Q_{ms} / D / t_f or T	Initial fiber mass (g)	Initial Avicel mass (g)	Percentage fiber loss
(1)	0.5	0	2.6
fines-free	0.5	0	4.0
Kraft hardwood	0.75	0	1.3
fibers	1.0	0	1.4
$Q/ Q_{ms}=1.1$	1.25	0	1.5
D = 2 mm	1.4	0	1.7
t_f = 20 min	(average)		(2.1)
(2)	0.5	0	2.9
fines-free	0.75	0	1.8
TMP fibers	1.0	0	3.4
Q/ Q_{ms} = 1.1	1.25	0	2.7
D = 2 mm	(average)		(2.7)
t_f = 40 min			
(3)	0.59	0.4	2.0
kraft hardwood	0.69	0.3	4.2
fibers	0.79	0.2	2.3
Q/Q_{ms} = 1.0	0.90	0.1	1.6
D = 4 mm	0.90	0.1	1.8
T = 0.97	(average)		(2.4)

Table 4-3: Percentage solids removal of Avicel-fiber mixtures with $Q = Q_{ms}$ and $D = 4$ mm

Fibers	Initial fiber mass (g)	Initial Avicel mass (g)	Amount of solids removed (g)
(1) TMP	0.61	0.2	0.23
	0.61	0.3	0.27
	0.61	0.4	0.38
(2) Kraft hardwood	0.90	0.1	0.11, (0.10)
	0.79	0.2	0.20, (0.20)
	0.69	0.3	0.26, (0.27)

4.5.2 Elutriated Particles from a Recycled Pulp Suspension

In a recycled pulp suspension both ink and pulp fines have sizes of the same order of magnitude. Fines comprise about 33% (Kajaani FS-200) and ink about 1.5-2% of the net paper weight [1]. The remainder is relatively long fibers of wide size distribution. The average fiber length is 1.3 mm. Although the selective removal of ink and the recovery of all pulp is desirable, fibers and fines may be lost in deinking operations. When deinking utilizes the difference in size between ink particles and fibers, fines are removed with ink as in the case of washing and the present technique of elutriation. The percentage pulp loss from washing systems ranges from 24-42% for fine wire to 40-54% for coarse wire [1]. From a flotation cell the loss is between 5 and 12% [10]. The yield of a deinking plant may be lower than 60% [1].

The particle elutriation results show that when the ink is well dispersed into small particles during pulp preparation (i.e. without relatively large specks), both ink

and fines are removed by the exit stream. The total percentage of these two types of particles is about 35%. This is almost the same as the average percentage solids removal obtained in experiments carried out with $Q/Q_{ms}=1.05$ for the various inlet diameters and the same initial solids hold-up of 1.0 g as tabulated in Table 4-4. Although the operating flow rates differed among these cases (e.g. the value of Q_{ms} for D=6 mm is about 10 times that for D=1), almost the same percentage of solids was removed. However, increasing the inlet diameter decreased the required elutriation time (Fig.4.7) but increased the water consumption (Table 4-4). On the other hand, the percentage solids removal varies with Q/Q_{ms} as shown in Fig.4.9 for two constant inlet diameters, 4 and 6 mm with m =1.0 g. From the results of the experiments performed with Avicel-fiber suspension (Table 4-3), neither the initial solids hold-up nor the initial fraction of particles resulted in a noticeable change on the percentage solids removal. Increasing Q/Q_{ms} is the only parameter that increased the percentage solids removal. This is due to a deflocculating effect resulting from expansion of the pulp bed (which causes a reduction in the fiber consistency which, in turn, determines the size of the floc [23]) and due to an increase in the shear effects and flow instability. Consequently, increasing Q/Q_{ms} resulted in the presence of a larger fraction of individual fibers that would be easily carried by the upward stream.

These results show that elutriation-spouting is an efficient technique for fines-fiber separation. It may have application in the separative treatment of fines and fibers (which is receiving a growing interest since both have different surface properties). In deinking, the loss of fines is a major disadvantage. This disadvantage may be overcome by having a subsequent ink-fines separation, perhaps using a flotation cell which removes ink selectively from the residual suspension. This is better than direct flotation since the load to the flotation cell is decreased by about 70% (after removing all fibers in elutriation-spouting) and the disadvantage of the loss of long fibers [10] in flotation is eliminated. Another possibility is to selectively flocculate the fines and forming large particles that can be spouted in a second stage spouted bed from which the ink particles can be elutriated.

Table 4-4: The percentage solids removal and water consumption at different inlet diameters with m= 1.0 g and Q/Q_{ms} = 1.05

Inlet Diameter D (mm)	Percentage solids removal	Water consumption (L/g initial pulp)
1	39	4.1
2	37	4.2
3	33	4.4
4	34	4.5
6	38	4.8
(Average)	36	

4.5.3 Elutriation Coefficient

Figure 4.10 shows the values of k_e for the two cases of D = 4 mm (empty squares) and 6 mm (filled squares) with m=1.0 g. The elutriation coefficient is a measure of the specific rate of particle wash-out (or liquid replacement when the particle size is small enough), hence it is related to the reciprocal of the liquid residence time in the vessel. Consequently, it increases with increasing inlet flow rate and with decreasing volume of bulk liquid (i.e. the volume outside fiber flocs). The effect of the flow rate is more pronounced than that of the external voidage because the bed is very dilute and the fiber flocs do not have a permanent structure.

Figure 4.11 shows the effect of inlet diameter on the elutriation coefficient at two values of Q/Q_{ms}= 1.05 (empty squares) and 1.2 (filled squares) with m=1.0 g. At constant Q/Q_{ms}, increasing inlet diameter increases the operating flow rate (see Chapter 2) and thus the elutriation coefficient.

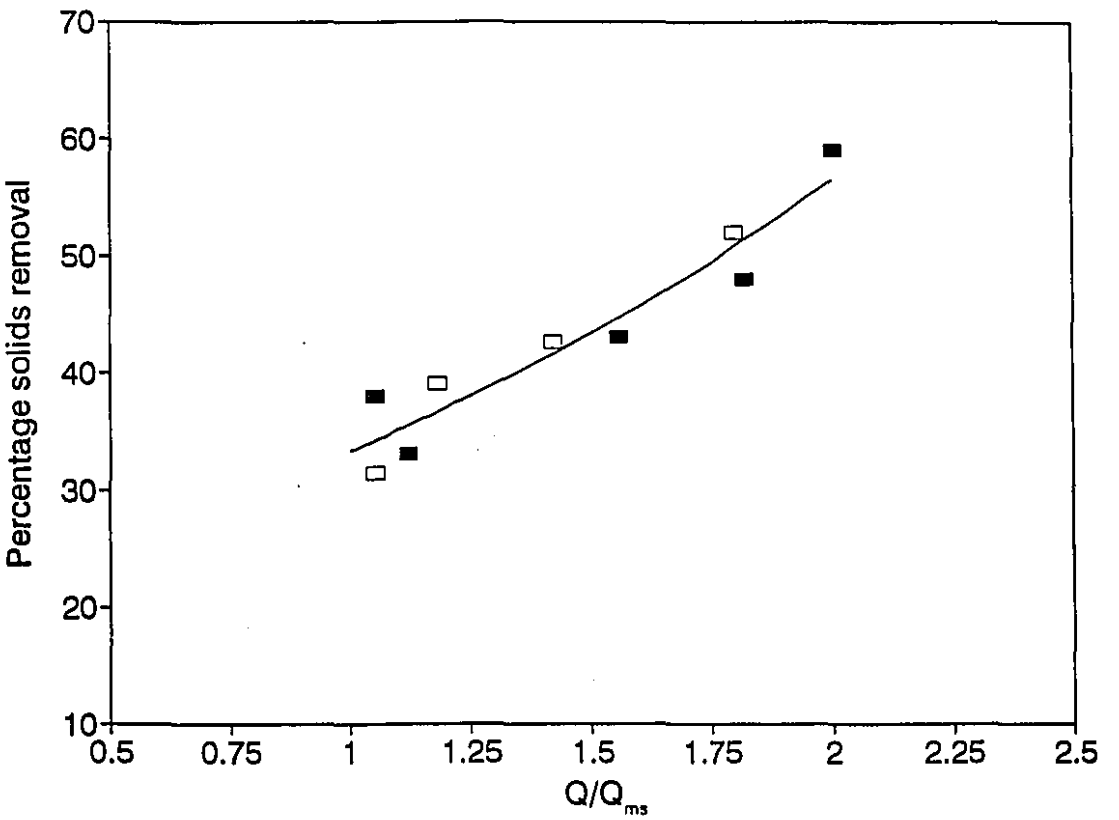

Figure 4.9: Percentage solids removal as a function of the ratio of flow rate to minimum spouting flow rate (Q/Q_{ms}) for the two cases of inlet diameter D = 4 mm (empty squares) and 6 mm (filled squares). The initial solids hold-up was 1.0 g.

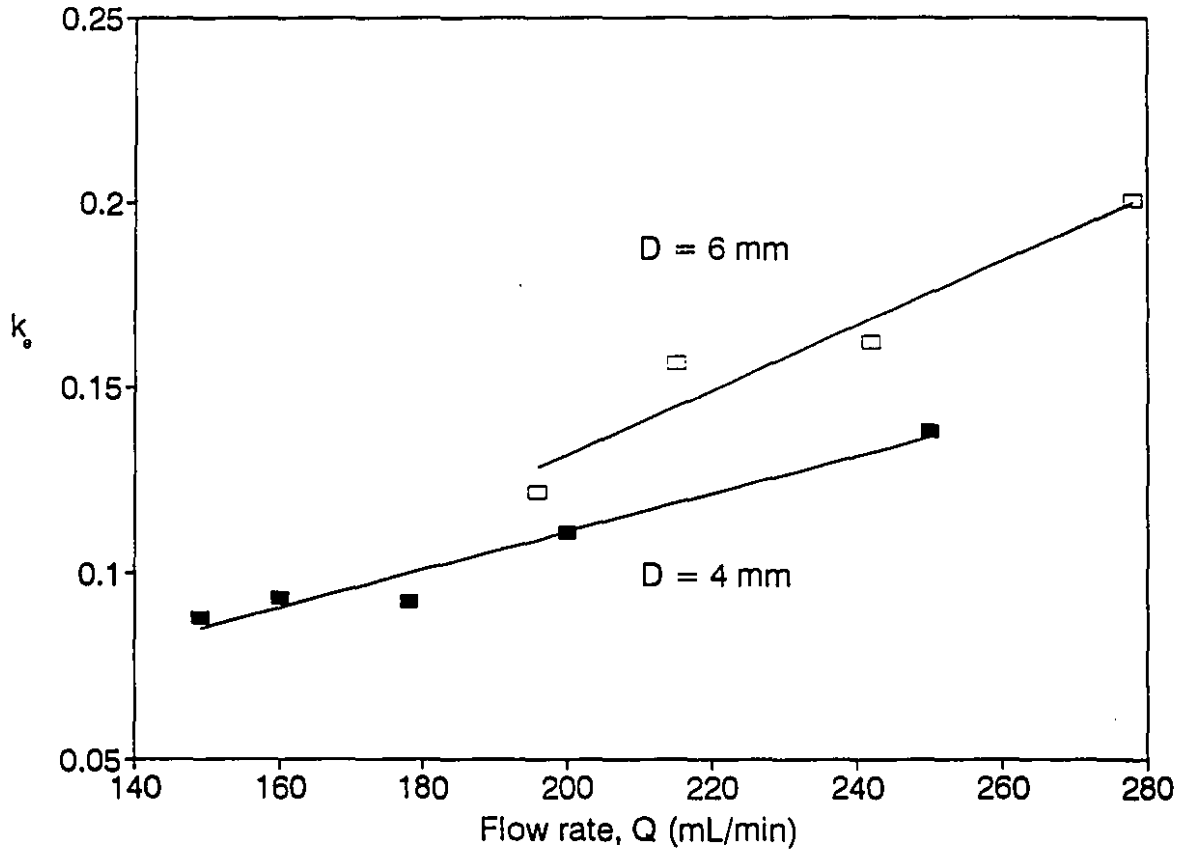

Figure 4.10: The elutriation coefficient (k_e) as a function of the flow rate (Q) for the two cases of D = 4 mm and 6 mm with m = 1.0 g.

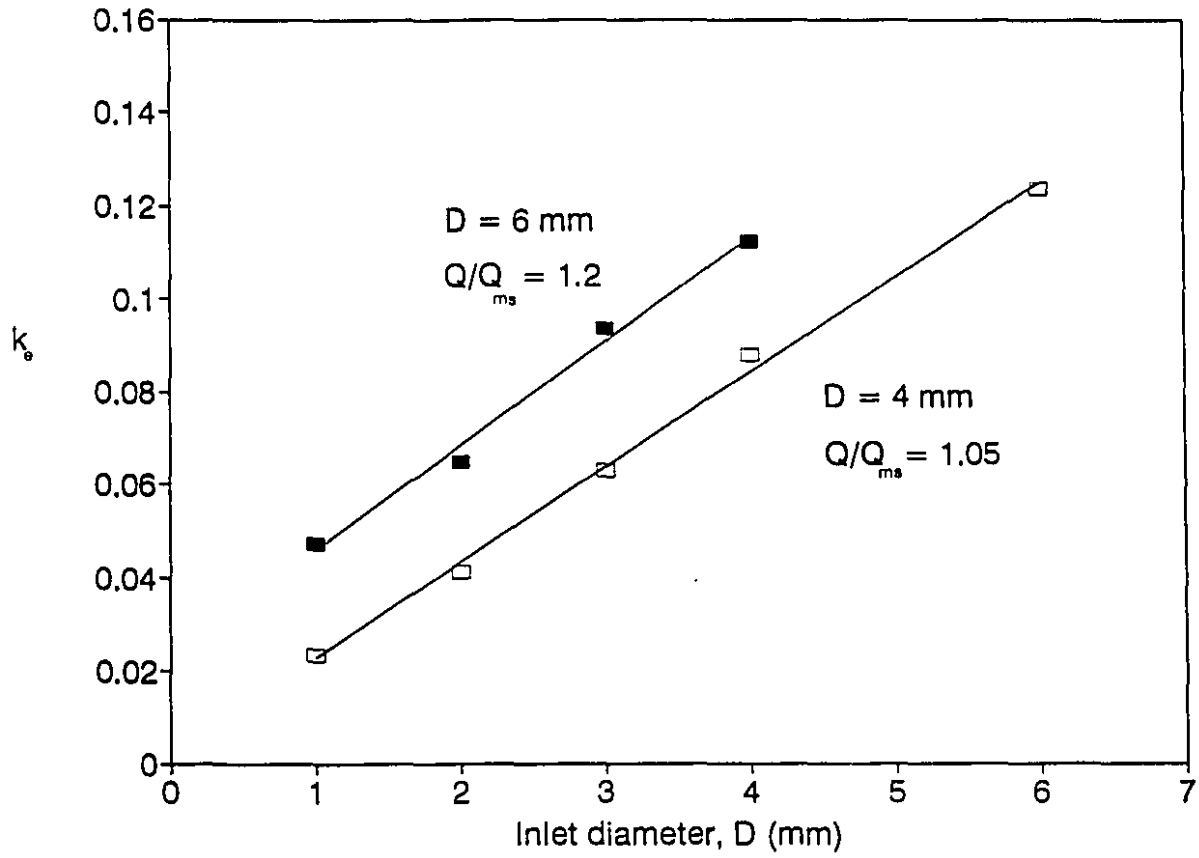

Figure 4.11: The elutriation coefficient (k_e) as a function of the inlet diameter (D) for the two cases of Q/Q_{ms} = 1.05 and 1.2. The initial solids hold-up was 1.0 g.

Figure 4.12 shows the effect of initial solids hold-up (m) on the elutriation coefficient. The triangles are for experiments with Q=160 mL/min and D=4 mm, the empty squares are for experiments with Q/Q_{ms} = 1.26 and D = 4 mm and the filled squares are for experiments with Q/Q_{ms}=1.07 and D=2 mm. These results show that m has little effect. The slight increase in k_e with increasing m at constant Q/Q_{ms} is attributed mainly to the increase in the operating flow rate (since Q_{ms} increases with m, see Chapter 2).

These findings are similar to those obtained by Ishikura et al. [21] on particle elutriation from a conventional liquid spouted bed of a binary mixture of rigid particles. They reported that the elutriation coefficient increased with increasing liquid velocity, while the initial solids hold-up and the inlet diameter (at constant flow rate) had little effect.

4.5. Conclusions

The elutriation-spouting technique removes ink and pulp fines from a recycled pulp suspension with small fiber loss (2%). It has the potential for being used in both deinking and fines-fiber separation.

The exit particle concentration was measured on-line as a function of time. The elutriation curve was similar to that reported for conventional spouted beds containing a binary mixture of rigid particles. The elutriation coefficient was dependent mainly on the flow rate. Increasing the flow rate, by increasing the ratio of flow rate to minimum spouting flow rate (Q/Q_{ms}) at the same inlet size and initial solids hold-up or by operating at larger inlet diameter or larger initial solids hold-up at the same Q/Q_{ms}, increased the elutriation coefficient. Operation at larger Q/Q_{ms} resulted in more fiber loss.

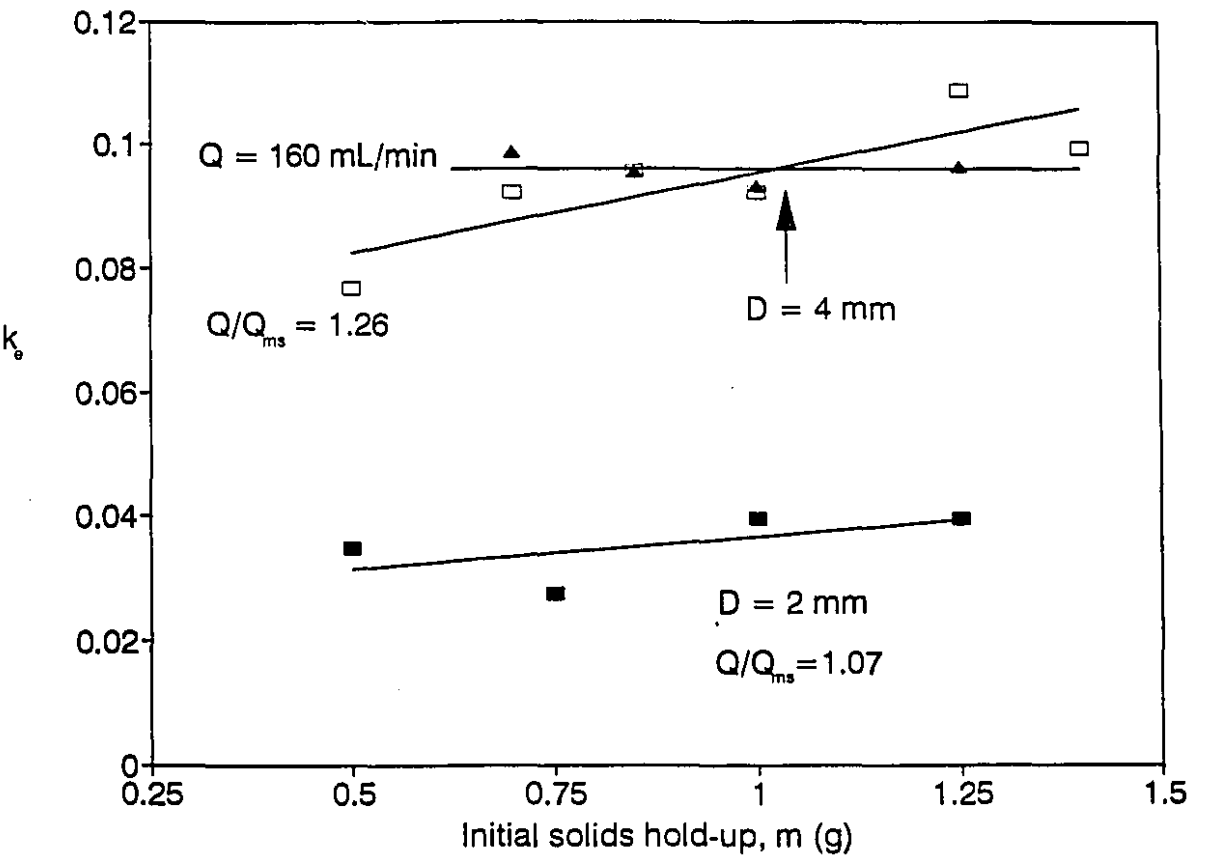

Figure 4.12: The elutriation coefficient (k_e) as a function of the initial solids hold-up (m). The triangles are for experiments with constant flow rate, Q = 160 mL/minute and inlet diameter of 4 mm. The squares are for experiments with constant ratio of flow rate to minimum spouting flow rate Q/Q_{ms}, the empty ones are with Q/Q_{ms}=1.26 and inlet diameter of 4 mm, the filled ones are with Q/Q_{ms}=1.0 and inlet diameter of 2 mm.

Nomenclature

A	Absorptivity (m^2 kg^{-1})
b	Path length (m).
c	Concentration of fines (kg m^{-3}).
c_o	Initial concentration of fines (kg m^{-3}).
C	Dimensionless concentration of fines.
D	Inlet diameter (m).
k_c	Elutriation coefficient (s^{-1})
m	Total initial mass of solids in the bed (g).
Q	Inlet liquid flow rate (m^3s^{-1})
Q_{ms}	Inlet liquid flow rate at minimum spouting conditions (m^3s^{-1}).
T	Transmittance of the exit stream.
T_o	Initial value of transmittance.
t	Time (s).
t_f	Total time for elutriation experiment (s).
Δm	Amount of particle removal by the liquid stream (g).

References

(1) E.D. Clark, F. R. Hamilton and J. H. Kleinau, "Economics of secondary fiber", in *Pulp and Paper Manufacture, Vol. 3,* Secondary Fibers and Non-Wood Pulping, (M.J. Kocurek, Ed.), 151-158 (1987).

(2) R.G. Horacek, "Washing ink from the pulp slurry", in *Pulp and Paper Manufacture, Vol. 3,* Secondary Fibers and Non-Wood Pulping, (M.J. Kocurek, Ed.), 179-188, (1987)

(3) M.A. McCool and L. Silveri, " Removal of specks and nondispersed ink from a deinking furnish", *Tappi, 70, 75-79* (1987).

(4) L. Pfalzer, "Deinking of secondary fibers, A comparison of washing and flotation", *Tappi, 63, 113-116* (1980).

(5) R.G. Horacek and A. Dewan, "Getting the most out of washing", *Tappi, 65, 64-68* (1982).

(6) R.A. Koffinke, "Modern newsprint system combines flotation and washing deinking", *Tappi, 68, 61-63* (1985).

(7) A. Shrinath, J. T. Szewczak and I. J. Browen, "A review of ink-removal techniques in current deinking technology", *Tappi, 74, 85-93* (1991).

(8) R.G. Horacek, "Using less water in deinking, The increasing significance of high-consistency washing", *Tappi, 62, 39-42* (1979).

(9) H.E. Ortner, "Flotation deinking", in *Pulp and Paper Manufacture, Vol. 3,* Secondary Fibers and Non-Wood Pulping, (M.J. Kocurek Ed.), 206-220 (1987)

(10) R.W. Turvey, "Why do fibers float", *JPPS, 19, 52-57* (1993).

(11) D. R. Crow and R.F. Secor, "The ten steps of deinking", *Tappi, 70, 101-106* (1987).

(12) J.M. Zabala and M.A. McCool, "Deinking at Papelera Peninsular and the philosophy of deinking system design", *Tappi, 71, 62* (1988).

(13) T. Allen, "Particle Size Measurement", 110-119 Chapman & Hall, London (1968).

(14) I. Tanaka, H. Shinohara, H. Hirosue and Y. Tanaka, "Elutriation of fines from fluidized bed", *J. Chem. Eng. Japan, 5, 51-56* (1972).

(15) I. Tanaka and H. Shinohara, "Elutriation of fines from fluidized bed-Study of transport disengaging height", *J. Chem. Eng. Japan, 5, 57-61* (1972).

(16) U.P. Ganguly, "Elutriation of solids from liquid fluidized bed systems, Part I: Onset of elutriation", *Can. J. Chem. Eng., 60, 466-469* (1982).

(17) U.P. Ganguly, "Elutriation of solids from liquid fluidized bed systems, Part II: Prediction of equilibrium bed concentration", *Can. J. Chem. Eng., 60, 470-474* (1982).

(18) U.P. Ganguly, "Elutriation of solids from liquid fluidized bed systems, Part III: A study of the possible cases of non-linearity in the elutriation of fine particles from fluidized beds", *Can. J. Chem. Eng., 64, 171-174* (1982).

(19) M. Leva, "Elutriation of fines from fluidized systems". *Chem. Eng. Progr.,47, 39-45* (1951).

(20) T. Ishikura, H. Shinohara and I. Tanaka, " Behaviour of fine particles in a spouted bed consisting of fine and coarse particles", *Can. J. Chem. Eng., 61, 317-324* (1983).

(21) T.Ishikura and I. Tanaka, "Behaviour and removal of fine particles in liquid-solid spouted bed consisting of binary mixtures", *Can. Chem. Eng. J., 70, 880-886* (1992).

(22) Report of the Physical and Chemical Standard Committee, Technical Section, CPPA, Standard C.4 (1950)

(23) R.J. Kerekes and C.J. Schell, "Characterization of fiber flocculation regimes by a crowding factor", *J.Pulp. Paper Sci., 18, p.32* (1992)

Chapter Five

Modeling Fines Elutriation from a Spouted Bed of Pulp Fibers

Abstract

A model was developed to describe the elutriation of fines from a spouted bed of aggregated coarse particles. The analysis was carried out for the general case of three liquid regions inside and around the coarse particle resulting from its porosity and rotation. The deaggregation of the coarse particles was accounted for by a particle source term. A system of three ordinary differential equations describing the particle balance in these regions was solved numerically. Depending on the size and the permeability of the coarse particle, the existence of each of the three regions in practical situations can be realized. The model can be simplified readily into a two regions model. The two region model was applied to the elutriation of fines from a spouted bed of pulp fibers with a first order source term for the release of particles (short fibers) from the fiber flocs. A good fit was obtained to the experimental elutriation curves of Chapter 4.

5.1. Introduction

In this thesis, the elutriation-spouting technique is investigated for the separation of small particles (including ink and pulp fines) from pulp fibers for the purpose of deinking and/or fines-fiber separation. Understanding this process requires the analysis of the behavior of pulp spouting and particle elutriation. In Chapter 3, a model for minimum spouting velocity for pulp spouting is presented. This chapter is concerned with a general model for particle elutriation from a spouted bed of a mixture of fines and aggregated coarse particles. Experimental elutriation curves from Chapter 4 are compared with the model developed here.

Data for particle elutriation from a spouted bed of recycled pulp suspension is reported in Chapter 4 where it is shown that both pulp fines and ink particles are elutriated at a rate which decreases with time. This qualitative behavior is similar to that reported in conventional applications of fluidization and spouting [1-7].

Models for particle elutriation from spouted (and fluidized) beds have been developed using two assumptions: (1) the bed is perfectly mixed, and (2) the rate of elutriation is proportional to the concentration of particles remaining in the vessel. The elutriation curves are characterized by a single parameter, the elutriation coefficient. At large times of elutriation, this model was found to disagree with experimental findings under certain circumstances (see Ref. 5 and Chapter 4). A model with a stronger physical basis which can describe particle elutriation for all times is needed.

The model developed below is based on the idea that when a porous coarse particle is subjected to a shear flow, there are three liquid regions within the vessel: the bulk of the liquid which is accessible to the external liquid flow, the region of open streamlines inside the porous particle which is accessible to liquid perfusion, and the region of closed streamlines inside the particle which is separated from the flow. Under certain circumstances only two regions are present depending on the

dimensionless radius of the coarse particles. When a mixture of fines and porous coarse particles is handled, the three regions contain particles that can be exchanged from one region to another by different mechanisms depending on the liquid transport process between them.

5.2. Development of the Model

When a solid particle is freely suspended in a fluid and has a different relative velocity from the fluid, there exists a hydrodynamic layer surrounding the particle due to the no-slip condition at its surface. The shape of this layer depends on the type of fluid flow, the relative velocity and the shape of the particle. For the case of a spherical particle subjected to a simple shear flow at low Reynolds number, there are two flow regions: the bulk of the fluid where the flow is represented by open streamlines and the hydrodynamic layer which forms a separated region in which the flow is represented by closed streamlines [8]. When a mixture of coarse and fine particles is present in such a flow field, some of the fine particles will be captured inside the hydrodynamic layer and orbit within it.

In the case of spherical particles and in the absence of flow disturbance or any repulsive force between the fines and the coarse particles, fines circulate around the coarse particle in closed orbits i.e. the fines remain near the coarse particles. However, fines may be detached (and re-attached as well) from the separated liquid region if there is a driving force for particle transport between the hydrodynamic layer and the bulk of the fluid. Such transport forces may be repulsive forces between the two particles and/or unsteady state effects which makes the streamlines open or make the separation surface change position thus resulting in liquid exchange between the two regions. As well, if the coarse particle is not spherical, the hydrodynamic layer will have spiral streamlines and consequently fines may enter this region, orbit the non-spherical particle a number of times and then leave [9].

In a spouted bed of pulp fibers, the coarse particles are fiber flocs which are

three dimensional porous networks (see Chapter 2 and 3). The flow patterns around a porous particle are different from those described above. Due to the permeability of the fiber floc some of the flow may perfuse the floc and a region of closed streamlines may be established inside the porous particle. In principle, modelling particle elutriation from beds of coarse porous particle should consider these liquid region.

The flow through and around a porous spherical particle in a creeping flow was investigated theoretically by Adler [10] for a uniform velocity and for a simple shear flow. A porous particles in a uniform flow is perfused by open streamlines, while for a porous particle in a simple shear flow, there are both open and closed streamline regions. The geometry of the region of closed streamlines is related to the dimensionless parameter ξ_1, defined by

$$\xi_1 = \frac{a}{k_p^{1/2}} \tag{5.1}$$

where a is the radius of the coarse porous particle and k_p is its permeability. At $\xi_1 = 10.89$ the surface separating the regions of closed and open streamlines coincides with the surface of the sphere (in the direction perpendicular to the flow, see Fig.5.1 a) [10]. When $\xi_1 < 10.89$, the porous sphere is partially perfused by open streamlines. When ξ_1 is very small, there are no closed streamlines and the porous particle is completely perfused. When $\xi_1 > 10.89$, the porous particle is surrounded by a region of closed streamlines similar to the case of a solid sphere.

The three regions are shown in Fig.5.1a. In addition to the liquid bulk outside the aggregated particle, region 1, there exist a region of open streamlines which perfuse part of the porous particle and a region of closed streamlines, region 2 and 3, respectively. The region of closed streamlines resembles the shape of a spheroid. Thus, part of it may be outside the surface of the porous particle (region 3a). Due to the rotation of the sphere and due to the fact that the flow in a spouted bed is

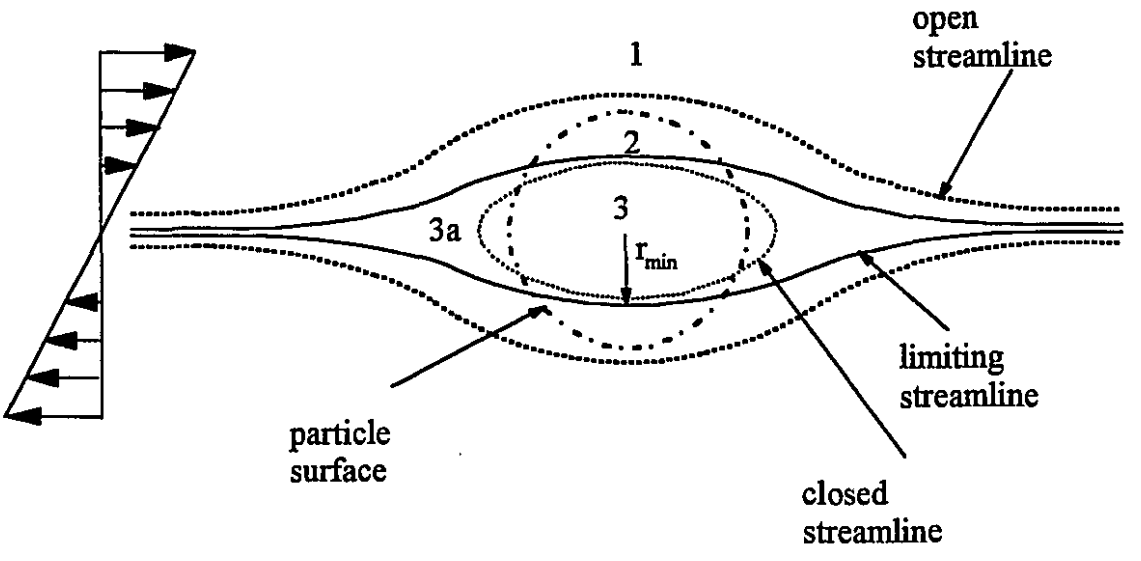

(a) Streamlines inside and around a spherical porous particle in a simple shear flow

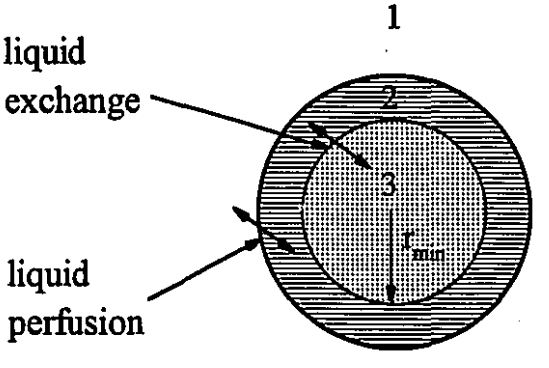

(b) The three regions considered in the model

Figure 5.1: The liquid regions inside and around a porous spherical particle: (a) in a simple shear flow, (b) the considered regions in the model.

continuously fluctuating, region 3a is rapidly equilibrated with the bulk. The part of region 3 which is between r_{min} and 1 is continuously exchanged with region 2 due to particle rotation. Consequently, region 3 can be considered as a sphere with radius r_{min}. For the purpose of particle transfer between the various regions, the three regions can be viewed, then, as shown in Fig.5.1b. Regions 2 and 3 are separated by a separation surface, the coordinate of which is given by the dimensionless radius (r_{min}) (non-dimensionalized with respect to a) [10]. The value of r_{min} is dependent on ξ_1 and thus the value of ξ_1 specifies the fraction of the liquid inside the porous particle that is accessible to liquid perfusion and the fraction that is separated (when $r_{min} < 1$).

The streamlines can be viewed as the trajectories of infinitesimally small particles. The existence of open streamlines crossing a porous particle requires that mass (or particle) transfer from inside the porous particle to the bulk occurs by convection. The rate of particle transfer between regions 1 and 2 should be given by the difference between the two convective fluxes. Vanishingly small particles cannot cross the separation surface between regions 2 and 3, hence they will not be removed if the flow is steady. The flow in a spouted bed is not steady because of the circulating motion of the aggregated particles between the spout and the annulus as well as the instability of jet flow (see Chapters 2 and 3). These phenomena change the flow conditions in the surroundings of the aggregated particle and cause de-aggregation and re-aggregation of the coarse particles. The separation surface between regions 2 and 3 inside the aggregated particle is not fixed but changes position. This fact, in addition to the rotation of the coarse particle, result in the exchange of material between regions 2 and 3. This process is referred to as liquid exchange. The volume of the exchanged liquid divided by the frequency of this process gives the rate of liquid exchange. Since each liquid fraction will contain particles in a concentration that is equal to the concentration in the region of its source, a net rate of particle transport will be achieved.

When the aggregated particles are composed of particles small enough to be

carried by the upward liquid flow upon de-aggregation, a net particle generation rate is obtained from the release of these particles into the liquid bulk. The source strength depends on the bond strength in the aggregated particle, the rate of re-aggregation and the size of the de-aggregated material. Aggregated particles may be composed of particles with a wide size distribution such that some of them have settling velocities larger than the upward liquid velocity. Alternatively some particles may be bonded to the aggregated structure by strong bonds, and thus they will be retained within the vessel providing a permanent solids hold-up which remains spouted (retentive hold-up). In this case, the particle generation term is a decreasing function with time since it depends on the difference between the present solids hold-up and the retentive solids hold-up. However, spouting of pulp fibers results in non-coherent flocs (see Chapter 3 and ref 11). In this case a pseudo-dynamic equilibrium is established between floc formation and break-up. During this process short fibers can be released from the structure of the floc and carried in the upward flow. The results of the material balance of Chapter 4 indicated that a fraction of the removed solids was generated during the period of elutriation since the obtained solids removal was larger than the initial fraction of fines. The fractional solids removal increased by increasing the ratio of flow rate to minimum spouting flow rate (see Fig.4.9).

The elutriation model is a mass balance for particles in the three liquid regions with different particle removal rates and a source term in the liquid bulk. Region 1 communicates with region 2 by liquid perfusion, while region 2 communicates with region 3 by liquid exchange. The net rate of particle elutriation from a spouted bed is dependent on the rates of particle transfer between these regions and the fractional volume of each region.

5.3. Elutriation Model

The following assumptions are made:

- The aggregated coarse particles are porous spheres with a constant radius "a".

- Inside the aggregated coarse particle, there are two regions, assumed to be concentric spheres. See Fig. 5.1 b.
- The two interior regions (regions 2 and 3) and the region exterior to the coarse particles (region 1) are well mixed (CSTR).
- The diameter of the inner region (region 3) of closed streamlines is constant at $2r_{min}$ (non-dimensionalized with respect to a). The diameter of the outer region (region 2) is 2.
- The outer region (region 2) is perfused by a constant flow Q_i.
- Between regions 2 and 3, liquid is exchanged at a constant volumetric rate Q_r.
- Elutriable particles are generated at a mass rate G_m.

Particle removal from a spouted bed of aggregated particles is represented schematically in Fig.5.2. The three CSTR cells represent the three regions shown in Fig 5.1. The mass balance equations for each of the regions shown in Fig.5.2 are:

$$V \epsilon \frac{dc_1}{dt} = Q_i (c_2 - c_1) - Q c_1 + V \epsilon G_m \tag{5.2}$$

$$V \epsilon_i \frac{dc_2}{dt} = Q_r (c_3 - c_2) - Q_i (c_2 - c_1) \tag{5.3}$$

$$V (1 - \epsilon - \epsilon_i) \frac{dc_3}{dt} = Q_r (c_2 - c_3) \tag{5.4}$$

where c_1, c_2, and c_3 are the particle concentrations in region 1, 2, and 3 respectively, t is the time, V is the total volume where spouting occurs, Q is the total volumetric flow rate to the vessel, G_m is the mass rate of release of particles by de-aggregation per unit total volume, ϵ is the external voidage (i.e. the fractional liquid volume which is outside the aggregated particle in region 1) and ϵ_i is the internal voidage (i.e.

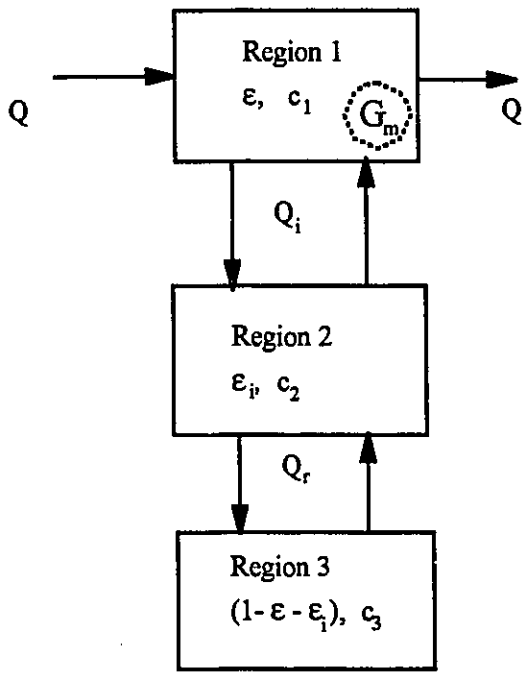

Figure 5.2: A schematic representation of the three regions particle elutriation model.

the fraction of the liquid volume inside the aggregated particle which is accessible to an internal flow). The volume fraction of the individual fibers is neglected since it is too small.

The concentrations (c_1, c_2, and c_3) are nondimensionalized as follows:

$$C_1 = \frac{c_1}{c_o}, \quad C_2 = \frac{c_2}{c_o}, \quad C_3 = \frac{c_3}{c_o} \tag{5.5}$$

where C_1, C_2 and C_3 are the dimensionless concentrations in regions 1, 2 and 3 respectively, and c_o is the initial concentration of small particles in the vessel. The time is non-dimensionalized with respect to the average residence time of the liquid in a solid-free vessel i.e.

$$t_r = \frac{t}{V/Q} \tag{5.6}$$

Implementing these dimensionless variables in eqns.5.2-4 results in the following system of equations

$$\epsilon \frac{dC_1}{dt_r} = -(1 + q_i) C_1 + q_i C_2 + \epsilon G \tag{5.7}$$

$$\epsilon_i \frac{dC_2}{dt_r} = q_i C_1 - (q_i + q_r) C_2 + q_r C_3 \tag{5.8}$$

$$(1 - \epsilon - \epsilon_i) \frac{dC_3}{dt_r} = q_r (C_2 - C_3) \tag{5.9}$$

where

$$q_i = \frac{Q_i}{Q}, \quad q_r = \frac{Q_r}{Q}, \quad G = \frac{V\, G_m}{Q\, c_o} \tag{5.10}$$

The rate of particle release from fiber flocs is proportional to the mass of short fibers that can be released (i.e. difference between the present mass of fibers and the retentive mass). Thus, the particle generation term is approximately an exponential decay term. As an approximation, a first order source term with respect to the concentration in the bulk (C_1) can be used;

$$G = K_g\, C_1 \tag{5.11}$$

where K_g is a dimensionless particle generation coefficient. For the purpose of comparison a constant source term was also tested.

The following initial conditions are required to solve the above system of first order ordinary differential equations (O.D.E) (eqns. 7-9):

$$at\ t_r=0 \quad C_1=1, \quad C_2=1, \quad C_3=1 \tag{5.12}$$

In addition to the dimensionless source term, four dimensionless parameters are required to characterize the system: ϵ, ϵ_i, q_i and q_r. Both of ϵ and ϵ_i are geometrical parameters and can be determined from the following equations, respectively:

$$\epsilon = 1 - \phi \tag{5.13}$$

$$\epsilon_i = (1-\epsilon)\ (1-r_{min}^3) \qquad (5.14)$$

where ϕ is the volume fraction of the aggregated coarse particles. For pulp fibers, ϕ is defined by eqn 3.7 and r_{min} is determined by the value of ξ_1 (see ref.10). The parameters q_i and q_r are determined by fitting experimental results.

Equations 5.7-9 are a linear system of first order O.D.E.'s. They can be solved mathematically by determining the eigenvalues and eigenvectors of the system matrix. Since the elements of the matrix are non-linear expressions of the parameters, the analytical solution is complex and the effects of the parameters are not easily seen. Hence, the system was solved numerically using the fourth order Runge-Kutta technique. Figures 5.3-5.5 show theoretical elutriation curves determined from the solution of the above model.

The effects of the transfer rates (q_i and q_r) are shown in Figures 5.3 and 5.4 with zero source term. Although both of them do not have large effects on the elutriation curves specially at large particle concentrations, the effect of q_i is more pronounced since it communicates with the bulk in which the concentration gives the elutriation curve. This fact shows that although three liquid regions may be present in practical application, the model can be simplified into two regions model as shown schematically in Fig.5.6. This simplification represents also the limiting cases of either very small values of ξ_1 or $\xi_1 > 10.89$, where only two regions exist communicating by liquid perfusion or liquid replacement, respectively. For pulp spouted bed, the value of $\xi_1 \approx 12$ i.e. the two regions model can be used to describe fines elutriation from a spouted bed of pulp fibers (see Chapter 4).

Figures 5.3 and 5.4 show also that when the source term is zero, the initial slope of the elutriation curve is always less than -1 since its absolute magnitude is proportional to the reciprocal of the external void fraction ($\epsilon < 1$). However, the existence of a source term may lead to elutriation curves with slopes larger than -1

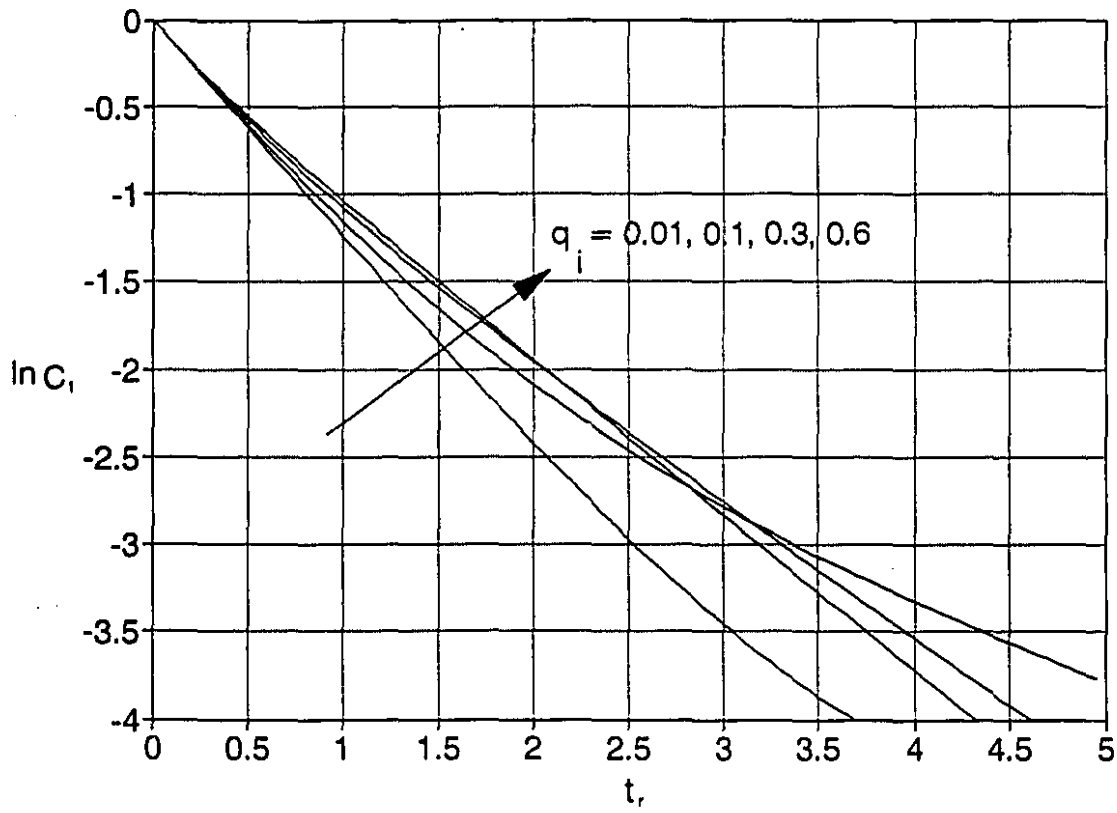

Figure 5.3: Effect of q_i on the theoretical elutriation curves for the three regions model. The values of the parameters are as follows: $\epsilon = 0.8, \epsilon_i = 0.1, q_r = 0.5$ and G=0

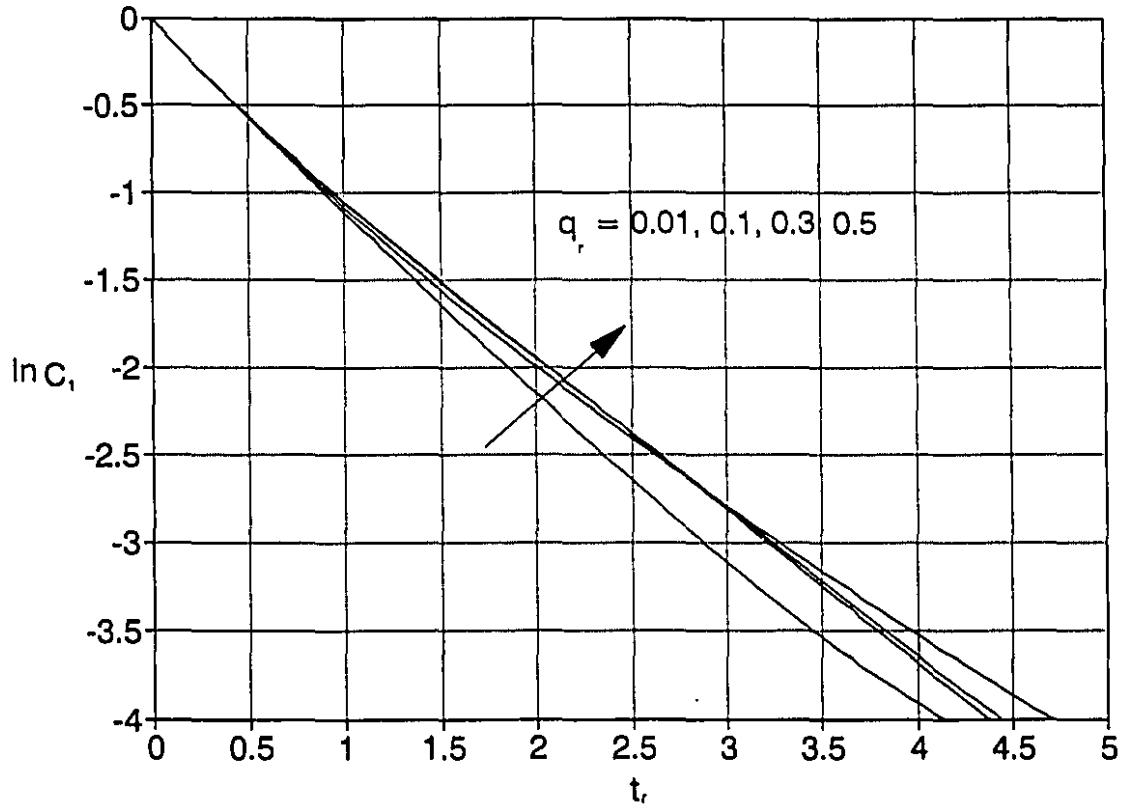

Figure 5.4: Effect of q_r on the theoretical elutriation curves for the three regions model. The values of the parameters are as follows: $\epsilon = 0.8$, $\epsilon_i = 0.1$, $q_i = 0.5$ and G=0.

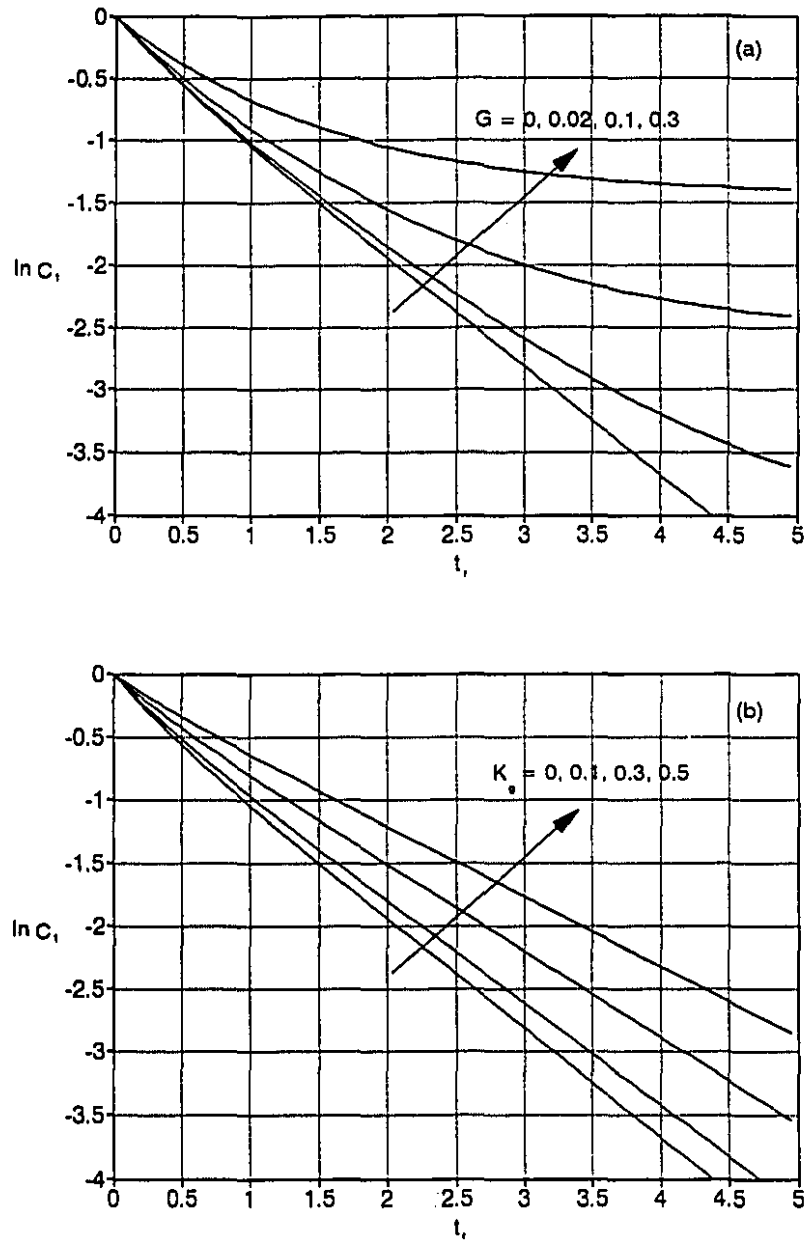

Figure 5.5: Effect of the strength of the source term on the theoretical elutriation curves. (a) Constant source and (b) first order source. The values of the parameters are as follows: $\epsilon = 0.8, \epsilon_i = 0.1, q_i = 0.5$ and $q_r = 0.5$.

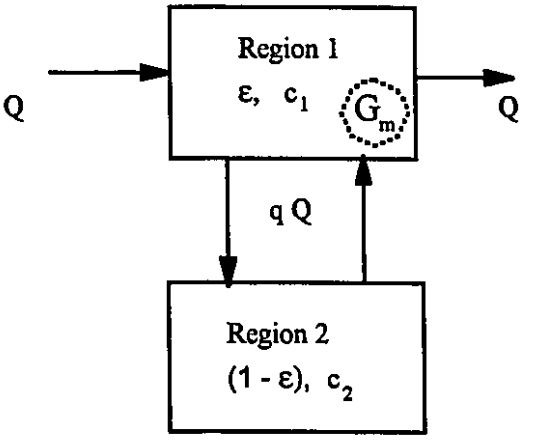

Figure 5.6: A schematic representation of the two regions particle elutriation model.

as shown in Fig.5.5 for the two cases of constant (figure a) and first order (figure b) source terms. The dimensionless plots of the experimental elutriation curves of Chapter 4 (see below) resulted in dimensionless curves with initial slopes larger than -1. This fact, in addition to the above mentioned fact of the solids removal being larger than the initial fraction of fines, indicated that the source term is essential to describe particle elutriation from spouted beds of recycled pulp suspensions. Since part of the fibers are relatively long, they will be attached to the floc network by stronger bonds than the short ones and even if they are released their settling velocity is higher than that of the short ones, consequently, there is pulp which cannot be carried by the upward liquid velocity. This indicates that the driving force of the generation term is governed by the difference between pulp hold-up and the retentive pulp hold-up which in turn is a decreasing function of time. Hence, the first order source term was chosen. Also, the constant source term resulted in larger shifts of the ln C_1 against t_r from linearity than the first order source term (compare Figs 5.5 a and b).

The two regions model with the first order source term which is used to fit experimental results of fines elutriation from pulp spouted bed is represented by the flowing system of PDE's and the corresponding initial conditions:

$$\epsilon \frac{dC_1}{dt_r} = -(1+q)\,C_1 + q\,C_2 + \epsilon\,K_g\,C_1 \qquad (5.15)$$

$$(1-\epsilon)\frac{dC_2}{dt_r} = q\,(C_1 - C_2) \qquad (5.16)$$

$$at\ t_r=0 \quad C_1=1, \quad C_2=1 \qquad (5.17)$$

where q is the dimensionless transfer rate between region 1 and 2 (see Fig.5.6).

An analytical solution of these equations was obtained which is very long and for this reason not included here.

Figures 5.7 to 5.9 show the effects of the three parameters of the two regions model (ϵ, q and K_g) on the elutriation curves. Figure 5.7 shows that increasing ϵ decreases the initial rate of particle elutriation since it is proportional to the reciprocal of ϵ. Figure 5.8 shows that increasing q decreases the initial rate of particle elutriation since it results in faster particle transfer from region 2 into region 1. Figure 5.9 shows that increasing K_g decreases the initial rate of particle generation since it increases the concentration of particles in region 1.

5.4. Comparison of Experimental Results with the Model

The experimental results of Chapter 4 indicated that the spouting region was followed by a fiber-free plug flow region in which the residence time (t_d) was given by the initial period of constant exit transmittance (or concentration). Hence, the time in the spouting region is non-dimensionlized as follows:

$$t_r = \frac{t_m - t_d}{V_T/Q - t_d} \tag{5.18}$$

where t_m is the measured time, and V_T is the total volume of the vessel and the additional tube volume between the exit from the vessel and the cell of the spectrophotometer (see Chapter 4). Figures 5.10 and 5.11 show two typical dimensionless plots for experiments with thermomechanically treated pulp using the blender and the British standard disintegrator, respectively.

Three dimensionless parameters are required to characterize the case of two regions with first order source term: ϵ, q and K_g. Equation 5.13 indicates that $\epsilon \approx 0.8$. Although ϵ is dependent on initial solids hold-up, a constant value of 0.8 is considered to be a good approximation in the range of operating conditions. The

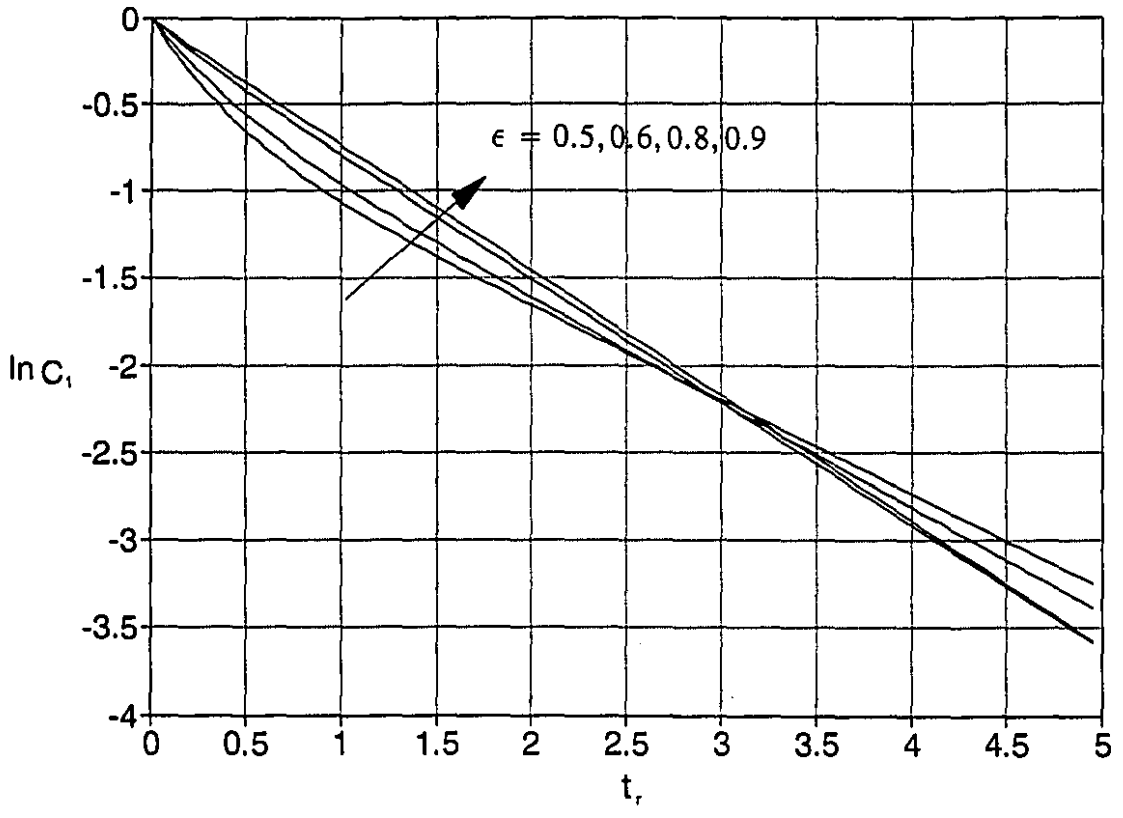

Figure 5.7: Effect of ϵ on the theoretical elutriation curves for the two regions model. The values of the parameters are as follows: q=0.5 and K_g=0.3.

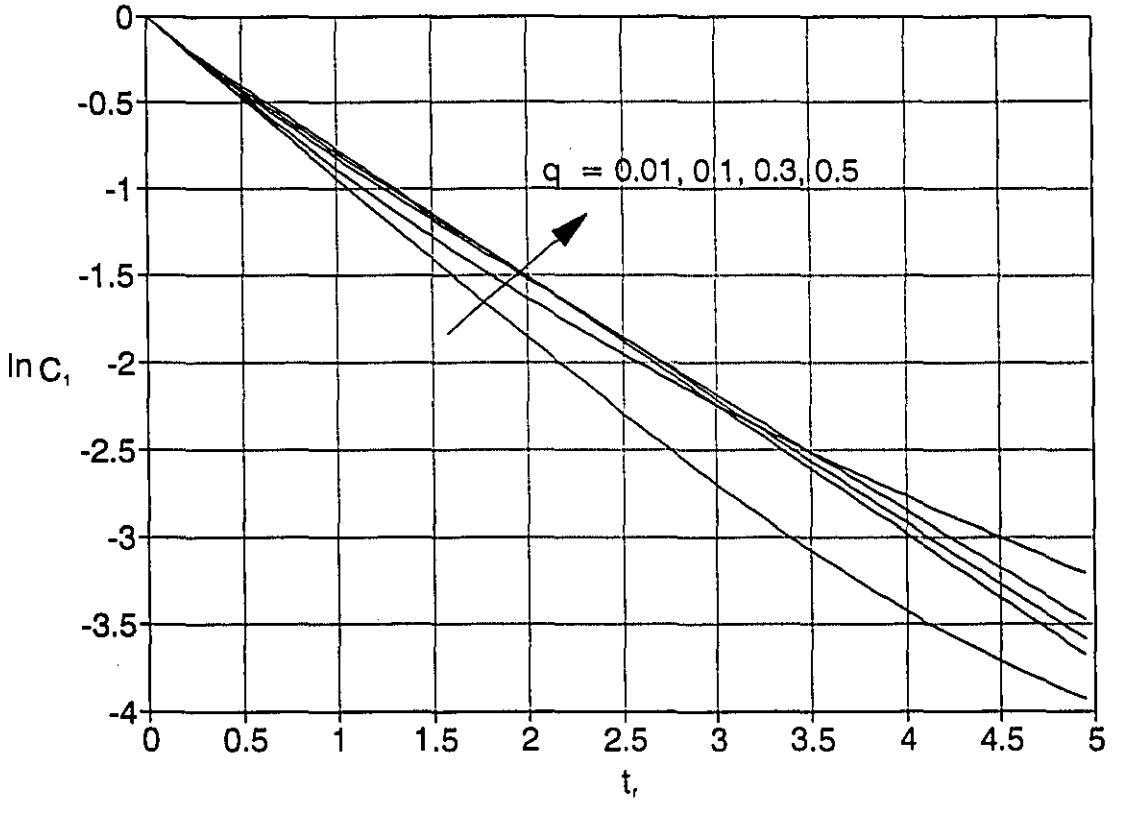

Figure 5.8: Effect of q on the theoretical elutriation curves for the two regions model. The values of the parameters are as follows: ϵ=0. 8 and K_g=0.3.

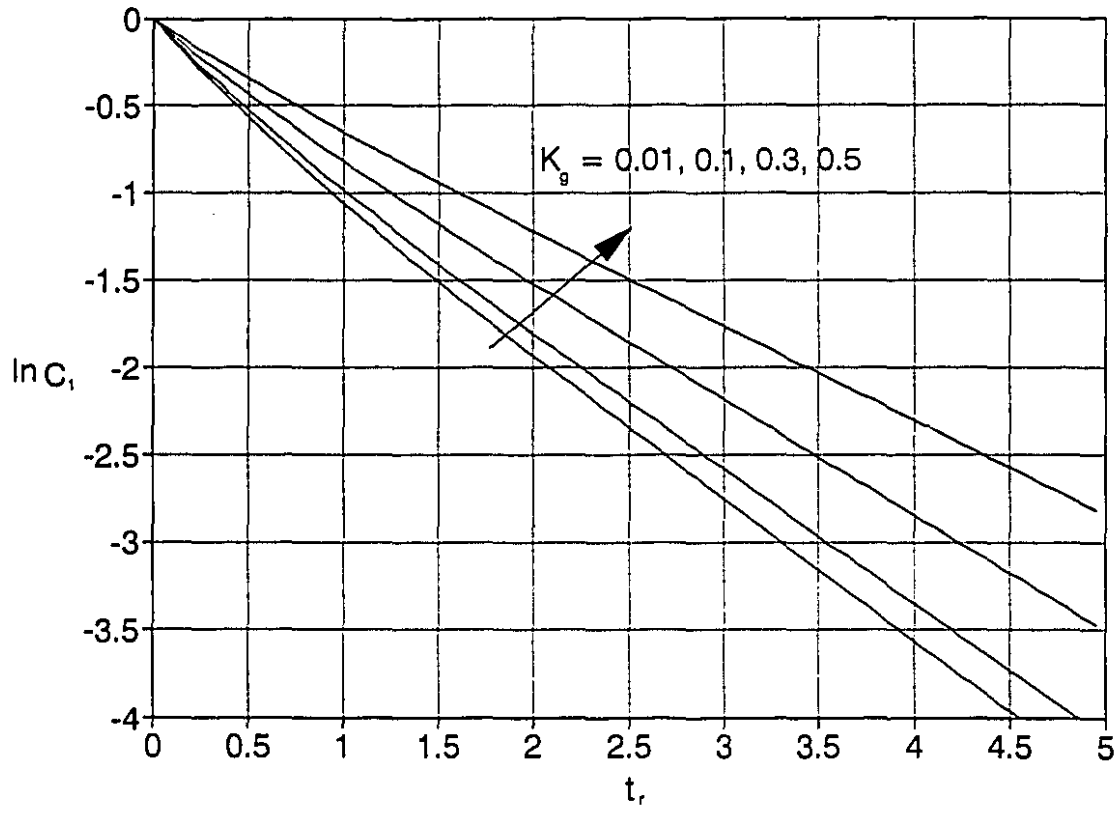

Figure 5.9: Effect of K_g on the theoretical elutriation curves for the two regions model. The values of the parameters are as follows: ϵ=0.8 , q=0.5.

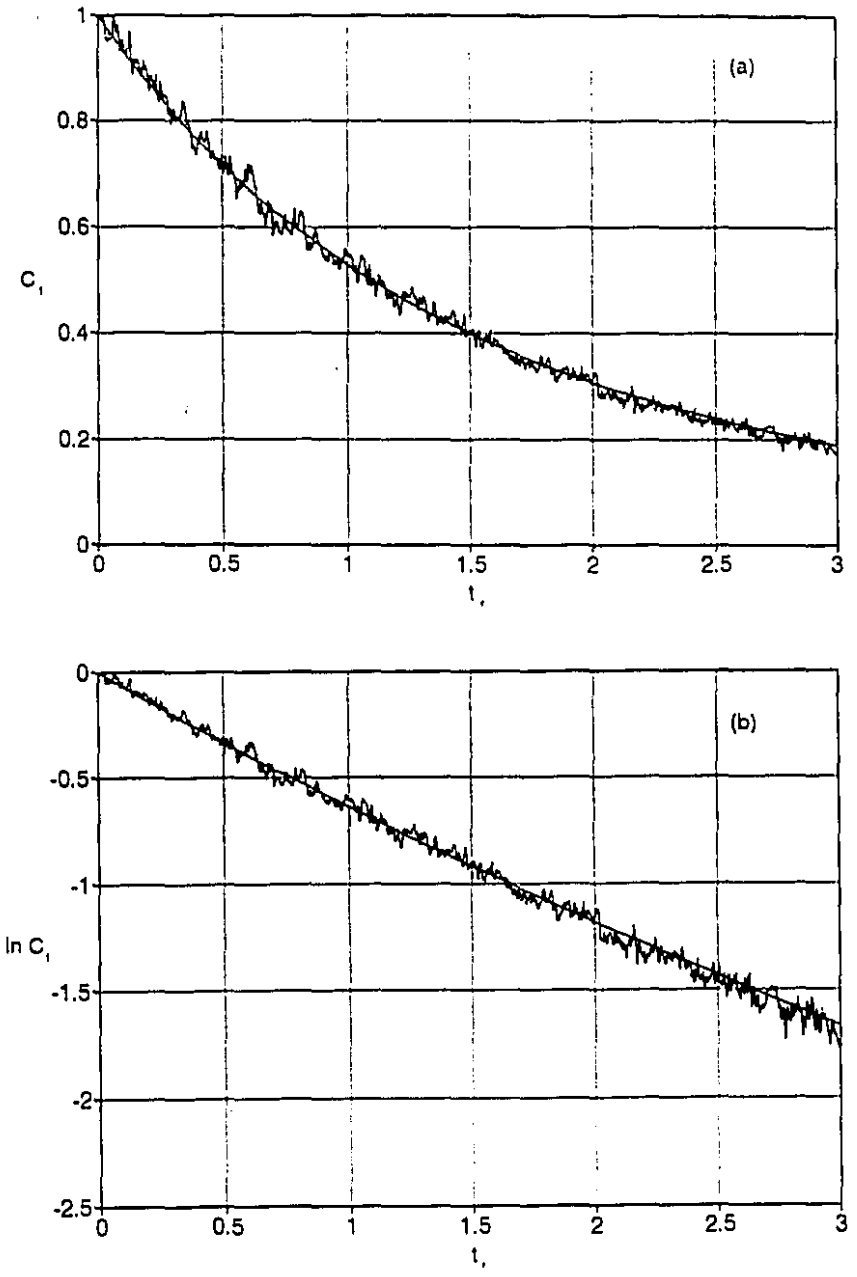

Figure 5.10: Dimensionless experimental elutriation curve from experiment with thermomechanically treated recycled pulp disintegrated in the blender compared with the theoretical prediction from the two regions case with first order source term. (a) C_1 against t_r (b) ln C_1 against t_r. The initial solids hold-up was 1.4 g, the inlet size was 4 mm and the flow rate was 200 mL/min. The values of the parameters are as follows: $\epsilon = 0.8, q = 0.14$ and $K_s = 0.56$.

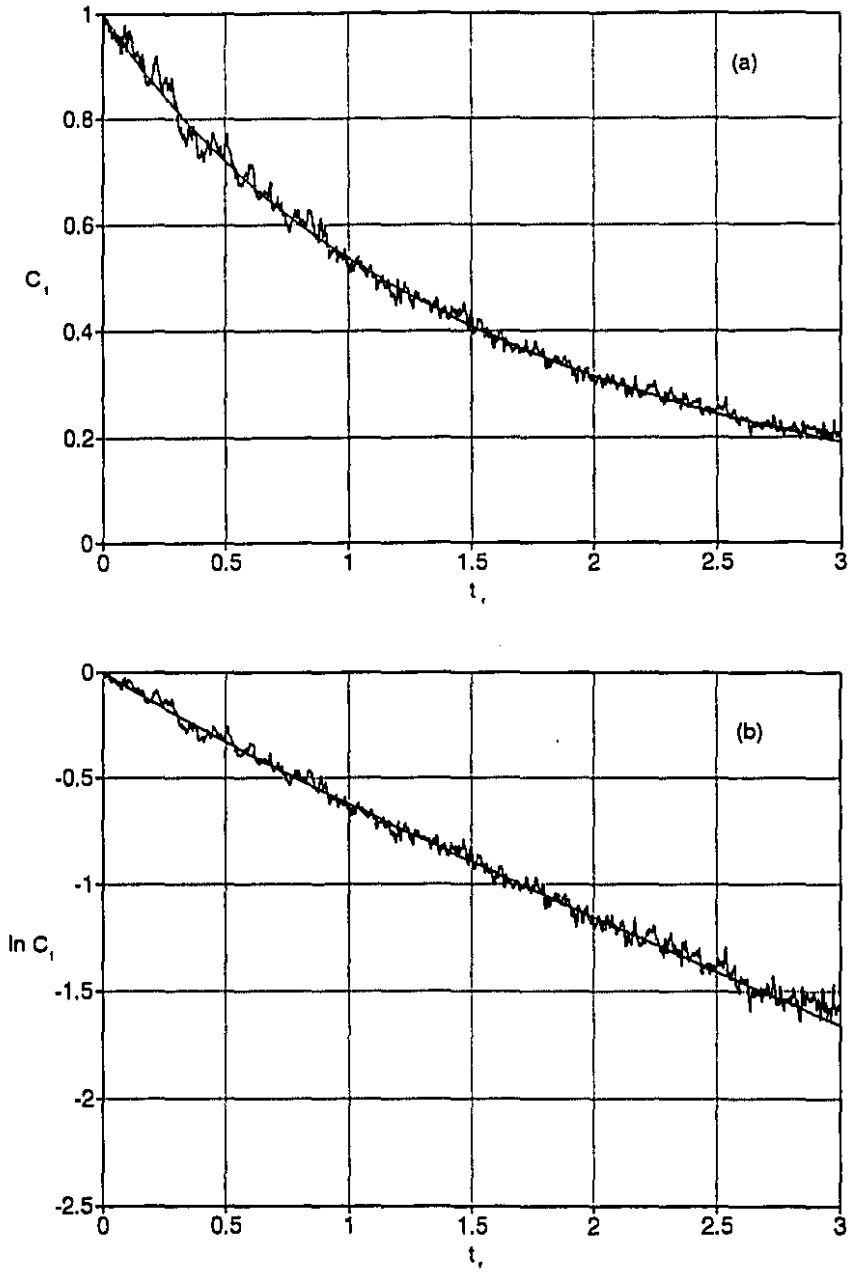

Figure 5.11: Dimensionless experimental elutriation curve from experiment with thermomechanically treated recycled pulp disintegrated in the British standard disintegrator compared with the theoretical prediction from the two regions case with first order source term. (a) C_t against t_r (b) ln C_t against t_r. The initial solids hold-up was 1.4 g, the inlet size was 4 mm and the flow rate was 200 mL/min. The values of the parameters are as follows: $\epsilon = 0.8, q = 0.24$ and $K_g = 0.55$.

values of q and K_g were determined from the best fit of the experimental elutriation curve (ln C_l vs. t_r plot). The fit minimized the summation of the normalized square deviations between the experimental and model values (E); the function E is defined as follows:

$$E = \sum \left(\frac{\ln C_{l,\,exp} - \ln C_{l,\,model}}{\ln C_{l,\,exp}} \right)^2 \qquad (5.16)$$

where the subscripts exp and model refer to experimental and theoretical curves respectively. The function E was minimized by numerical iteration for the optimum values of K_g and q. The obtained values of q and K_g were 0.14 and 0.56 for pulp from the blend, respectively, and 0.24 and 0.55 for pulp from the standard British disintegrator, respectively. Figures 5.10 and 5.11 show the fits for the two cases mentioned above.

The amount of particles released by the generation term is given by the integration of the source term between the initial and final particle concentrations. For an elutriation period between $C_l=1$ to $C_l=0$, the fraction of solids that has been released from the fiber flocs during elutriation is proportional to K_g. There is not much difference between the two values of K_g obtained from the fits of the curves from the two different disintegration methods; the amount of the generated particles is almost the same in both cases. The amount of generated particles (and consequently K_g) is expected to be dependent mainly on the size distribution of fibers and the differences between fibers settling velocities and the upward liquid velocity. Hence, for the same pulp, the value of K_g should be dependent mainly on the ratio of flow rate to minimum spouting flow rate (Q/Q_{ms}). Figure 5.12 shows a dimensionless plot for thermomechanically treated pulp in the blender at $Q/Q_{ms}=1.05$. The obtained values of q and K_g are 0.13 and 0.23 respectively. The corresponding value of Q/Q_{ms} in Fig.5.10(with the same pulp as in Fig.5.12) is 1.25. Increasing Q/Q_{ms} increases the net solid removal (see Fig.4.9) and thus increases the

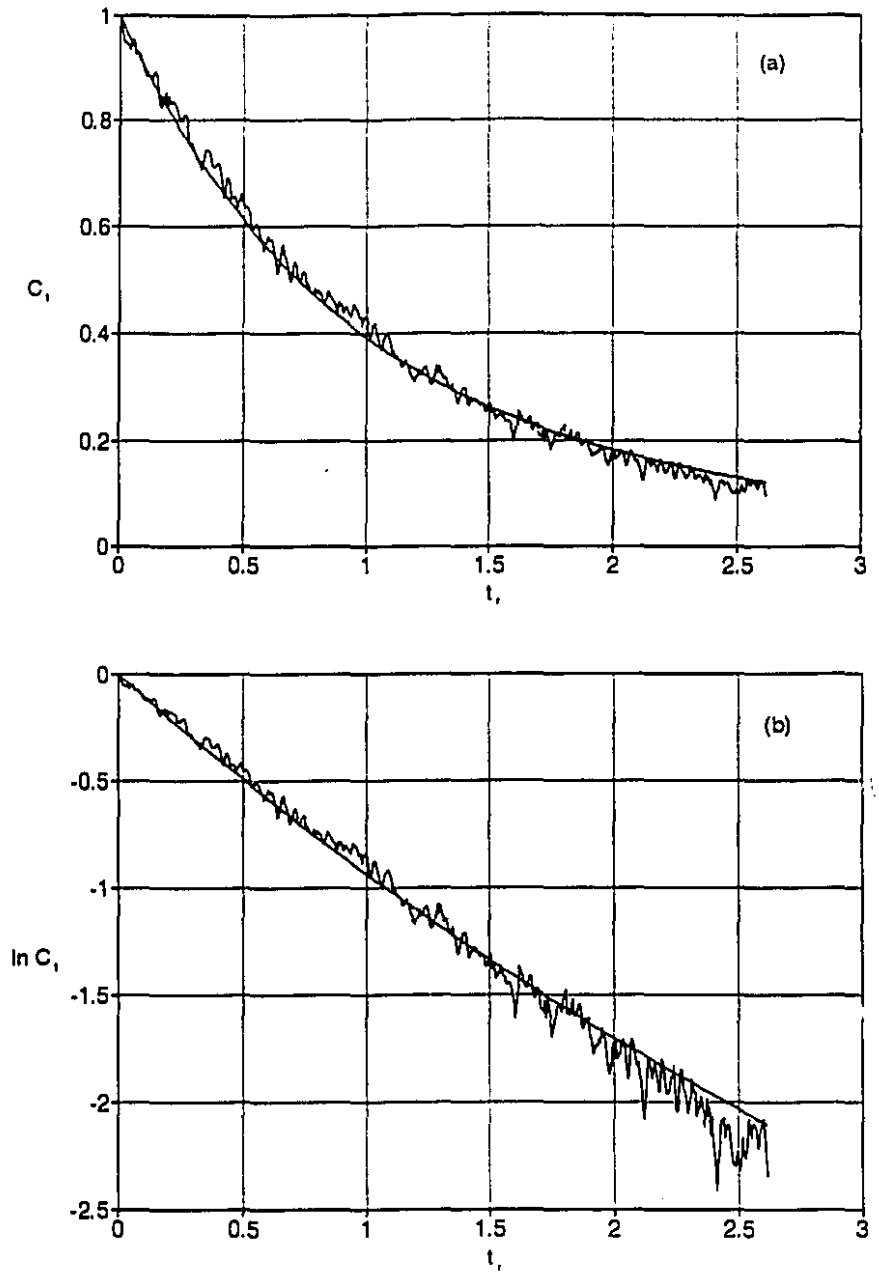

Figure 5.12: Dimensionless experimental elutriation curve from experiment with thermomechanically treated recycled pulp disintegrated in the blender compared with the theoretical prediction from the two regions case with first order source term. (a) C_1 against t_r (b) ln C_1 against t_r. The initial solids hold-up was 1.0 g, the inlet size was 3 mm and the flow rate was 100 mL/min (Q/Q_{ms} = 1.05). The values of the parameters are as follows: ϵ = 0.8, q= 0.13 and K_g= 0.23.

amount of released particles.

Disintegration in the standard British disintegrator produced more loose flocs than in the blender since the fibers were more stiff. Fiber flocculation and the strength of a fiber floc is enhanced by the flexibility of the fibers. When the fiber floc is loose, the process of de-flocculation and re-flocculation is more frequent. Thus, in this case, the rate of liquid exchange between regions 1 and 2 is large. Hence, the value of q for pulp from standard British disintegrator is larger than that for pulp from the blender. Comparing the values of q from the fits in Fig.5.10and 5.12 at different Q/Q_{ms} indicates that the value of q is not affected considerably by the flow rate (or Q/Q_{ms}) i.e. it is mainly dependent on the state of the floc.

5.5. Conclusions

A general model for particle elutriation from a spouted bed of a mixture of fines and coarse aggregated particles was developed from mass balance equations in the different liquid regions present inside and around the aggregated particles. The number of liquid regions can be determined from the permeability and size of the aggregated particle. For the case of particle elutriation from a spouted bed of a recycled pulp, the experimental elutriation curves are well fitted by the two regions model with a first order source term that accounts for the release of short fibers from the fiber flocs.

Nomenclature

- a Radius of the aggregated coarse particle, or fiber floc, (m).
- c_1 Concentration of fines in liquid bulk (far from aggregated particle) (kg m^{-3}).
- c_2 Concentration of fines in the region of open streamlines inside the aggregated particles (kg m^{-3}).
- c_3 Concentration of fines in the region of closed streamlines inside the aggregated particle (kg m^{-3}).
- C_1 Dimensionless concentration of fines in liquid bulk.
- C_2 Dimensionless concentration of fines in the region of open streamlines inside the aggregated particle.
- C_3 Dimensionless concentration of fines in the region of closed streamlines inside the aggregated particle.
- c_o Initial concentration of fines in the vessel (kg m^{-3}).
- G_m Source term; rate of particle release from aggregated coarse particles per unit total volume (kg m^{-3} s^{-1}).
- G Dimensionless source term.
- k_p Permeability of the aggregated particle (m^2).
- K_g Dimensionless particle generation coefficient.
- Q Volumetric flow rate fed to the vessel (m^3 s^{-1}).
- Q_i Volumetric flow rate perfusing the aggregated particle (m^3 s^{-1}).
- Q_r Volumetric liquid exchange rate between regions 2 and 3 (m^3 s^{-1}).
- q_i Dimensionless value of Q_i.
- q_r Dimensionless value of Q_r.
- q Dimensionless rate of liquid transport between the two regions in the case of two liquid regions.
- Q_{ms} Minimum spouting flow rate (m^3 s^{-1}).
- r_{min} Minimum distance of approach i.e. the coordinate of the boundary between the regions of open and closed streamlines (dimensionless).
- V Total volume occupied by pulp suspension (m^3).
- V_T Total volume of the vessel and the tubings (m^3).

t time (s).

t_m measured time (s).

t_d dead time between the surface of the spouted bed and the spectrophotometer (s)

t_r dimensionless time.

ϵ external void fraction in a spouted bed of aggregated particles.

ϵ_i internal void fraction.

ξ_1 dimensionless radius of the aggregated particle defined by eqn. 5.1

ϕ volume fraction of the aggregated particles in the vessel.

References

(1) I. Tanaka, H. Shinohara, H. Hirosue and Y. Tanaka, "Elutriation of fines from fluidized bed", *J. Chem. Eng. Japan, 5, 51-56* (1972).

(2) I. Tanaka and H. Shinohara, "Elutriation of fines from fluidized bed-Study of transport disengaging height", *J. Chem. Eng. Japan, 5, 57-61* (1972).

(3) U.P. Ganguly, "Elutriation of solids from liquid fluidized bed systems, Part I: Onset of elutriation", *Can. J. Chem. Eng., 60, 466-469* (1982).

(4) U.P. Ganguly, "Elutriation of solids from liquid fluidized bed systems, Part II: Prediction of equilibrium bed concentration", *Can. J. Chem. Eng., 60, 470-474* (1982).

(5) U.P. Ganguly, "Elutriation of solids from liquid fluidized bed systems, Part III: A study of the possible cases of non-linearity in the elutriation of fine particles from fluidized beds", *Can. J. Chem. Eng., 64, 171-174* (1982).

(6) T. Ishikura, H. Shinohara and I. Tanaka, " Behaviour of fine particles in a spouted bed consisting of fine and coarse particles", *Can. J. Chem. Eng., 61, 317-324* (1983).

(7) M. Leva, "Elutriation of fines from fluidized systems". *Chem. Eng. Progr.,47, 39-45* (1951).

(8) S.V. Kao, R.G. Cox, S.G. Mason, "Streamlines around single spheres and trajectories of pairs of spheres in two-dimensional creeping flows", *Chem. Eng. Sci. 32, 1505* (1977)

(9) Z. Adamczyk and T.G.M. van de Ven, " Pathlines around freely rotating spheroids in simple shear flow", *Int. J. Multiphase Flow, 9, 203-217* (1983)

(10) P.M. Adler, " Streamlines in and around porous particles", *J. Colloid Interface Sci., 81, 531-535* (1981).

(11) R.J. Kerekes and C.J. Schell, "Characterization of fiber flocculation regimes by a crowding factor", *J. Pulp. Paper Sci., 18, p.32* (1992)

Chapter Six

Continuous Elutriation of Fines from a Wedge-Shaped Vessel

Abstract

A continuous particle elutriation process was demonstrated in a wedge-like vessel having the required geometry for the continuous removal of fines from a recycled pulp suspension. The vessel had an inclined tube at one vertical end wall that served as an inlet for the suspension. Near the other vertical end, the suspension flow was split into a bottom stream containing the recovered pulp and a top stream containing the separated fines. The effect of the operating conditions on both the hydrodynamic behavior and the separation efficiency was investigated.

There were two critical limits for the operating flow rates of the feed suspension: below a minimum flow rate fibers settled near the bottom exit and above a maximum flow rate fibers escaped in the top stream. These limiting flow rates did not show a strong dependence on the other operating conditions. There was a maximum inlet consistency above which the pulp bed expanded into the exit section and no separation took place.

The particle concentration in the top stream was measured with a spectrophotometer, from which the separation efficiency was determined as a function of the inlet and outlet flow rates and the inlet consistency. The separation efficiency increased with increasing split ratio (i.e. the ratio of top to bottom streams) and with decreasing consistency of the feed suspension. Fiber loss in the top stream was about 1% of the fibers fed.

6.1. Introduction

The process of spouting-elutriation can remove pulp fines and ink from a recycled pulp suspension in a semi-batch operation mode in a conical vessel. An industrial application of this process would require continuous operation. In this chapter, continuous elutriation is demonstrated experimentally in a wedge-like vessel.

6.2. Experimental Apparatus and Procedure

The wedge-like vessel used in this chapter is shown in Fig.6.1. It consisted of a lower diverging channel of 30° angle opening to an upper converging channel of 60° angle. The total height of the vessel was 36.6 cm and the length was 25.4 cm. The vessel was closed at the bottom and the top by flat strips with widths of 12 and 10 mm, respectively. Five identical tubes of 3 mm ID spaced 5 cm apart and centered the vessel through the top and the bottom strips. The outermost tubes were 2.7 cm from the vertical side walls. The bottom tubes served as an inlet for a crossflow and the top tubes as an outlet for the stream containing the elutriated particles. The suspension inlet was a tube of 1 cm ID inclined at an angle of 31° between its axis and the vertical vessel wall. It was placed at a height of 11.5 cm from the bottom of the vessel and centered at that height. The bottom outlet was a vertical tube of 1 cm ID placed adjacent to the vertical wall at the opposite end from the inlet. The vessel and the tubes were made from Plexiglas.

The system flowsheet is shown in Fig.6.2. A continuously mixed vessel of about 37 L volume was the main reservoir for the pulp suspension. The pulp suspension was prepared in a way similar to that described in Chapter 4, using the thermomechanical treatment method, and diluted in the vessel to the required consistency (X_s). A centrifugal pump transported the pulp suspension to a tank which was designed with an overflow to provide a constant head feed for the process

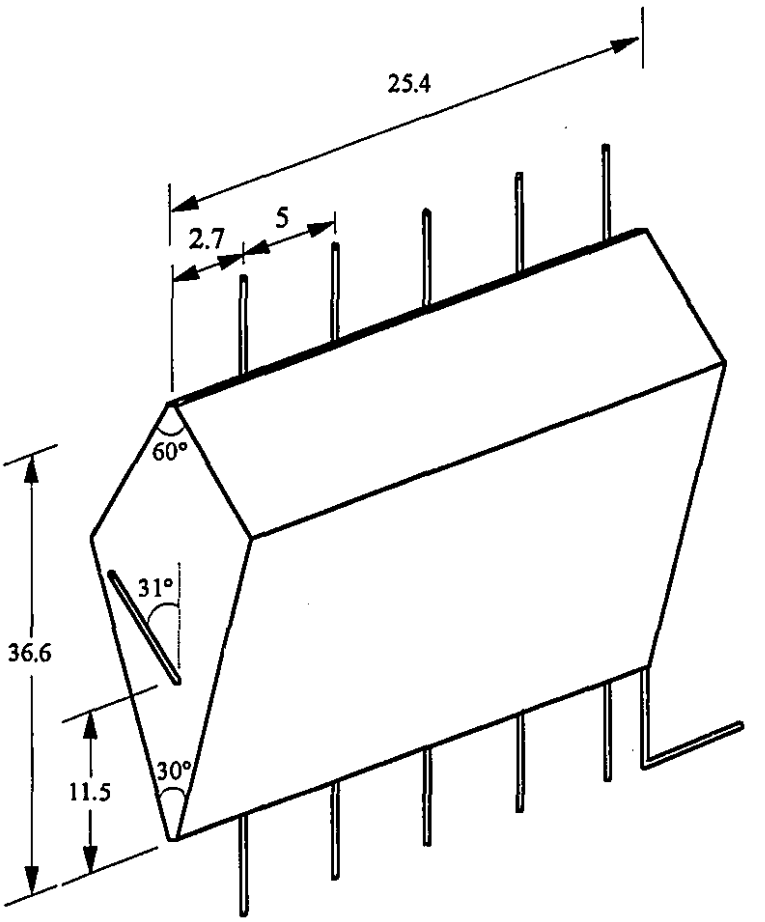

Figure 6.1: The wedge-like vessel. Dimensions in cm

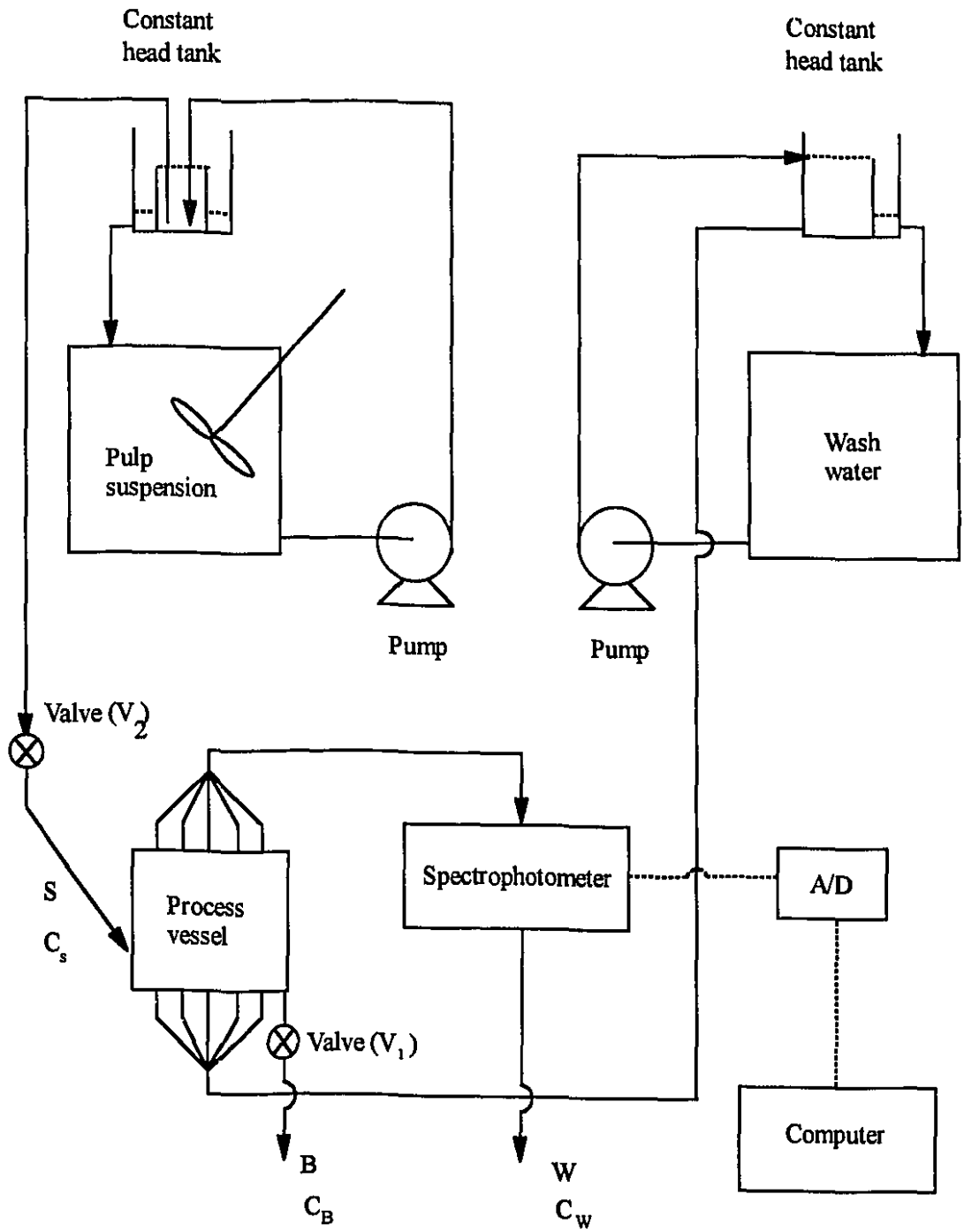

Figure 6.2: The experimental set-up

vessel. The overflow was circulated back to the pulp reservoir. The circulation rate was high enough to keep the solids suspended in the constant head vessel. The suspension feed (S) flowed by gravity to the wedge-like process vessel. The flow rates were controlled manually by valves (V_1 and V_2). Within the process vessel, the suspension was split into a bottom stream (B) containing the recovered pulp and a top stream (W) containing the elutriated particles. The top stream passed through a spectrophotometer to measure the transmittance, as described in Chapter 4. The measured transmittance was shown on the computer screen in real time. The concentration of fines was determined by the Beer-Lambert law.

In order to investigate the mechanism of particle separation, experiments were performed with suspensions of small particles (Avicel particles of 20 μm size, see Chapter 4) and fines-free fiber suspensions (kraft hardwood). Both suspensions were prepared as described in Chapter 4. In these cases, the bottom stream flowed through a second spectrophotometer which was also connected to the computer. For experiments with fines-free fiber suspensions, the percentage fiber loss from the feed in the top stream was determined by filtrating a known volume of the top stream over a 150 mesh screen as described in Chapter 4.

In some experiments, a cross-flow of fiber and particle-free water was introduced to the vessel through the five bottom tubes (see Fig.6.1). For this purpose a flow circuit similar to that for the pulp suspension was used.

The cross-flow water flow rate was measured using a flowmeter, while the two exit streams were measured by sample collection over known time intervals. The suspension feed rate was determined from the overall mass balance. Since the flow rates were adjusted manually, it was difficult to set them to the required values and the accumulation of fibers within the vessel during the time required to reach steady state caused a deviation in the flow rates from the pre-set values. Hence, there was an error of the order of a few percent in the mentioned flow rates.

In addition to the determination of particle concentration in the top stream, small samples of the suspensions from both the feed and the bottom streams were taken and subsequently dried to determine the solid content.

6.2.1. Data and Analysis

The experiment required about 30 minutes to reach steady state operation since the volume of the process vessel was large (about 7.5 L). A typical example of a start-up transient is shown in Fig.6.3 for the case of an inlet consistency of 0.5 g/L, feed flow rate of 740 mL/minute and split ratio (W/B) of 1.4. The figure shows the measured transmittance of the top stream as a function of time for an experiment with a recycled pulp suspension fed into a liquid-filled, solid-free vessel. The transmittance decreased with time to a constant value of T_{w_s} at steady state.

The separation efficiency η is defined as the fractional removal of small particles from the feed suspension at steady state i.e.

$$\eta = \frac{C_w W}{C_s S} \tag{6.1}$$

where W and S are the flow rates of the top stream and the feed suspension and C_w and C_s are the particle concentrations in W and S, respectively. Since all streams have densities close to 1 g/L, the overall mass balance may be written

$$S = W + B \tag{6.2}$$

where B is the flow rate of the bottom stream. Combining eqns 6.1 and 6.2

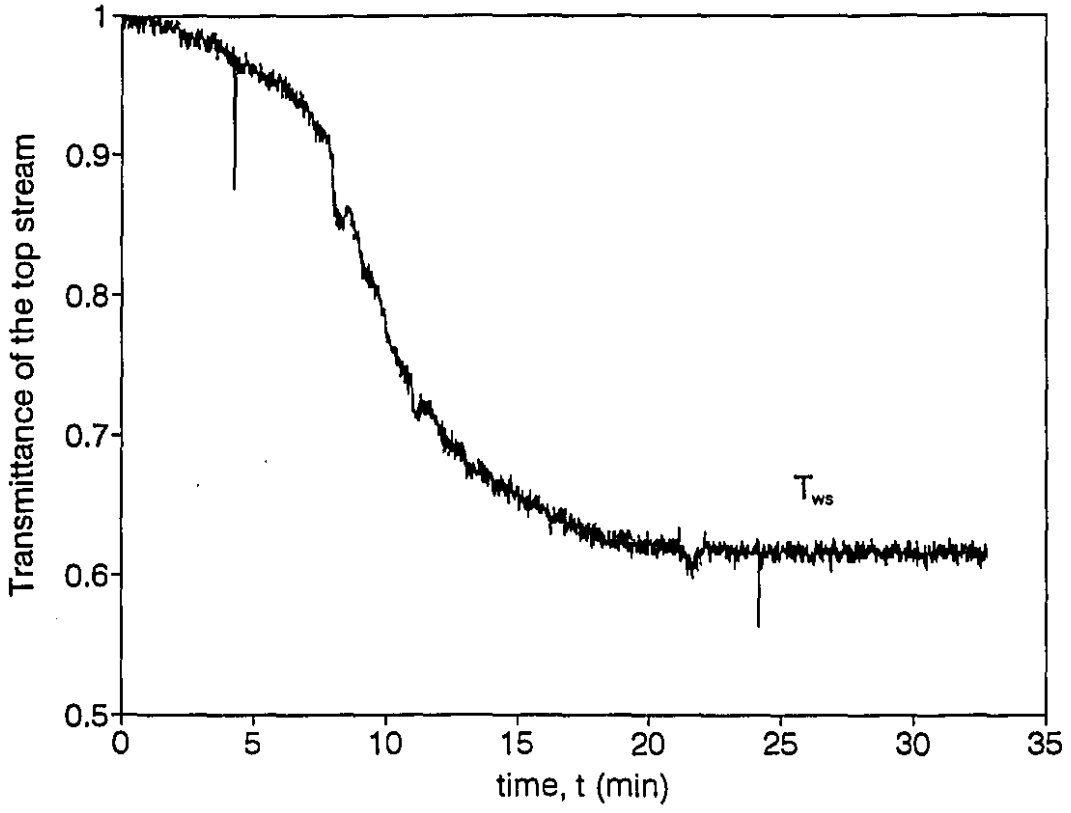

Figure 6.3: A typical example of the measured transmittance of the top stream as a function of time for an experiment with recycled pulp suspension fed into a liquid-filled, solid free process vessel. The inlet consistency was 0.5 g/L, the feed flow rate was 740 mL/minute and the split ratio (W/B) was 1.4. The steady state transmittance is T_{ws}.

$$\eta = \frac{C_w}{C_S} \frac{W/B}{1 + W/B} \tag{6.3}$$

The experimental separation efficiency was calculated from eqn 6.3 using C_w determined from the measured steady state transmittance (T_{ws}) through the Beer-Lambert law:

$$C_w = \frac{1}{A\ b} \ln \left(\frac{1}{T_{ws}}\right) \tag{6.4}$$

where A and b are the absorptivity and the path length, respectively. An approximate value of the product "Ab" for fines from a recycled pulp suspension was determined from experiments with the conical vessel of Chapter 4. In the semi-batch process, the initial transmittance of the exit suspension corresponded to the initial concentration of fines. Measuring the initial transmittance with different initial solids hold-ups, and knowing that the initial fraction of small particles (ink and pulp fines) was about 0.35 (Chapter 4), gave the transmittance-concentration calibration. The curve is shown in Fig.6.4. The estimated value of the product "Ab" in eqn.6.4 was 3.0 L/g.

The concentration of particles in the feed, C_s, may be expressed as a fraction of the inlet consistency.

$$C_s = y\ X_s \tag{6.5}$$

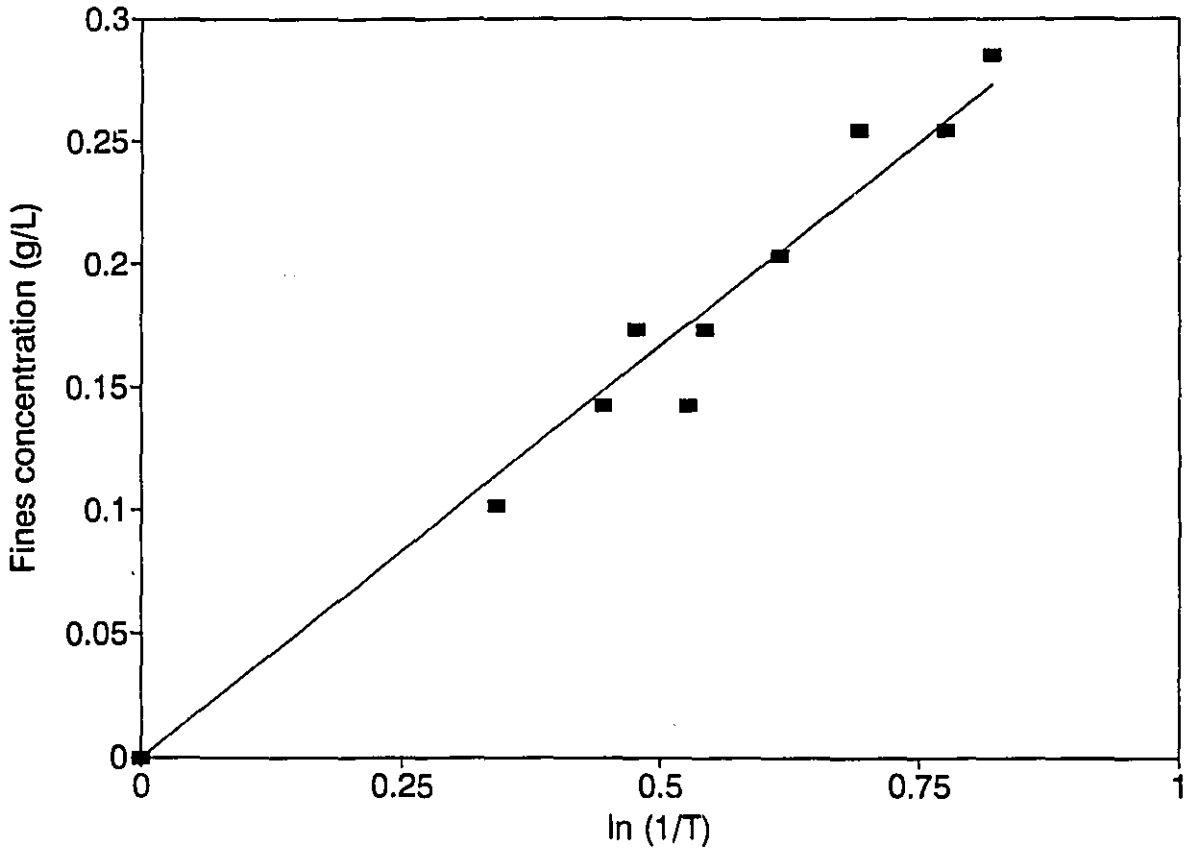

Figure 6.4: Calibration curve of the spectrophotometer for suspensions of fines from a recycled pulp suspension.

where y is the fraction of fines in the total suspended solids (g fines/g total pulp) and X_s is the feed consistency (g pulp/L suspension). Typical values of y are in the range of 0.3 to 0.4. Combining eqns. 6.3, 6.5 and 6.6 yields the following equation which was used to calculate the separation efficiency from experimental values of the feed consistency, the split ratio and the steady state transmittance of the top stream.

$$\eta = F \frac{W/B}{1 + W/B} \frac{1}{X_s} \ln \left(\frac{1}{T_{ws}}\right) \tag{6.6}$$

where

$$F = \frac{1}{yAb} \tag{6.7}$$

For a given feed suspension, A is a constant. For the recycled pulp used here, $y \approx 0.35$ and $F = 1.02$ g/L $\pm$ 3%.

6.3. Results and Discussion

6.3.1. Spouting Mechanism

Fines can be separated from fibers if at some height in the process vessel the liquid velocity is higher than the terminal settling velocity of the fines and less than that of the flocs of fibers. This requirement was achieved when the suspension was fed between certain limiting flow rates. The flow pattern for successful operation is shown schematically in Fig. 6.5 a. The increase in the cross sectional area of the vessel in the vertical direction satisfied the required conditions for the settling of

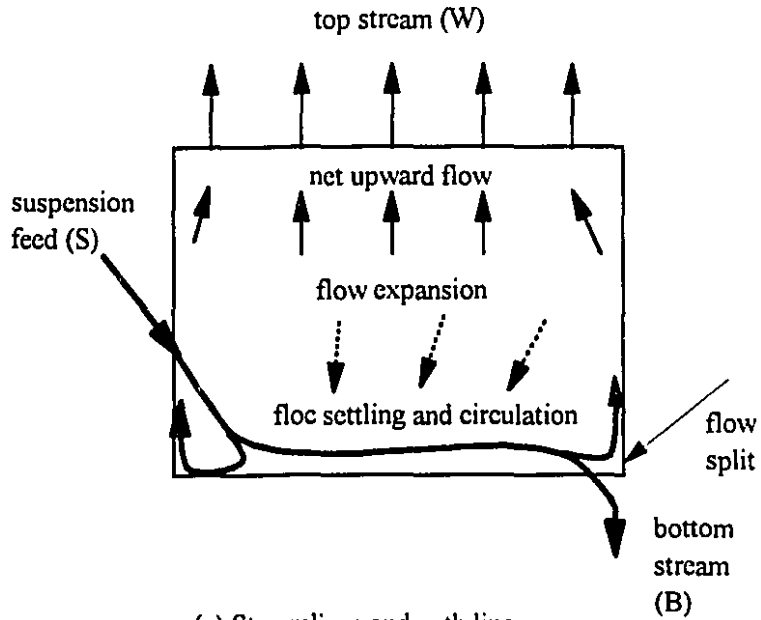

(a) Streamlines and path lines.
represents the streamlines of suspension flow,
represents the streamlines of floc-free liquid flow and
represents the path lines of flocs

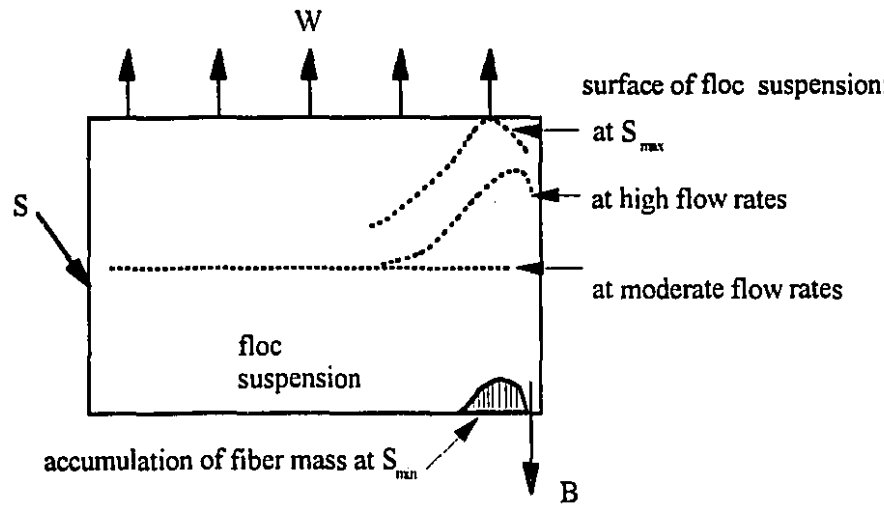

(b) Location of floc suspension. The dotted curve indicates the interface between the floc suspension and floc-free liquid. The shaded area is the region of pulp deposition at $S < S_{min}$

Figure 6.5: Schematic representation of flow in process vessel

fiber flocs after they rose to a certain height within the vessel. The horizontal flow near the bottom of the vessel was strong enough to prevent the permanent accumulation of fiber mass. This horizontal flow was split into an upward flow and a downward bottom stream. The resulting bed consisted of a continuous phase of floc suspension filling the lower part of the vessel.

At low feed rates, fibers tend to settle near the bottom exit where the horizontal flow splits (see Fig.6.5 b). For a fixed ratio of W/B, when the feed flow rate was decreased below S_{min}, a mass of fibers accumulated near the bottom outlet and grew with time as more fibers settled. As the fiber mass grew, the flow rate of the bottom stream decreased until the process was terminated.

In addition to the lower limit on feed flow rate (S_{min}), there was an upper limit at which flocs of fibers escaped in the top stream. The height of the pulp suspension phase within the vessel was a function of the inlet flow rate. At moderate flow rates, the surface of the pulp bed was nearly flat (Fig.6.5 b). At higher flow rates, the suspension surface rose near the opposite wall of the vessel (see Fig.6.5 b). This height increased with increasing inlet feed flow rate up to a flow rate (S_{max}) where the pulp suspension reached the first tube exit and fiber flocs were carried out of the vessel, resulting in considerable fiber loss. The lower (S_{min}) and the upper (S_{max}) operating feed rates were determined experimentally as functions of the flow split ratio (W/B) and the inlet consistency (X_s). Results are shown in Fig.6.6. The values scatter due to the difficulty in adjusting the flow conditions precisely. The inlet consistency (X_s) did not cause a measurable change in S_{min} and S_{max} for values between 0.5 to 1.0 g/L. When X_s was increased to about 2.0 g/L, the pulp suspension filled the whole vessel resulting in the fiber carryover. A value of $X_s \approx 1.5$ g/L represents the maximum inlet consistency for this geometry. The split ratio had little effect on S_{min} or S_{max} although there was a tendency for S_{max} to decrease with W/B. As an approximation, S_{max} and S_{min} can be considered to be 1000 and 500 mL/min, respectively, for the vessel used in this work. The limiting flow rates should

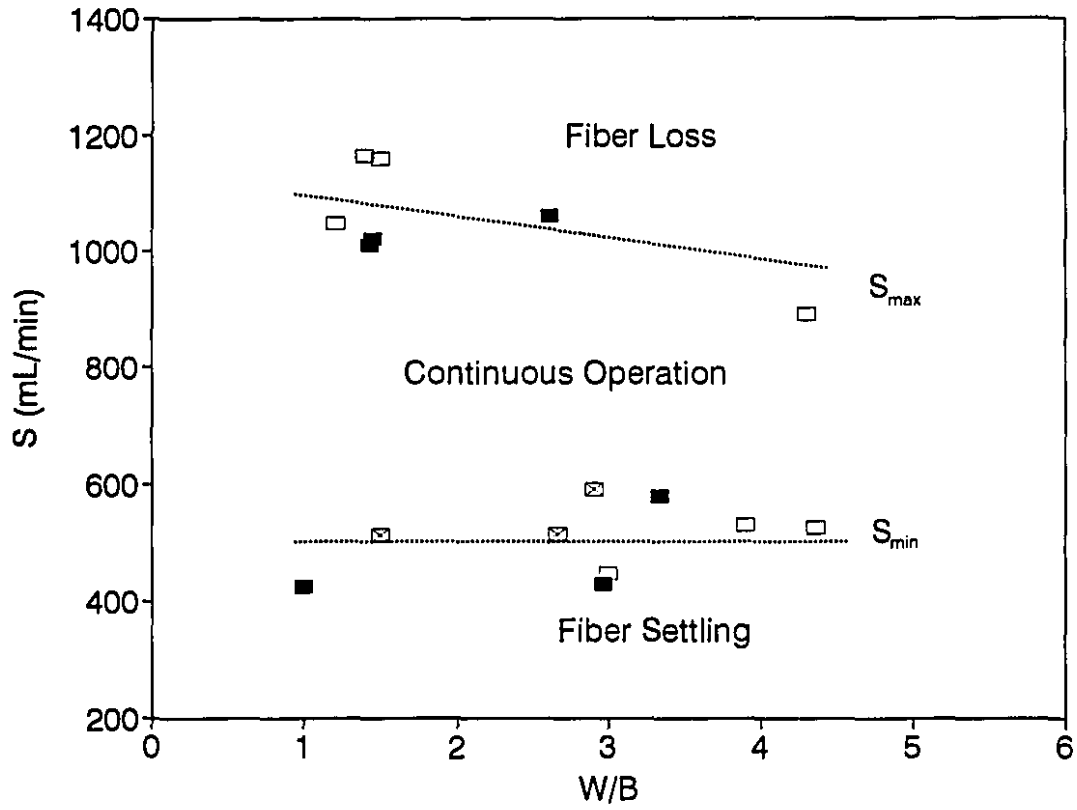

Figure 6.6: Regimes of operation. The symbols refer to different inlet consistencies as follows: empty square for 0.5 g/L, square with cross for 0.8 g/L and filled square for 1.0 g/L.

depend on geometrical parameters which were not varied, such as the design of the inlet and outlets, the position and the angle of inclination of the feed tube, the vessel length, height and the two angles, etc.

In order to study the feasibility of improving the separation efficiency, a cross flow stream was introduced from the bottom of the vessel in the form of five parallel jets injected through the five bottom tubes (see Fig.6.1). In this case, fibers settled between the jets. The settled mass of fibers grew with time and steady state operation could not be reached in 70 minutes.

6.3.2. Separation Mechanism

If the fines are so small that their settling velocity is much less than the liquid velocity, they may be considered as mathematical points in the flow field. If the particles do not interact with the flocs, the particle concentration is the same in all streams ($C_W=C_S$) and from eqn. 6.3, the separation efficiency is determined only by the flow split ratio, i.e.

$$\eta_s = \frac{W/B}{1 + W/B} \tag{6.8}$$

and the solids recovery R_s (g recovered solids / g solids in the feed) is given by

$$R_s = 1 - y\,\eta_s \tag{6.9}$$

Experiments were performed with pulp-free suspensions of Avicel particles fed into a liquid-filled, solid-free process vessel. The dimensionless exit concentrations of the two outlet streams, C_w/C_s and C_B/C_s, were determined from measured transmittances. Figure 6.7 shows these concentrations as functions of time for a

feed concentration (C_s) of 0.7 g/L, a feed flow rate (S) of 750 mL/minute and a split ratio (W/B) of 1.8. At steady state the two exit concentrations approached the feed concentration, confirming that for these small particles (20 μm) the separation efficiency is η_s.

On the other hand, when the settling velocity of the suspended particle is large enough compared to the upward liquid velocity, they can be excluded from the top stream. This is the case of fiber flocs; they are large enough, so they leave in the bottom stream. Figure 6.8 shows the measured transmittance of the two outlet streams as functions of time for an experiment with a fines-free fiber suspension fed into a liquid-filled, solid-free vessel. The inlet consistency (X_S) was 0.75 g/L, the feed flow rate (S) was 630 mL/minute and the split ratio (W/B) was 2.1. The steady state value of the transmittance of the top stream is very close to 1.0 which is equivalent to solid-free water indicating that the fiber concentration in the top stream is small. The fiber loss in the top stream was determined from filtration and drying. The measured percentage fiber loss in the top stream relative to fibers in the feed stream is tabulated in Table 6-1 for different operating conditions. The average fiber loss was about 1%. The fibers were retained in the bottom stream resulting in an increase in its consistency compared to the feed consistency, and thus the steady state transmittance of the bottom stream was much lower than that of the feed.

These results (Figure 6.5 and 6.6 and Table 6-1) indicate that the mechanism of the separation in the continuous wedge-like vessel is based on the exclusion of fibers from the top stream and the split of fines into the two streams. Fines split occurs according to flow split ratio when the fines are very small and fiber flocs do not release short fibers nor capture fines. This continuous technique produces a partial separation because fines are retained in the bottom even if no fibers are lost in the top stream. The removal selectivity of small particles can be improved by increasing the split ratio (e.g. up to 4) for which about 80% particle removal can be expected.

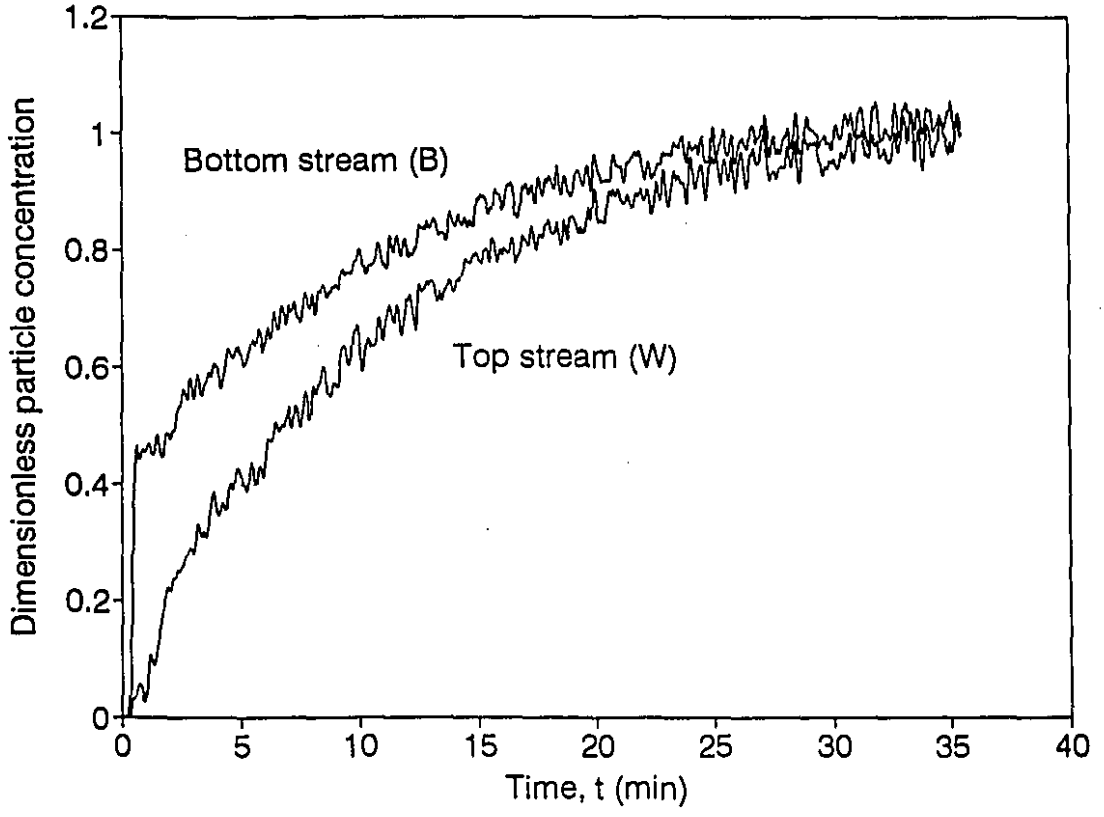

Figure 6.7: Dimensionless particle concentrations (C_w/C_s and C_b/C_s) as functions of time for a pulp-free Avicel particle suspension. The feed concentration was 0.7 g/L, the feed flow rate was 750 mL/min and the split ratio (W/B) was 1.8.

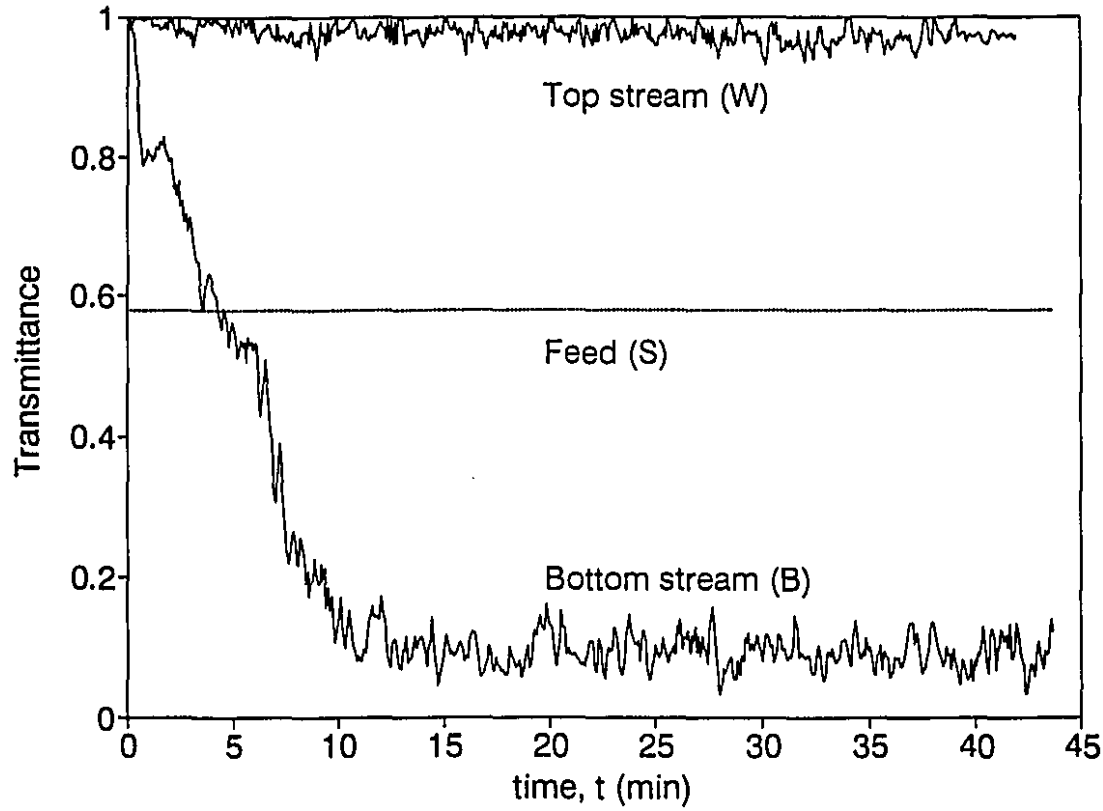

Figure 6.8: The top and bottom transmittances as function of time for an experiment with a fines-free fiber suspension fed into a liquid-filled, solid-free process vessel. The feed consistency was 0.75 g/L, the feed flow rate was 630 mL/min and the split ratio (W/B) was 2.1. The dashed line is the corresponding transmittance of the feed consistency.

Table 6-1: Percentage fiber loss in the top stream

Feed consistency X_s (g/L)	Feed flow rate S (mL/min)	Split ratio W/B	Percentage fiber loss
1.1	830	2.9	0.8
1.1	640	1.8	0.2
0.94	690	2.1	1.4
0.94	630	1.4	0.8
0.75	630	2.1	1.8
(average)			1.0

For experiments with recycled pulp suspensions, the solid recovery (g in stream B/ g in stream S) was measured from the dried samples from the bottom and feed streams. Table 6-2 shows results at different operating conditions. The last column gives the estimated pulp recovery i.e. R_s (eqn.6.9). The experimental results agreed with the estimated values within 10%. This difference is attributed to the errors in determining the solid contents and the flow rates.

6.3.3. Separation Efficiency

The separation efficiency was measured as a function of the split ratio (W/B), the suspension feed flow rate (S) and consistency (X_s).

The effect of the split ratio (W/B) on the separation efficiency (η) is shown in Fig 6.9, for the case of an a inlet pulp consistency of 0.5 g/L, and a feed flow rate of

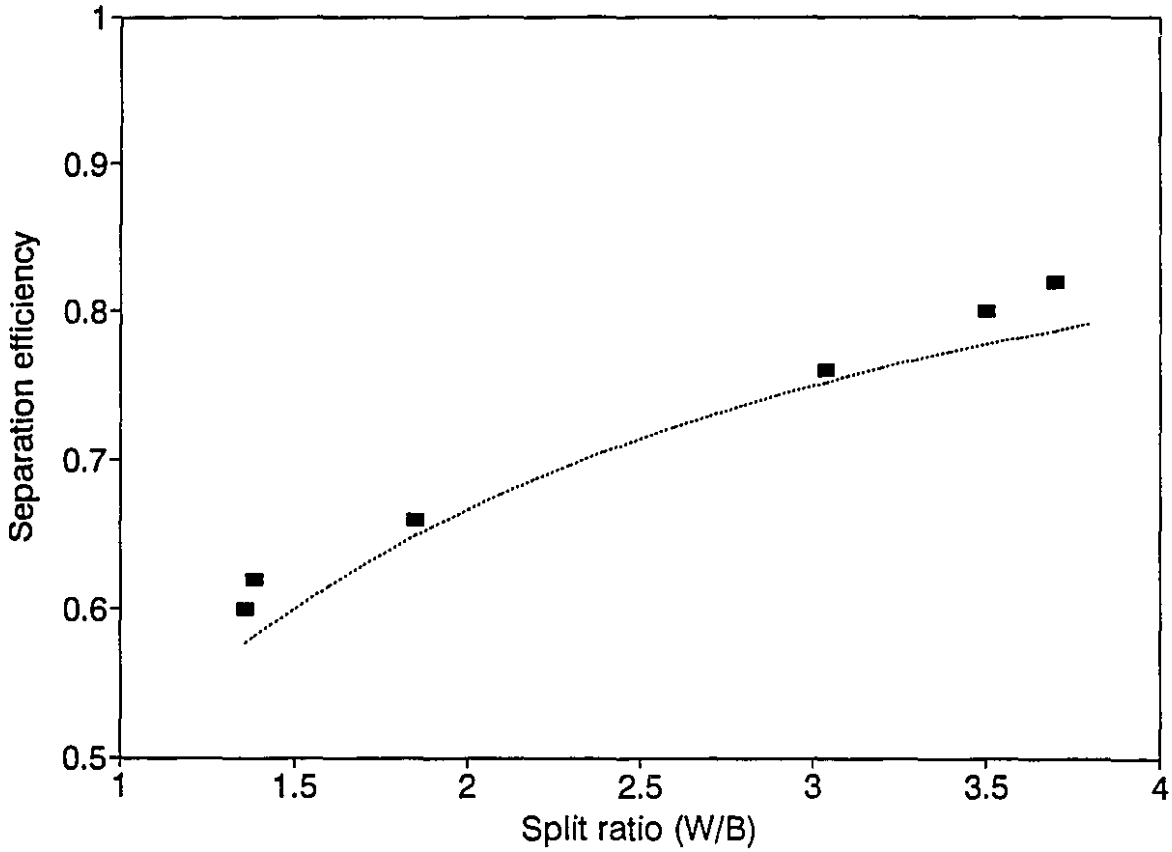

Figure 6.9: Separation efficiency (η) as a function of split ratio (W/B). The inlet consistency was 0.5 g/L and the feed flow rate was 730 mL/min. The dashed line is η_s calculated from eqn.6.8.

730 mL/min. The dashed line shows the limiting value, η_s. The experimental results are close to η_s, hence at low consistency (0.5 g/L) and moderate feed rate, the fines removal was governed by the flow split ratio.

Table 6-2: Percentage solid recovery

Feed flow rate S (mL/min)	Split ratio W/B	Inlet pulp consistency X_s (g pulp/L)	Pulp Recovery (measured)	pulp recovery (R_s; eqn. 6.9)
670	1.85	0.70	0.70	0.77
620	1.73	0.64	0.73	0.78
630	1.70	1.50	0.68	0.78

The effect of feed flow rate (S) on the separation efficiency is shown in Fig.6.10 for an inlet consistency of 0.5 g/L and a split ratio of 1.8. The dashed line is the limiting value, η_s. For moderate flow rates, $\eta=\eta_s$ while at flow rates of 800 mL/min $\eta>\eta_s$. This means that the measured top concentration of particles was larger than the particle concentration in the feed (C_s), which provided that there was particle generation within the process vessel. This was similar to what has been found in Chapters 4 and 5 with the semi-batch process when the operating flow rate is much higher than the minimum spouting flow rate. At high feed rates more de-flocculation took place and the surface of the pulp suspension rose higher and closer to the opposite wall of the vessel (see Fig.6.5 b). The released short fibers were easily carried in the top stream before being associated with the fiber flocs again resulting in increasing the separation efficiency.

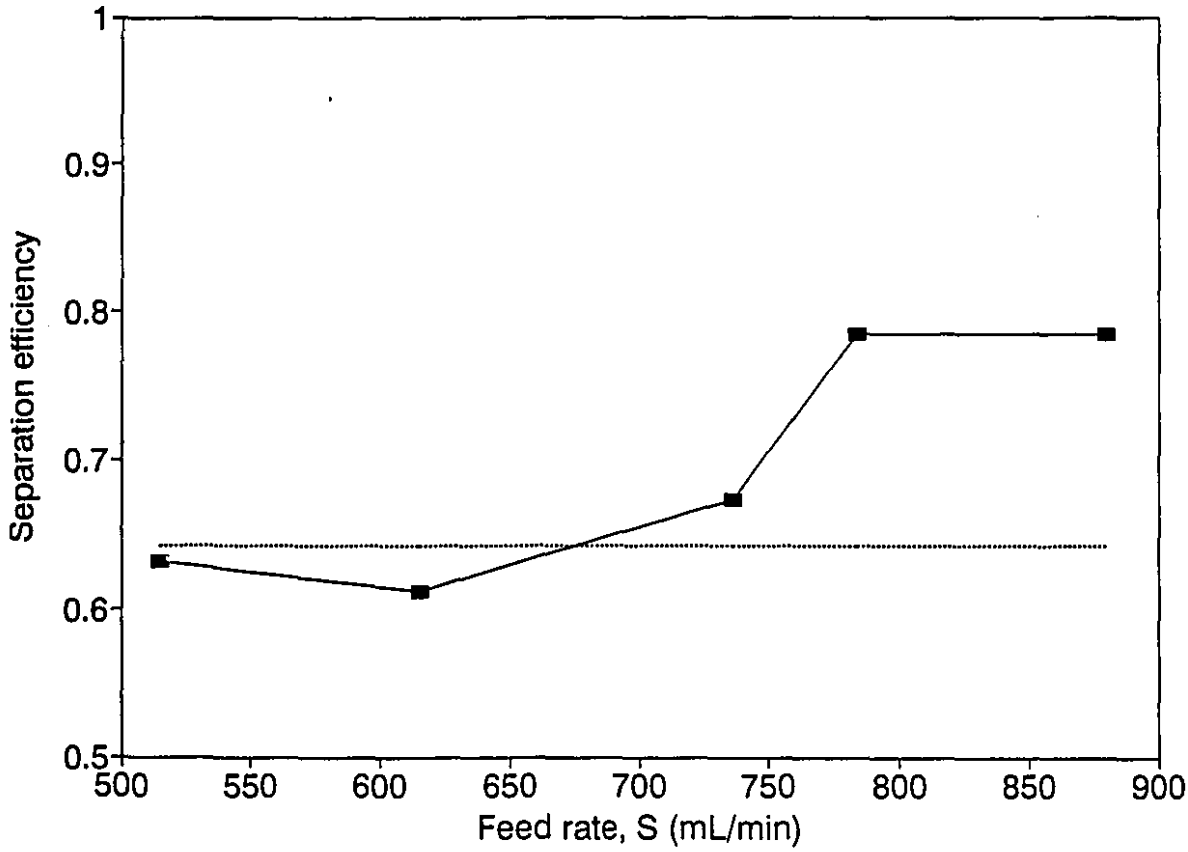

Figure 6.10: Separation efficiency (η) as a function of feed flow rate (S). The inlet consistency was 0.5 g/L and the split ratio (W/B) was 1.8. The dashed line is η_s.

Figure 6.11 shows the measured separation efficiency as a function of inlet consistency for a feed rate of 630 mL/min and a split ratio of 2.1. The dashed line is the value of η_s. At low inlet consistency, $\eta \approx \eta_s$, while at high inlet consistency, $\eta < \eta_s$. When the consistency was relatively high, the structure of a fiber floc was more permanent and hence the liquid inside the floc was not easily or rapidly exchanged with the bulk. In such a case, the residence time of the suspension within the vessel might not permit liquid exchange (which is accompanied with particle exchange). This fact in addition to the decrease in the external void fraction with increasing consistency resulted in having a small fraction of particles that was able to follow the liquid streamlines and thus to be split between the two exit streams. Most of the particles that were captured inside the flocs left in the bottom stream resulting in a lower particle concentration in the top stream than the expected value and consequently a separation efficiency less than η_s was obtained.

6.4. Conclusions

Particle fractionation by "elutriation-spouting" was achieved in a continuous operation in a wedge-like vessel. The process operates between lower and upper limits of the feed flow rate. These limits are nearly independent of the split ratio. There is a maximum inlet consistency above which the suspension phase expands and leaves in the top stream. The mechanism of separation is based on the exclusion of fibers from the top stream and the split of fines in the two outlet streams in proportion to the flow split ratio. The separation efficiency increased with increasing split ratio and decreased with increasing inlet consistency.

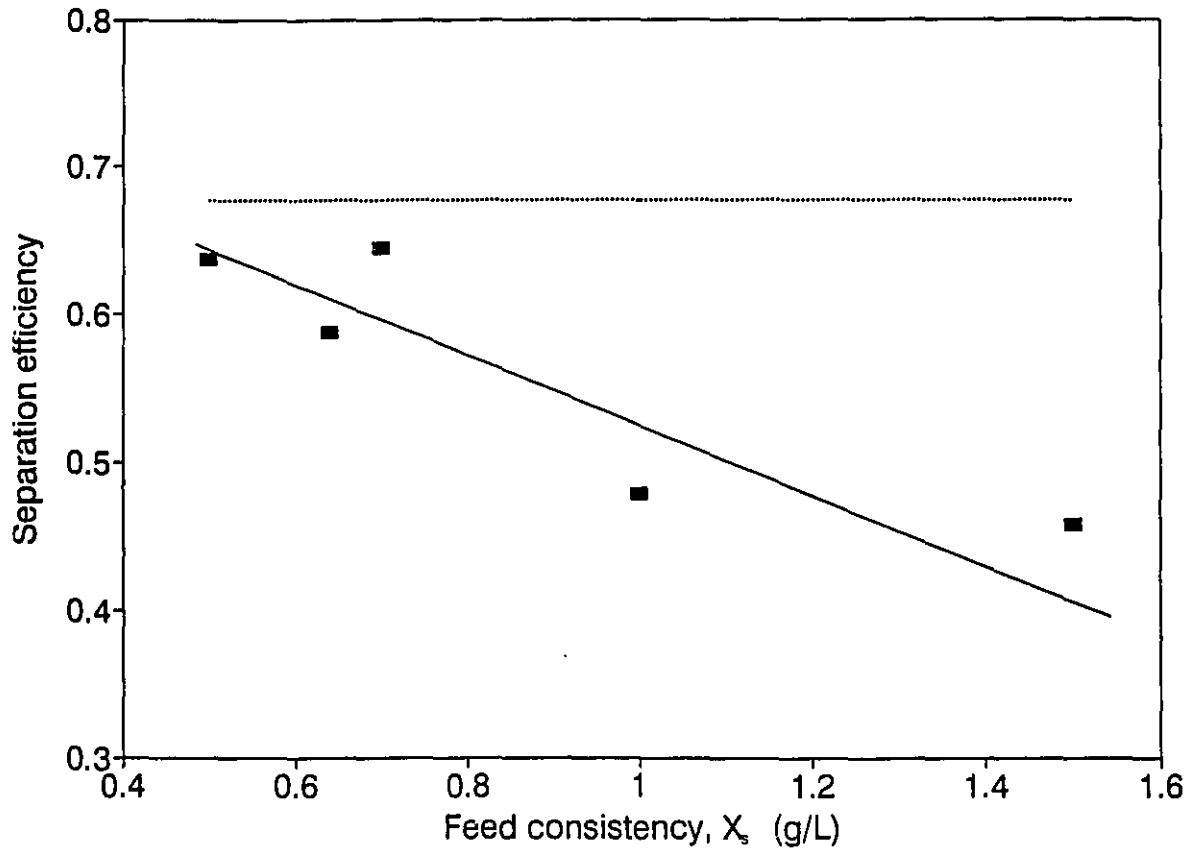

Figure 6.11: Separation efficiency (η) as function of inlet consistency (X_s). The feed flow rate was 630 mL/min and the output ratio (W/B) was 2.1. The dashed line is η_s.

Nomenclature

A	Absorptivity ($m^2 kg^{-1}$)
b	Path length through the cell of the spectrophotometer (m).
B	Bottom flow rate ($m^3 s^{-1}$).
C_w	Concentration of fines in the stream W ($g\ m^{-3}$).
C_s	Concentration of fines in the stream S ($g\ m^{-3}$).
C_B	Concentration of fines in the stream B ($g\ m^{-3}$).
F	Constant (g/L).
R_s	Estimated solids recovery.
S	Suspension feed flow rate ($m^3 s^{-1}$).
t	Time (s).
T_{ws}	Top transmittance at steady state.
W	Top flow rate ($m^3 s^{-1}$).
X_s	Consistency of pulp in the feed suspension ($g\ m^{-3}$).
y	Fraction of fines in a pulp suspension (g/g)
η	Separation efficiency.
η_s	Limiting separation efficiency for very small particles.

Chapter Seven

Summary, Contributions to Knowledge and Recommendations for Further Research

7.1 Summary of the Thesis

The feasibility of separating small particles from a recycled pulp suspension by an upward liquid flow has been investigated in this thesis. The work was started by trying to fluidize pulp fibers. It was found that handling pulp fibers required a flow field with sufficiently high shear to break the large fiber masses resulting from flocculation. This was acheived in a conical vessel for semi-batch operation and in a wedge-like vessel for continuous operation. In both vessels small particles were elutriated by an upward liquid flow.

The minimum spouting velocity in a conical vessel was measured for both pulp fibers and rigid rounded particles. Pulp spouting has been compared to conventional spouting. The flow patterns of liquid flow through the conical vessel used in the spouting experiments were visualized. The observations were used as a base for developing a model for estimating the minimum spouting velocity for pulp spouting. For the continuous vessel, the limits of the operating conditions required for continuous operation have been determined experimentally.

The effectiveness of the two operation modes, semi-batch and continuous, for the removal of small particles have been determined from mass balance analysis. Solid recovery has been estimated by measuring the solid content in the residual suspension or the bottom stream for both vessels. For suspensions of pulp fibers, fiber loss in the top stream has been determined by filtrating the top stream over 150 mesh and measuring the mass of the collected fibers. The behavior of particle elutriation has been investigated by measuring the transmittance of the top stream that contained the removed particles for both the semi-batch and the continuous vessels. An on-line technique for measuring particle concentration has been used for this purpose. For the semi-batch vessel, the time variation in the exit particle concentration (elutriation curve) was measured and from it the elutriation coefficient was estimated. A model for semi-batch elutriation was developed. For the continuous vessel, the steady state particle removal efficiency has been determined

from the measured exit transmittance.

7.2 Contributions to Knowledge

The work made the following original contributions to knowledge:

1) Liquid spouting of rigid particles in a conical vessel is similar to the known gaseous spouting behavior.

2) Pulp fibers are spouted in water in a conical vessel when the inlet Reynolds number (Re) is above a certain critical value and when the pulp consistency is within a certain range which permits the formation of non-coherent fiber flocs. Single fibers can not be spouted. Pulp spouting is different from conventional spouting.

3) Liquid flow through a conical diffusor at low Re has two flow regimes: (a) a steady straight jet and (b) an unsteady expanding jet. Flow transition between these two regimes occurs at a critical value of the Reynolds number that depends on the vessel geometry.

4) The flow field in a conical spouted bed of pulp fibers is of an unsteady expanding jet type. The minimum spouting occurs near the jet-flow transition. The presence of fibers in a spouted bed affects mainly the viscosity of the medium. Increasing the mass of fibers increases the viscosity and thus increases the minimum value of Re for pulp spouting.

5) A mixture of pulp fibers and small particles are separated in semi-batch operation using a conical spouted bed. Both ink and pulp fines can be removed from a recycled pulp suspension. The rate of particle removal may be characterized by an elutriation coefficient which increases with increasing flow rate. A fiber loss of about 2% occurs when the flow rate is close to the minimum spouting flow rate. Increasing the flow rate results in larger fiber loss.

6) Pulp fibers can be spouted in continuous operation in a wedge-like vessel having an inclined tube pulp inlet, a top outlet for water and elutriable particles and a bottom outlet for pulp exit. Certain ranges of flowrates and consistency are required.

7) Continuous elutriation of small particles can be achieved in a wedge-like vessel. The fibers are largely excluded from the top stream while the small particles are split between the two outlet streams according to the ratio of their flow rates.

7.3 Recommended Further Research

The following projects are suggested as continuations of the various aspects of this thesis.

1) Further study of pulp spouting in a conical vessel: The aim of this study is to investigate the feasibility of increasing the operating consistency. The following parameters can be investigated:

a) The vessel geometry, including
   - the cone angle, height and other inlet geometries.
   - diverging vessel with square cross-sectional area (instead of circular one) which will affect the jet flow patterns and thus the minimum spouting flow rate.

b) Manipulating the size of fiber flocs by adding flocculating agents such as polymers.

2) Further study of continuous elutriation-spouting to

a) increase the operating consistency by changing the vessel geometry e.g. wide angle, higher height, different positions of the tubes of the different streams, etc.

b) investigate a possible geometry with a cross flow stream that may improve

the separation efficiency.

c) optimize the geometrical parameters to achieve maximum particle separation with maximum operating consistency and flow rates

3) Particle deposition onto pulp fibers in spouted bed: This study can be carried in both semi-batch and continuous vessel. The first provides a well characterized flow field for investigating the deposition phenomena. The second may lead to an industrial application for fiber filling.

4) Investigating the feasibility of ink flotation from a mixture of fines and ink (i.e. the top exit suspension from an elutriation-spouting process). This study is recommended to overcome the disadvantage of fines loss in the use of elutriation-spouting as a deinking procedure.

5) A study of liquid spouting of rigid particles in conical vessels to determine the minimum spouting velocity and pressure drop across the bed as well as the stability of spouting. The following variables should be investigated:

a) Vessel geometry including the cone angle, height and the inlet geometry

b) Particle size for the same material.

c) Particle density for different materials with the same particle size.

d) Liquid density and viscousity

e) Spouting of particle mixtures.

6) A study of particle elutriation from liquid spouted beds containing mixtures of rigid particles of different particle sizes and/or different particle densities. Examples of possible systems are glass particles of different sizes or a mixture of glass and zinc particles of same particle size. The following parameters can be investigated:

a) The minimum elutriation velocity.

b) The elutriation curve.

c) The existence of a critical particle size ratio below which particles can not be separated.